A UNITED STATES DEPARTMENT OF COMMERCE PUBLICATION

SECTION C

UNIVERSITY OF MICHIGAN
AUG 10 1971
ENGINEERING LIBRARY

JOURNAL OF RESEARCH

of the NATIONAL BUREAU OF STANDARDS

Volume 75C No. 1 Jan.-Mar. 1971

Engineering and Instrumentation

U.S. DEPARTMENT OF COMMERCE
National Bureau of Standards

Journal of Research
of the
National Bureau of Standards

C. Engineering and Instrumentation

Jan.-Mar. • 1971

VOLUME • 75C

NUMBER • 1

Editor: Martin Greenspan

Associate Editors: G. F. Montgomery, R. V. Smith, A. F. Schmidt

Publication dates:
Feb. 15, May 15, Aug. 15, Nov. 15, 1971

J. Res. Nat. Bur. Stand. (U.S.), C
CODEN: JNBCA 75C (1) 1-67 (1971)

JOURNAL OF RESEARCH

The National Bureau of Standards Journal of Research reports research and development in the fields of activity shown at right. Also included from time to time are survey articles on topics closely related to the Bureau's scientific and technical program.

The Journal is published in three separate sections as follows:

A. Physics and Chemistry

Contains papers of interest primarily to scientists working in these fields. Issued six times a year. Annual subscription: domestic, $9.50; foreign, $11.75. Single copy, varies.

B. Mathematical Sciences

Presents studies and compilations designed mainly for the mathematician and the theoretical physicist. Issued quarterly. Annual subscription: domestic, $5.00; foreign, $6.25. Single copy, $1.25.

C. Engineering and Instrumentation

Reports research and development results of interest chiefly to the engineer and the applied scientist. Issued quarterly. Annual subscription: domestic, $5.00; foreign, $6.25. Single copy, $1.25.

The National Bureau of Standards[1] was established by an act of Congress March 3, 1901. The Bureau's overall goal is to strengthen and advance the Nation's science and technology and facilitate their effective application for public benefit. To this end, the Bureau conducts research and provides: (1) a basis for the Nation's physical measurement system, (2) scientific and technological services for industry and government, (3) a technical basis for equity in trade, and (4) technical services to promote public safety. The Bureau consists of the Institute for Basic Standards, the Institute for Materials Research, the Institute for Applied Technology, the Center for Computer Sciences and Technology, and the Office for Information Programs.

THE INSTITUTE FOR BASIC STANDARDS provides the central basis within the United States of a complete and consistent system of physical measurement; coordinates that system with measurement systems of other nations; and furnishes essential services leading to accurate and uniform physical measurements throughout the Nation's scientific community, industry, and commerce. The Institute consists of a Center for Radiation Research, an Office of Measurement Services and the following divisions:

Applied Mathematics—Electricity—Heat—Mechanics—Optical Physics—Linac Radiation[2]—Nuclear Radiation[2]—Applied Radiation[2]—Quantum Electronics[3]—Electromagnetics[3]—Time and Frequency[3]—Laboratory Astrophysics[3]—Cryogenics[3].

THE INSTITUTE FOR MATERIALS RESEARCH conducts materials research leading to improved methods of measurement, standards, and data on the properties of well-characterized materials needed by industry, commerce, educational institutions, and Government; provides advisory and research services to other Government agencies; and develops, produces, and distributes standard reference materials. The Institute consists of the Office of Standard Reference Materials and the following divisions:

Analytical Chemistry—Polymers—Metallurgy—Inorganic Materials—Reactor Radiation—Physical Chemistry.

THE INSTITUTE FOR APPLIED TECHNOLOGY provides technical services to promote the use of available technology and to facilitate technological innovation in industry and Government; cooperates with public and private organizations leading to the development of technological standards (including mandatory safety standards), codes and methods of test; and provides technical advice and services to Government agencies upon request. The Institute also monitors NBS engineering standards activities and provides liaison between NBS and national and international engineering standards bodies. The Institute consists of the following technical divisions and offices:

Engineering Standards Services—Weights and Measures—Flammable Fabrics—Invention and Innovation—Vehicle Systems Research—Product Evaluation Technology—Building Research—Electronic Technology—Technical Analysis—Measurement Engineering.

THE CENTER FOR COMPUTER SCIENCES AND TECHNOLOGY conducts research and provides technical services designed to aid Government agencies in improving cost effectiveness in the conduct of their programs through the selection, acquisition, and effective utilization of automatic data processing equipment; and serves as the principal focus within the executive branch for the development of Federal standards for automatic data processing equipment, techniques, and computer languages. The Center consists of the following offices and divisions:

Information Processing Standards—Computer Information—Computer Services—Systems Development—Information Processing Technology.

THE OFFICE FOR INFORMATION PROGRAMS promotes optimum dissemination and accessibility of scientific information generated within NBS and other agencies of the Federal Government; promotes the development of the National Standard Reference Data System and a system of information analysis centers dealing with the broader aspects of the National Measurement System; provides appropriate services to ensure that the NBS staff has optimum accessibility to the scientific information of the world, and directs the public information activities of the Bureau. The Office consists of the following organizational units:

Office of Standard Reference Data—Office of Technical Information and Publications—Library—Office of Public Information—Office of International Relations.

[1] Headquarters and Laboratories at Gaithersburg, Maryland, unless otherwise noted; mailing address Washington, D.C. 20234.
[2] Part of the Center for Radiation Research.
[3] Located at Boulder, Colorado 80302.

U.S. DEPARTMENT OF COMMERCE
Maurice H. Stans, Secretary
NATIONAL BUREAU OF STANDARDS
Lewis M. Branscomb, Director

Order all publications from the Superintendent of Documents
U.S. Government Printing Office, Washington, D.C. 20402.

Use of funds for printing this publication approved by the Director of the Bureau of the Budget (June 22, 1966).

JOURNAL OF RESEARCH of the National Bureau of Standards — C. Engineering and Instrumentation
Vol. 75C, No. 1, January-March 1971

Rotary-Vane Attenuator With an Optical Readout

W. E. Little*, W. Larson*, and B. J. Kinder*

Institute for Basic Standards, National Bureau of Standards, Boulder, Colorado 80302

(May 13, 1970)

A precision x-band rotary-vane attenuator has been developed that follows its theoretical cosine squared law of attenuation to within 0.002 dB to a value of 20 dB. The best available attenuation measurement techniques verify this relationship to within the accuracy of the measurements. From 20 to 50 dB, the deviation from the theoretical value slowly increases and is frequency dependent. At present, three attenuators of this type have been constructed by NBS. Two of these attenuators have excellent attenuation versus frequency characteristics in the 20 to 50 dB range (0.08 dB deviation at 50 dB) while the third has a marked degree of frequency sensitivity (0.21 dB at 50 dB).

Key words: Attenuator; microwave; precision; rotary vane.

1. Introduction

The principle of the rotary-vane attenuator [1,2][1] has been known for a number of years, and relatively good attenuators have been commercially available for some time. A considerable amount of analysis [3,4,5,6,7] of this type of commercially available attenuator has been made, and some work has been directed toward the development of more precise attenuators [8,9]. Most of the major problems have been identified and analyzed.

The steps taken in the work described in this paper were to eliminate or reduce the major limiting errors. The results achieved using this approach were very gratifying. The evaluation of the three constructed attenuators has shown that the property of attenuation difference up to 20 dB is improved an order of magnitude over that reported previously. However, two of the attenuators retain their excellence above 20 dB, while the third shows some frequency dependence at higher values of attenuation. A description of the attenuators and the results of the measurement on two of them by the i–f substitution [10], d–c substitution [12], and modulated subcarrier [13] techniques of attenuation measurement are given.

The "true" rotary vane value is estimated by averaging the results from the three measurement techniques. Measurement results from the third attenuator by the subcarrier technique are also given.

2. Theory

As is well known, the ideal behavior of the rotary-vane attenuator is given by

$$\frac{E_{\text{in}}}{E_{\text{out}}} = \frac{1}{\cos^2 \gamma}$$

where E_{in} indicates the strength of the input wave and E_{out} is the strength of the output wave.

In decibels, this is

$$A = -40 \log_{10} (\cos \gamma).$$

Thus, ideally, the output wave is a simple function of the angle of rotation of the center section of the attenuator.

There are many problems encountered in the actual construction of this type attenuator which has many sources of error. The errors fall roughly into five categories: (1) read-out resolution and resettability; (2) basic mechanical precision such as vane alinement, rotating section eccentricity, resolution of vane angle setting, etc.; (3) external leakage, primarily from the rotating joints; (4) internal leakage (lack of absorption of the parallel component); and (5) internal reflections. Mariner [8] gives adequate analysis of categories 2, 4, and 5. James [9] also considers these errors as well as category 1 for the particular type tape readout which he was using. Larson [7] further considers the vane alinement error. The errors caused by category 3 have not been considered and in fact have not been readily observable in the attenuators that have been tested to date, primarily because there was not sufficient resolution to see the results of the leakage or the problem was not identified. In the development of the attenuators described here, this problem was identified and had to be corrected for before substantial improvement could be accomplished.

* National Bureau of Standards, Electromagnetics Division, Boulder, Colo. 80302

[1] Figures in brackets indicate the literature references at the end of this paper.

3. Description of the Attenuator

3.1 Readout

One of the major limitations of the design of this type of attenuator has been the technique used to determine the actual vane angle setting. In the commercial low-resolution (and some recent high-resolution) instruments, the technique is to simply use a gear reduction system with all the associated mechanical problems. These errors have been analyzed by Larson [4,6] and it is quite conclusive that the technique rapidly becomes the limiting factor in the design of an ultra-precision attenuator. James [9] used a tape-dial indicator arrangement but, again, it is not suitable for ultra-precision attenuators. (See fig. 1.)

To achieve the desired accuracy, the readout has to be a direct-reading device attached directly to the rotating cylinder. Fortunately, there are commercially available engraved glass scales with an optical readout that have the desired accuracy and resolution. Figure 2 shows a sketch of one of the scales mounted on the cylinder of the attenuator's rotating center section. The scale has an absolute accuracy of $\pm$ 1″ of arc and a resolution of the same amount; hence, the total uncertainty is $\pm$ 2″ of arc. Figure 3 shows the attenuation deviation in dB from nominal for the variation of $\pm$ 2″ of arc versus attenuator dial setting in decibels. If this were the only source of uncertainty, the values of the uncertainty in attenuation would be about $\pm$ 0.00025 dB and 0.003 dB at the dial setting of 10 and 50 dB respectively.

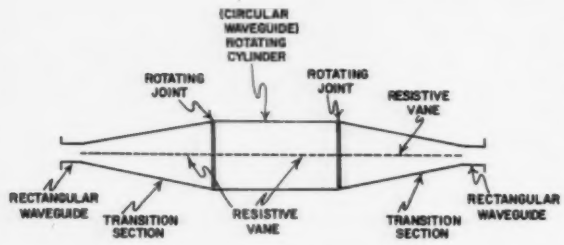

FIGURE 1. *Basic components of rotary-vane attenuator.*

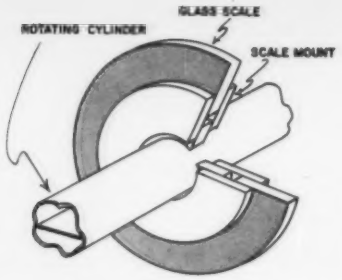

FIGURE 2. *Engraved glass scale mounted on rotating cylinder.*

A sketch of the dual microscope readout is illustrated in figure 4. Note the two viewing apertures are located 180 degrees apart in order to reduce the eccentricity error.

3.2 Mechanical Precision

The final quality of the attenuator, even with the engraved scales, is primarily a function of the precision and accuracy with which it is assembled. Larson [7] shows that the vane alinement is quite critical and a relatively small misalinement can cause a considerable error. Further, in order to utilize effectively the $\pm$ 1″ of arc resolution of the engraved scale, rotational precision is a must.

The required precision was obtained by carefully machining and strengthening the attenuator housing as shown in figure 5. In some of the later testing of attenuator No. 1, it was observed that even with the improved housing there was a nonrepeatability of setting of approximately 10 μB. The cause of this problem was found

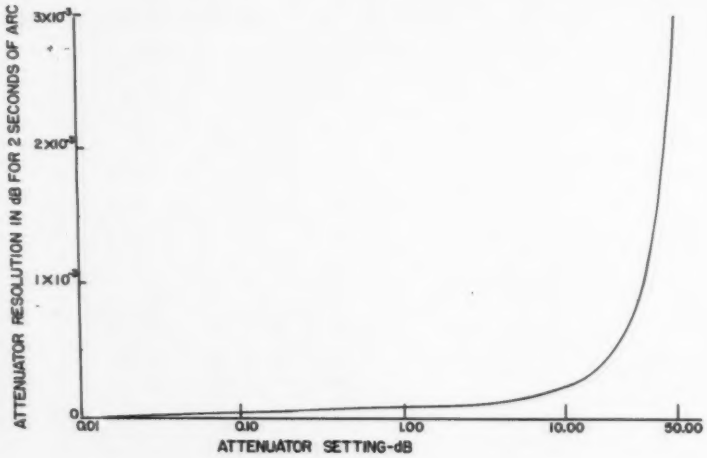

FIGURE 3. *Attenuator resolution.*

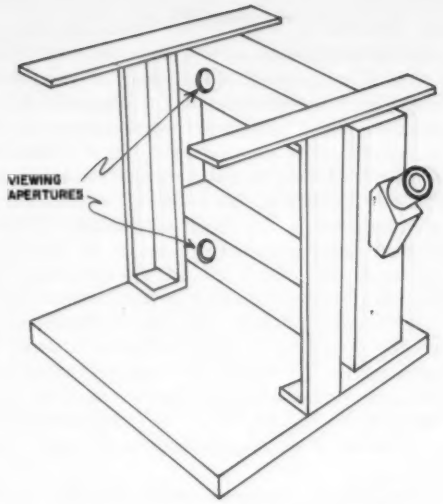

FIGURE 4. *Dual microscope mounted in attenuator housing.*

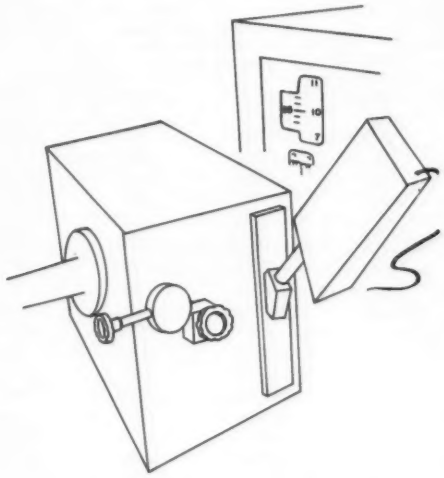

FIGURE 5. *Modified attenuator housing.*

to be the forces exerted on the rotating cylinder by the drive gear even though the finest quality triple A bearings had been used in the rotating joints. The problem was eliminated by driving the cylinder through a bellows as shown in figure 6. This addition was not made to attenuators No. 2 and 3.

3.3 External Leakage

The effects of external leakage are quite subtle and in many cases are very difficult to identify. In the early design of the attenuators, this leakage caused nonrepeatability problems at the lower values of attenuation and instability at the higher values. The primary source of the leakage signal was determined to be the rotating joints.

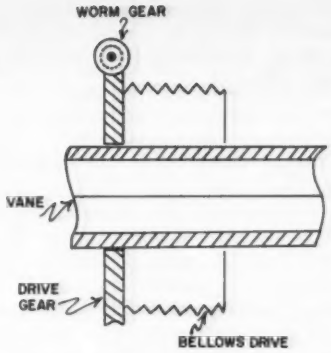

FIGURE 6. *Bellows drive of attenuator No. 1.*

The addition of chokes alone did not provide sufficient attenuation to stop the leakage. In some cases, the leaked power is down only 40 dB from the incident power in the waveguide and it is rarely down more than 60 dB. In the attenuators described here, the leakage was reduced to more than 120 dB below the incident power by liberal use of microwave-absorbing material in the design of the housing and rotating joints as shown in figure 7.

3.4 Internal Leakage

Internal leakage is the result of insufficient attenuation of the parallel component of the wave (the component that is in the plane of the resistive card). The card absorption was checked by measuring the maximum attenuation that could be achieve with a particular card. For commercially available cards, this ranged from 110 dB to 135 dB at 9 GHz. The results of this leakage component is a deviation from the $\cos^2\gamma$ law at the higher values of attenuation. Both Mariner [8] and James [9] analyzed

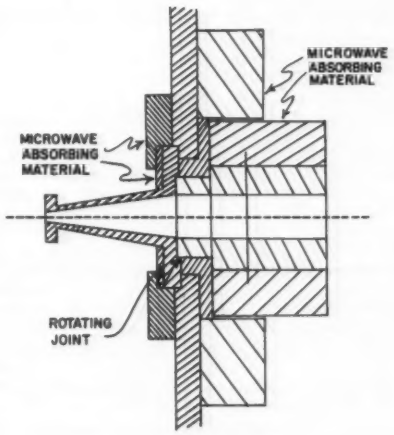

FIGURE 7. *Addition of microwave absorbing material around rotating joints.*

this error. The actual effect of this leakage for the attenuators is shown in figures 8, 9, and 10. Some work was done on the design of different types of cards but no improvement was achieved.

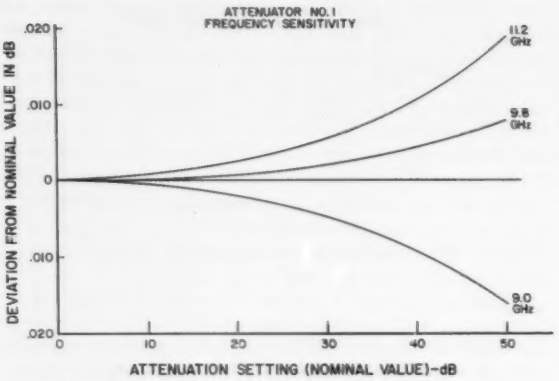

FIGURE 8. *Frequency sensitivity of attenuator No. 1.*

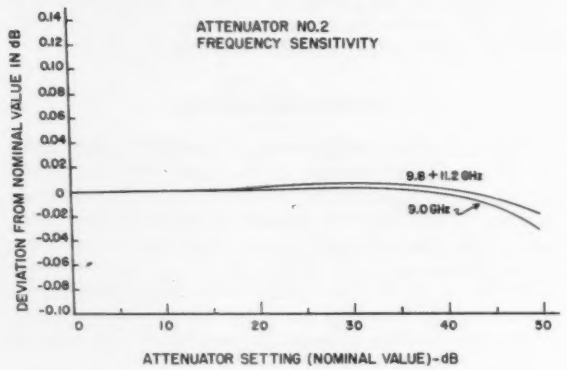

FIGURE 9. *Frequency sensitivity of attenuator No. 2.*

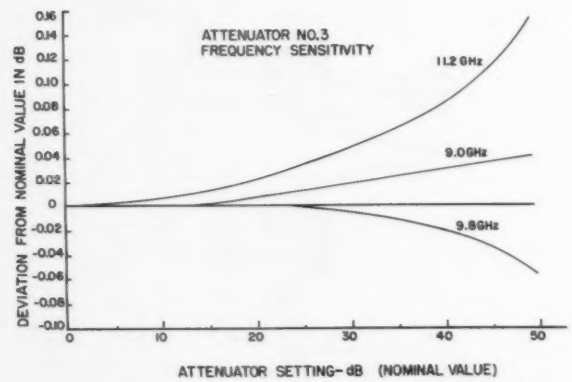

FIGURE 10. *Frequency sensitivity of attenuator No. 3.*

4. Results

In order to test the attenuators over the desired 50 dB range, several techniques of attenuation measurement were used. The d–c substitution [12] system is the most accurate technique of attenuation measurement available in the range of 0.01 to approximately 20 dB. The modulated subcarrier [13,14] technique is quite accurate in the range of 0.1 to 20 dB while the i–f [15] substitution technique is quite good in the range of 1 to 50 dB. All the techniques are comparable over parts of the overlapping range up to 20 dB. Above 20 dB, the d–c substitution technique loses resolution and the particular subcarrier system used for the measurements had not been carefully evaluated above 20 dB at the time of the measurements.

Attenuators No. 2 and No. 3 were calibrated by all three techniques of attenuation measurement at several values between 0.5 and 20 dB at *9 GHz* as shown in table 1. (Values above 20 dB were obtained by the i–f tech-

TABLE 1. *Comparison of calibration data for the same attenuator by three different methods*

Nominal value, dB		Average measured value, dB	Estimated limits to systematic error,	Standard deviation, dB
		Attenuator No. 2.		
0.5000	d–c	00.5006	0.0006	.0001
	i–f	00.4990	.0150	.1000
	sc	00.4996	.0050	.0005
1.0000	d–c	01.0018	.0013	.0006
	i–f	01.0002	.0150	.0023
	sc	00.9997	.005	.0016
3.0000	d–c	03.0016	.0047	.0001
	i–f	03.0000	.0150	.0023
	sc	02.9993	.0050	.0014
6.0000	d–c	06.0021	.0049	.0001
	i–f	05.9986	.0150	.0028
	sc	05.9984	.0050	.0025
10.0000	d–c	10.0020	.0053	.0055
	i–f	09.9990	.0150	.0013
	sc	09.9973	.0050	.0021
20.0000	d–c	20.0021	.0100	.0042
	i–f	19.9994	.0150	.0013
	sc	19.9946	.0100	.0023
		Attenuator No. 3.		
0.5000	d–c	0.5002	0.0006	0.0004
	i–f	.4988	.0150	.0010
	sc	.5007	.005	.0002
1.0000	d–c	1.0003	.0013	.0002
	i–f	0.9992	.0150	.0010
	sc	1.0003	.0050	.0011
3.0000	d–c	3.0007	.0047	.0002
	i–f	3.0010	.0150	.0010
	sc	3.0003	.0050	.0015
6.0000	d–c	6.0008	.0049	.0005
	i–f	6.0000	.0150	.0023
	sc	6.0007	.0050	.0027
10.000	d–c	9.9996	.0053	.0016
	i–f	9.9992	.0150	.0010
	sc	9.9994	.0050	.0025
20.0000	d–c	20.0069	.0100	.0014
	i–f	19.9964	.0150	.0013
	sc	20.0000	.0100	.0045

nique only and are shown in table 3). The estimated systematic error for each system is the summation of the estimated limits to all of the known system errors (this gives the estimated maximum possible systematic error) and the standard deviation is determined from the measurement data.

The estimated true values for the attenuators given in table 2 are the average of the values obtained from the three different systems.

TABLE 2. *Estimated true value for each nominal value determined from the average of the three different methods*

Nominal value, dB	Estimated true value, dB
Attenuator No. 2	
0.5000	00.4997
1.0000	01.0006
3.0000	03.0003
6.0000	05.9997
10.0000	09.9996
20.0000	19.9987
Attenuator No. 3.	
0.5000	00.4999
1.0000	00.9992
3.0000	03.0005
6.0000	06.0004
10.0000	10.0003
20.0000	20.0018

TABLE 3. *Measured values—i–f substitution technique*

Nominal value, dB	Average measured value, dB	Estimated limits to systematic error, dB	Standard deviation, dB
Attenuator No. 2			
30.000	30.001	±0.018	0.001
40.000	40.000	± .028	.003
50.000	49.968	± .085	.004
Attenuator No. 3			
30.000	29.995	±0.018	0.003
40.000	39.982	± .028	.003
50.000	49.945	± .085	.003

5. Conclusion

The development work outlined in this report confirms that over a limited range a precision-built, rotary-vane attenuator has excellent properties for a primary reference standard of attenuation difference. These properties are nearly ideal up to the attenuation value of 20 dB. Above this value of attenuation the rotary-vane attenuator is an excellent working standard. (The attenuator needs calibrating because of the frequency-sensitivity problem.) Solution of the remaining two outstanding problems (frequency sensitivity and internal leakage) will establish it as a primary reference standard over a much larger attenuation range.

The attenuator should find wide application for the evaluation of systems where it is not feasible to use section-by-section evaluation techniques. For example, in some of the dual channel i–f attenuation-measuring systems, the standard piston attenuator cannot be independently evaluated. In addition to being used in the straight rf substitution technique, this rotary-vane attenuator can be used in the same fashion that the 30 MHz waveguide-below-cutoff atenuator is presently used. For the higher frequencies (millimeter waves), a frequency down converter can be used to obtain the proper frequency and for the lower frequencies, an upconverter can be employed.

Another quite useful area for this rotary-vane attenuator is in the measurement of very small values of attenuation. To the authors' knowledge, there is no other way to achieve a change of attenuation of a few hundredths or tenths of the decibel to the accuracy and resolution that can be achieved with the ultra-precision rotary-vane attenuator.

6. References

[1] Southworth, G. C., (1959), Principles and Applications of Waveguide Transmissions, Ed., Princeton, J. J. (Von Nostrand, (1959) pp. 374–376.

[2] Hand, B. P., A precision waveguide attenuator which obeys a mathematical law, Hewlett-Packard J. **6,** 1–2 (Jan. 1955).

[3] Larson, Wilbur, Analysis of rotation errors of a waveguide rotary-vane attenuator, IEEE Trans. Instr. Meas. **IM-12,** No. 2, 50–55 (Sept. 1963).

[4] Larson, Wilbur, Table of attenuation error as a function of vane-angle error for rotary-vane attenuators, Nat. Bur. Stand. (U.S.), Tech. Note 177, 156 pages (May 1963).

[5] Larson, Wilbur, Table of attenuation as a function of vane angle for rotary-vane attenuators ($A = -40 \log_{10} \cos \theta$), Nat. Bur. Stand. (U.S.), Tech. Note 229, 188 pages (Jan. 1965).

[6] Larson, Wilbur, Gearing errors as related to alignment techniques of the rotary-vane attenuator, IEEE Trans. Instr. Meas. **IM-14,** 117–123 (Sept. 1965).

[7] Larson, Wilbur, Analysis of Rotationally Misaligned Stators in the Rotary-Vane Attenuator, IEEE Trans. Instr. Meas. **IM-16,** No. 3 (Sept. 1962).

[8] Mariner, P. F., An absolute microwave attenuator, Proc. IEE, pp. 415–419 (Sept. 1962).

[9] James, Allan V., A high-accuracy microwave attenuation standard for use in primary calibration Laboratories, IRE Trans. Instr. **I-11,** 285–290 (Dec. 1962).

[10] Gainsborough, G. F., A method of calibrating standard-signal generators and radio-frequency attenuators, J. IEE (London) **94,** Part III, 203–210 (May 1947).

[11] Grantham, R. E., and Freeman, J. J., (June 1968), A standard of Attenuation for Microwave Measurements, Trans. AIEE **67,** 329–335 (June 1968).

[12] Engen, G. F., and Beatty, R. W., Microwave attenuation measurements with accuracies from 0.0001 to 0.06 decibel over a range of 0.01 to 50 decibels, J. Res. Nat. Bur. Stand. (U.S.), **64C** (Eng. & Instr.), No. 2, 139–145 (Apr.-June 1960).

[13] Schafer, G. E., and Bowman, R. R., A modulated sub-carrier technique of measuring microwave attenuation, Proc. IEE (London) **109,** Part B. Suppl. No. 23, 783–786 (May 1962).

[14] Little, William E., Further analysis of the modulated sub-carrier technique of attenuation measurement, IEEE Trans. Instr. Meas. **13,** 71–76 (June-Sept. 1964).

[15] Weinschel, B. O., and Sorger, G. U., Waveguide below cut-off attenuation standard, Acta IMEKO **III,** 407–424 (1964).

(Paper 75C1–307)

JOURNAL OF RESEARCH of the National Bureau of Standards — C. Engineering and Instrumentation
Vol. 75C, No. 1, January-March 1971

Design and Operational Characteristics of a High-Speed (Millisecond) System for the Measurement of Thermophysical Properties at High Temperatures*

Ared Cezairliyan

Institute for Materials Research, National Bureau of Standards, Washington, D.C. 20234

(November 19, 1970)

Design and constructional details of a high-speed system for the measurement of selected thermophysical properties of electrical conductors at temperatures above 2000 K in experiments of subsecond duration are described. Operational characteristics of such a system are given. Various phenomena that affect the design and successful operation of the system are discussed and, whenever possible, quantitative results are given. Certain experimental checks to assess the operation of the system are also described.

Key words: High-speed measurements; high temperatures; thermodynamics; thermophysical properties.

1. Introduction

Interest in thermophysical properties at temperatures above the limit of accurate steady-state experiments has necessitated the development of high-speed measurement techniques. Most of the difficulties inherent in steady-state methods are eliminated in high-speed experiments. However, new problems arise due to the nature of rapid experiments, some of which increase rapidly with increasing speed. This suggests that an optimized system has to be designed for most accurate measurements.

The objective of this writing is to describe the details of a high-speed system for the measurement of selected thermophysical and related properties (heat capacity, electrical resistivity, hemispherical total and normal spectral emittances, melting point, etc.) of electrical conductors at temperatures above 2000 K in experiments of subsecond duration. Operational characteristics of such a system under actual experimental conditions are presented. Various phenomena that affect the design and successful operation of the system are discussed in the context of high-speed experiments and, whenever possible, quantitative results are given. Certain experimental checks to assess the operation of the system are described.

The method employed in the high-speed measurements is based upon rapid resistive heating of the specimen by a single pulse (subsecond duration) of direct current and measuring the pertinent quantities with millisecond resolution. Formulation of the relationships between various experimental quantities and properties is given in another publication [1][1]

* This work was supported in part by the Propulsion Division of the U. S. Air Force Office of Scientific Research under Contract ISSA-70-0002.

[1] Figures in brackets indicate the literature references at the end of this paper.

2. Measurement System

The high-speed measurement system consists of an electric power pulsing circuit and associated measuring and control circuits. A functional diagram of the complete system and a photograph of a portion of the system are presented in figures 1 and 2, respectively.

2.1. Pulsing Circuit

The pulse circuit includes the specimen in series with a battery bank, a standard resistance, a variable resistance, and a switching system. The battery bank consists of 14 series-connected 2 V batteries each having approximately 1100 A–h capacity. A standard resistance (0.001 Ω shunt) made of manganin strip is used to measure the pulse current flowing through the specimen. A variable resistance made of water-cooled Inconel tubes (total resistance = 30 mΩ) enables control of the heating rate of the specimen and the shape of the current pulse. The switching system consists of two series-connected, fast-acting switches. The second switch is used as a backup in the event the first one fails to open at the end of the heating period. The switches are operated by a series of pulse control units.

The pulsing circuit is a simple RL circuit whose dynamic characteristics, after closing of the switch, may be expressed by

$$E - L\frac{di}{dt} = i\,(R_s + R_c) \qquad (1)$$

where

R_s = resistance of the specimen
R_c = resistance of the circuit with the exception of the specimen

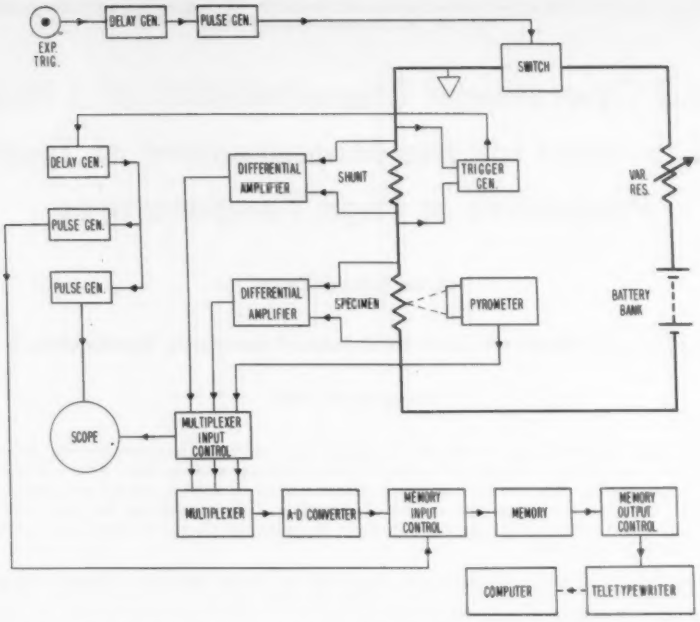

FIGURE 1. *Functional diagram of the complete high-speed measurement system.*

L = self-inductance of the complete circuit
E = battery potential
i = instantaneous current
t = time.

The solution of eq (1) is

$$i = \frac{E}{R}(1 - e^{-Rt/L}) \qquad (2)$$

where R = resistance of the complete circuit ($R = R_s + R_c$). Equation (2), which gives the increase of current as a function of time, is obtained on the assumption that the quantities E, L, and R are constant. In an actual experiment, this assumption is satisfied approximately for E and L, however, R increases with time as the specimen is heated. Therefore, the current versus time relationship is of a distorted exponential form. The circuit's "time constant," which is expressed by the quantity L/R, decreases with increasing R as the specimen is heated.

Energy stored in the magnetic field of an inductor, with no ferromagnetic material in its vicinity, is given by

$$W = \frac{Li^2}{2}. \qquad (3)$$

It may be noted that stored energy depends on the instantaneous value of the current and not on the current history. In a typical high-speed measurement system, in which inductance of the specimen is of the order of 10^{-7} H, and current is the order of 10^3 A, magnetic energy is of the order of 0.1 J. This is small compared to imparted energy, which is the order of 10^3 J. For a complete cycle of operation, consisting of closing the switch and after a finite period opening the switch, the stored energy in the specimen is zero.

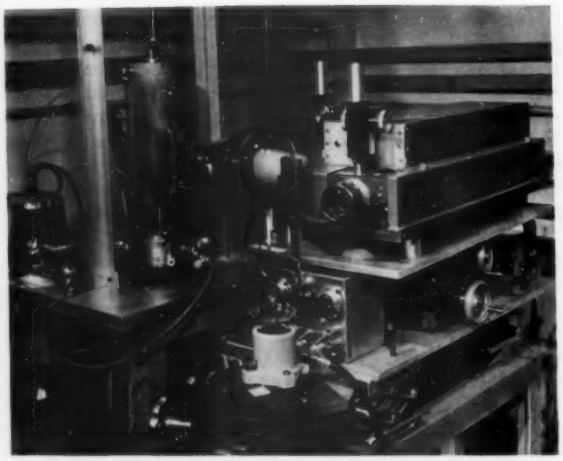

FIGURE 2. *The experiment chamber and the high-speed pyrometer.*

2.2. Measuring and Control Circuits

Voltage signals from both the standard resistance and the specimen are sent to the recording system via differential amplifiers. A potentiometric system is used to calibrate pulse-voltage and pulse-current measuring circuits including the differential amplifiers and the digital

recording system. A Kelvin bridge is used to measure resistance of the specimen at ambient temperature before and after a pulse experiment. A 400 Hz synchronous motor used in the high-speed pyrometer provides the time base for the data acquisition system. Timing of various events, such as closing of the switch and triggering of various electronic equipment, during a pulse experiment is achieved by a series of time-delay units. Triggering of the recording system and opening of the switch at the end of the desired heating period are automatically activated when the specimen temperature reaches preadjusted initial and final values.

2.3. Specimen

The specimen is a tube of the following nominal dimensions: length = 4 in (102 mm), outside diameter = 0.25 in (6.3 mm), wall thickness = 0.02 in (0.5 mm). A small rectangular hole (1 × 0.5 mm) is fabricated in the wall at the middle of the specimen to approximate blackbody conditions. In order to compensate for the cross-sectional nonuniformity created by the hole, a portion from the rest of the specimen is removed by grinding its surface. The criterion is that the cross section of the removed portion is equal to that of the opening created by the hole. From geometrical considerations this may be expressed as

$$ab = \frac{R^2}{2}\left(\frac{\pi\theta}{180} - \sin\theta\right) \tag{4}$$

where

a = width of hole
b = depth of hole (thickness of tubular specimen)
R = outer radius of specimen
θ = angle subtended by the arc corresponding to the ground flat.

After solving the above transcendental equation for the angle θ by iteration, the pertinent dimensions as shown in figure 3 may be obtained from the following relations:

$$L = 2R \sin\frac{\theta}{2} \tag{5}$$

$$C = R \cos\frac{\theta}{2}. \tag{6}$$

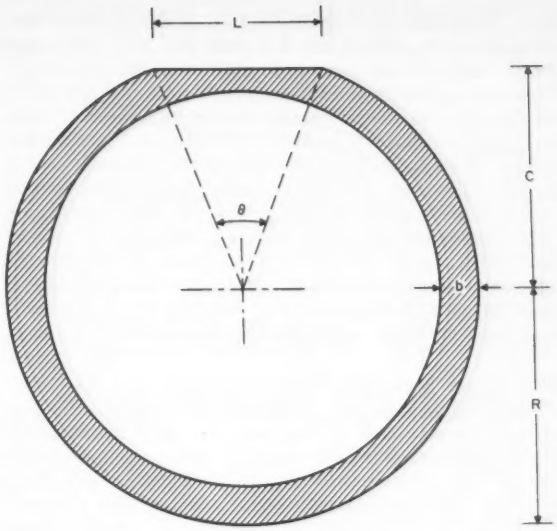

FIGURE 3. *Specimen cross section at the plane of the flat.*

A photograph of the specimen is shown in figure 4.

The rectangular sighting hole in the specimen wall is fabricated 0.8 mm offcenter to improve the blackbody quality. For the specimen geometry given in an earlier section, blackbody quality of the hole is estimated using De Vos' [10] method. Computations are made assuming four different specimen inner surface reflectances and for two specimen lengths, one corresponding to the "effective" length and the other to the actual length. The results (fig. 5) do not show any appreciable dependence of the blackbody quality on length and reflectance.

2.4. Experiment Chamber

The experiment chamber, shown schematically in figure 6, contains the specimen, the clamping electrodes, an expansion joint, potential probes, and other auxiliary components.

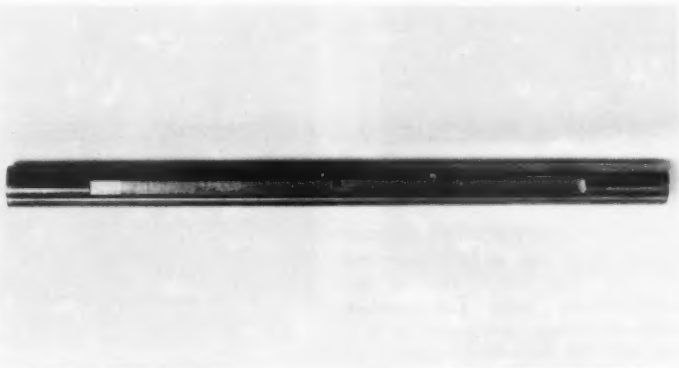

FIGURE 4. *Photograph of the specimen.*

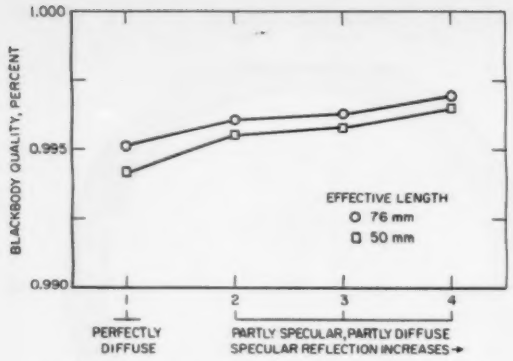

FIGURE 5. *Blackbody quality of a specimen computed for different inner wall reflectances and lengths.*

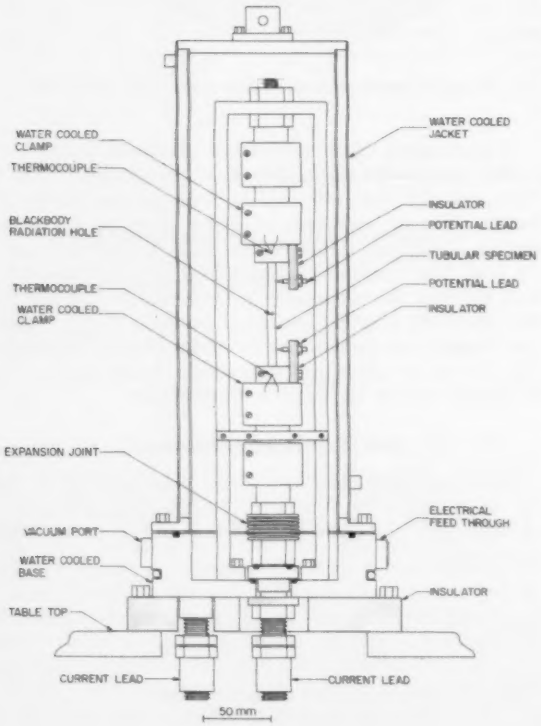

FIGURE 6. *Experiment chamber.*

The specimen is mounted vertically 6 mm offcenter with respect to the axis of the chamber to reduce the effect of internal reflections. The inner wall of the chamber is coated with nonreflecting paint. The chamber wall, as well as the specimen clamps, are water cooled. Thermocouples are connected (electrically insulated) to the two end clamps to measure the specimen temperature before each pulse experiment. An expansion joint allows the expansion of the specimen in the downward direction. The effect of specimen evaporation on the window transmission is minimized by placing a flat partial shield in front of the specimen.

The potential probes are knife-edges made of the specimen material and are placed at a distance approximately 13 mm from the end clamps. The knife-edges define an "effective" portion of the specimen, which should be free of axial temperature gradients for the duration of the experiment. A photograph of the specimen with the clamps and potential probes is shown in figure 7.

The chamber is designed for conducting experiments with the specimen either in vacuum or in a controlled atmosphere.

2.5. High-Speed Pyrometer

Temperature of the specimen is measured with a high-speed photoelectric pyrometer, which permits 1200 evaluations of the specimen temperature per second. The pyrometer alternately passes precisely timed samples of radiance from the specimen and a reference source through an interference filter (wavelength 650 nm, bandwidth 10 nm) to a photomultiplier. During each exposure the photomultiplier output is integrated and is recorded. Successive exposures to the reference source, which is a calibrated, gas-filled tungsten-filament lamp, are taken through a sequence of three different optical attenuators mounted on a rotating disk, resulting in a staircase of reference exposures with approximately 50 percent at-

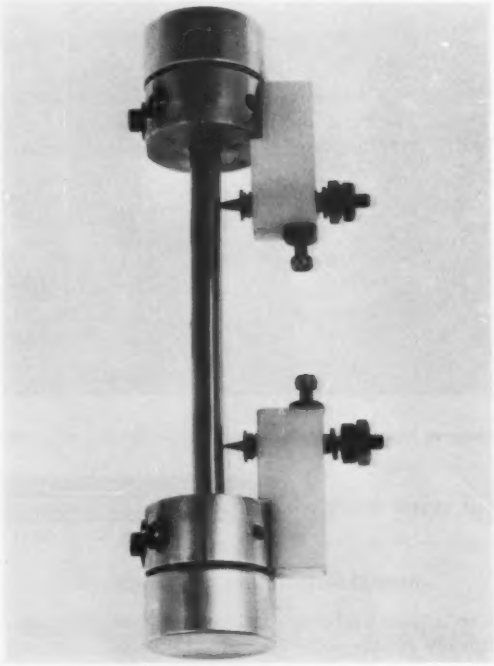

FIGURE 7. *Photograph of the specimen, clamps, and potential probes.*

tenuation for each step. This scheme is used for measurements up to 2500 K, the limit of reliable operation of gas-filled lamps. For measurements at higher temperatures calibrated optical attenuators are placed in the path of the radiation from the specimen. The details regarding the construction and operation of the pyrometer are given in the literature [2].

2.6. High-Speed Digital Data Acquisition System

The high-speed digital data acquisition system consists of a multiplexer, analog-to-digital converter, and a core memory together with control and interfacing equipment. All signals are brought to the multiplexer through differential amplifiers in order to avoid inaccuracies arising from common ground points. The multiplexed signals go to the analog-to-digital converter, which has a full scale reading of $\pm$ 10 V and a full-scale resolution of one part in 8192 ($8192 = 2^{13}$). Digital output from the converter consists of 13 binary bits plus a sign bit. This output is stored in a core memory having a capacity of 2048 words of sixteen bits each. The data acquisition system is capable of recording a set of signals corresponding to temperature, voltage, and current approximately every 0.4 ms. At the end of the pulse experiment, information stored in the memory is retrieved in the form of numeric printing and punched tape using a teletypewriter. Since the laboratory has access to a time-shared computer, it is possible to unload the memory directly to the computer, bypassing the intermediate stage of punching paper tape. A manuscript regarding the constructional and operational details of the high-speed digital data acquisition system is in preparation [3]. Oscilloscopes are used only to monitor the general pattern of the experimental results, and to detect any anomalies.

3. Operational Characteristics

Highest measurement precision is achieved when the experimental quantities are recorded close to the full-scale value of the data acquisition system. However, since quantities vary with time it is not possible to realize this completely. The recording of current can be optimized by adjusting the series resistance, which minimizes this variation. Also, the proper adjustment of the series resistance assures the quasi-linear variation of both voltage and current pulses. Oscilloscope trace photographs of typical voltage and current pulses are shown in figure 8. Radiance from the blackbody hole in the specimen, as well as that of the reference lamp, as seen by the pyrometer as a function of time is shown in figure 9. Dots forming the horizontal lines correspond to the three reference radiances. Temperature of the specimen is computed from the interpolation of its radiance between adjacent reference radiances.

In the computation of properties third-degree polynomial functions for voltage, current, and temperature as functions of time are obtained by least squares approximation of the data. Typical standard deviation of an individual point from the pertinent function is 0.02 percent for voltage, 0.03 percent for current, and 0.5 K for temperature.

Typical results on imparted power to the specimen, the heating rate of the specimen and the ratio of heating to cooling rate (M) for a molybdenum specimen computed from measurements of voltage, current, and temperature are shown in figures 10, 11, and 12, respectively. They represent a total of 40 experiments that were performed at two different speeds, designated as "fast" and "slow," over the temperature range 1900 to 2800 K. The smooth curves shown in the figures are obtained by fitting the computed points to third-degree polynomial functions using least squares approximation. The standard deviation of an individual point from the pertinent function is 0.5 percent for power, 0.7 percent for heating rate, and 0.8 percent for the ratio of heating to cooling rate. The small values of the standard deviations are an indication of the high degree of reproducibility of the current pulses and

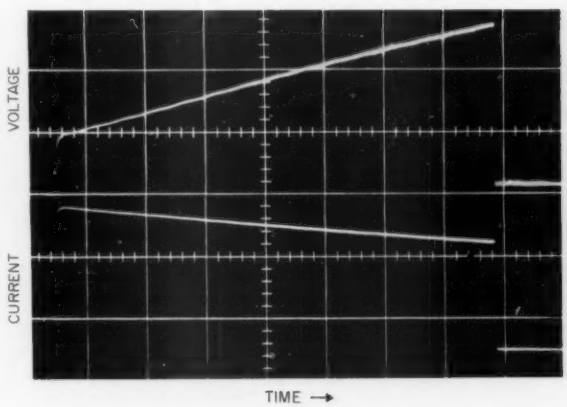

FIGURE 8. *Oscilloscope trace photographs of typical voltage and current pulses.*

Equivalence of each major division is: time = 50 ms, voltage = 2 V, current = 1000 A.

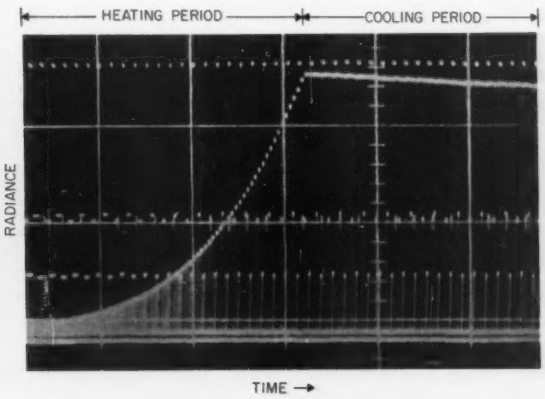

FIGURE 9. *Oscilloscope trace photograph of radiance of rapidly heating specimen.*

Dots forming the long horizontal lines correspond to radiances from the reference source. Equivalence of each major division is: time = 20 ms, radiance = arbitrary unit.

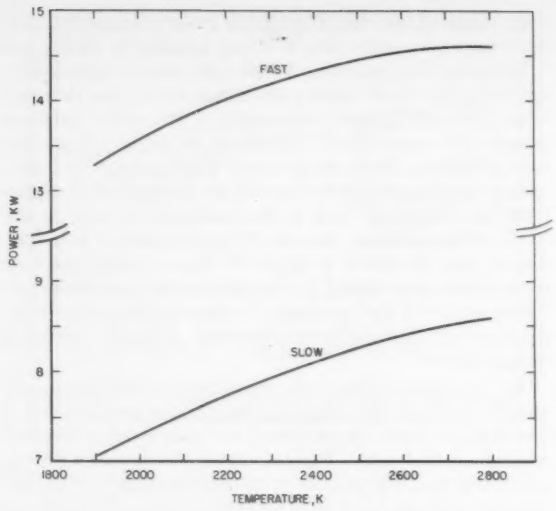

FIGURE 10. *Variation of the power imparted to a molybdenum specimen as a function of temperature.*

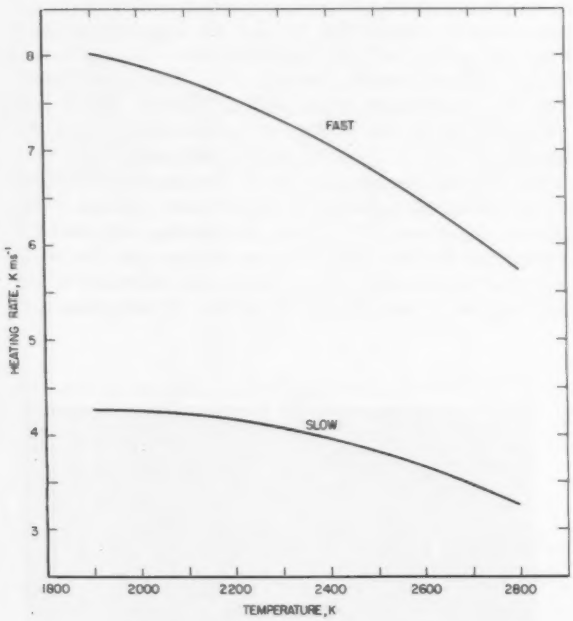

FIGURE 11. *Variation of the heating rate of a molybdenum specimen as a function of temperature.*

the entire measurement system. Reproducibility of the pulses was also determined by performing a total of 12 experiments at 5 min intervals. The maximum difference in the measured current values was less than 0.02 percent.

Although heating rate of the specimen depends, among other factors, on the power supply and the external circuit

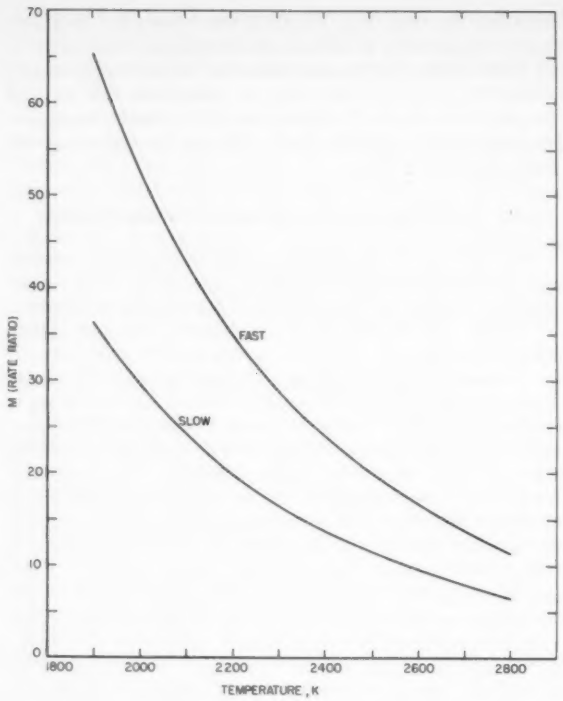

FIGURE 12. *Variation of the quantity M (ratio of heating to cooling rate) of a molybdenum specimen as a function of temperature.*

characteristics, the cooling rate following the opening of the switch depends on the specimen material and its geometry.

Power balance during cooling yields the following expression for the cooling rate of the specimen:

$$\left(\frac{dT}{dt}\right)_c = -BT^4 \tag{7}$$

where (8)

$B = \epsilon\sigma A/c_p n$
$A =$ effective surface area of specimen
$c_p =$ heat capacity
$n =$ weight of effective specimen
$T =$ specimen temperature
$\epsilon =$ hemispherical total emittance
$\sigma =$ Stephan Boltzmann constant (5.6697×10^{-8} W m^{-2} K^{-4})
$(dT/dt)_c =$ cooling rate.

The cooling rate as a function of temperature for a typical molybdenum specimen is shown in figure 13.

In order to obtain an expression for the specimen temperature during cooling as a function of time, eq (7) is rearranged and integrated. The resultant relation is

$$T = \left(\frac{1}{3Bt + \frac{1}{T_m^3}}\right)^{1/3} \tag{9}$$

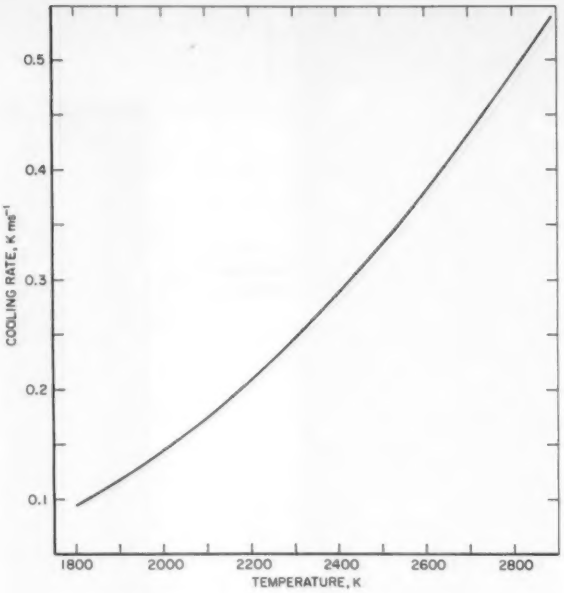

FIGURE 13. *Variation of the cooling rate of a molybdenum specimen as a function of temperature.*

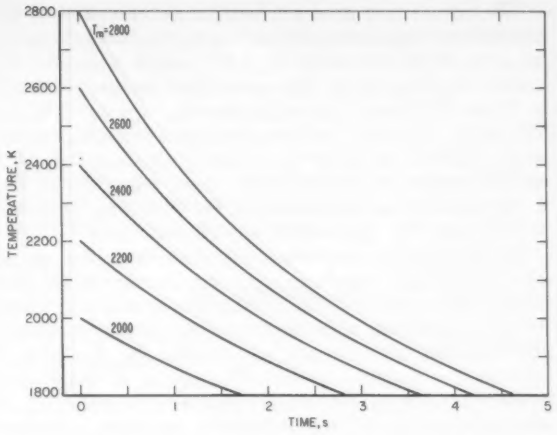

FIGURE 14. *Variation of the temperature of a molybdenum specimen during cooling from various initial temperatures.*

where

$t =$ time

$T_m =$ specimen temperature at the start of cooling (at $t = 0$).

Variation of the temperature of a molybdenum specimen during cooling as a function of time corresponding to different initial temperatures is shown in figure 14.

In preliminary calculations and also in computations related to error analysis it is necessary to know the quantity P_r/P_i, where P_r is power loss from the specimen due to thermal radiation and P_i is power input to the specimen. From power balances for heating and cooling periods the following relation is obtained:

$$\frac{P_r}{P_i} = \frac{1}{1+M} \tag{10}$$

where

$$M = \frac{(dT/dt)_h}{(dT/dt)_c}. \tag{11}$$

It may be seen that for the steady-state case $(dT/dt)_h = 0$, which implies that $M = 0$, and thus $P_r = P_i$.

4. Consideration of Various Phenomena

In this section various physical and electrical phenomena that affect the design and operation of high-speed thermodynamic measurement systems are presented.

4.1. Axial Temperature Distribution

Heat transfer from specimen to clamps causes the establishment of temperature gradients in the specimen. However, since the voltage probes are 12.7 mm away from the clamps, sharp temperature gradients near the clamps do not affect the measurements. The magnitude of the axial temperature gradient in the "effective" specimen is estimated by solving the transient heat conduction equation assuming constant properties and zero radial heat transfer [4]. The series solution is given by the following equation:

$$T = \left(\frac{i^2\rho l^2}{2\lambda A^2}\right)\left[1 - \frac{x^2}{l^2} - \frac{32}{\pi^3}\sum_{n=0}^{\infty}\frac{(-1)^n}{(2n+1)^3}\cos\left[\frac{(2n+1)\pi x}{2l}\right]\exp\left[-\frac{a(2n+1)^2\pi^2 t}{4l^2}\right]\right] \tag{12}$$

where

$i =$ electric current

$\rho =$ electrical resistivity

$A =$ cross-sectional area of specimen

$l =$ half length of "effective" specimen

$x =$ axial distance from midpoint of specimen

$\lambda =$ thermal conductivity

$a =$ thermal diffusivity.

If radial heat transfer is considered, the actual axial temperature gradient will be somewhat smaller than that given by eq (12).

The temperature gradient between the midpoint of the molybdenum specimen and various points along the specimen is calculated using eq (12) (with $n = 30$) for various heating pulses. The normalized results are shown in figure 15. Computations for heating pulses of 350 and 700 ms in duration indicate that specimen temperature at the plane of the potential probes is approximately 99.9 and 99 percent of its midpoint value, respectively. The respective average temperature of the "effective" specimen is 99.99 and 99.9 percent of its midpoint value.

To ascertain the temperature uniformity, a photograph of a molybdenum specimen was taken during the last part of the heating period. This photograph is shown in figure 16 in conjunction with the schematic of the specimen. No variations in exposure are detected for the portion between the potential probes. The region of sharp temperature gradients was studied photomicrographically. A photomicrograph of a molybdenum specimen, obtained after heating it to 2800 K for several times with pulses ranging from 0.4 to 0.8 s is shown in figure 17. Pertinent locations on the photomicrograph are identified with respect to the specimen. Two distinctly different grain structures may be seen. The portions of the specimen that were in the clamp or close to it have retained the original "drawn" pattern, while the portion that was heated to high temperatures shows a considerable grain growth. It is interesting to note a clear boundary between the two patterns, which correspond to a plane (P1) approximately 3 mm from the plane (P2) of the end clamp.

4.2. Radial Temperature Distribution

There is no exact solution for the time-dependent radial temperature distribution in conductors carrying pulse currents with radiative heat transfer from their surfaces. Even the numerical methods become very complicated because of the nonlinearity of the differential equation.

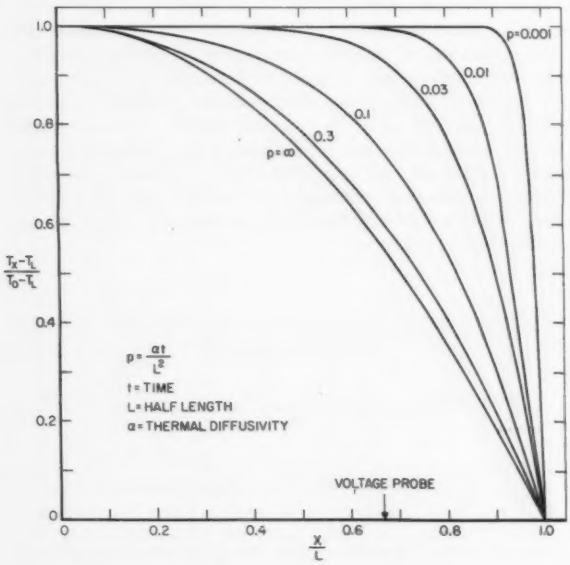

FIGURE 15. *Axial temperature distribution in a resistively self-heated specimen under transient conditions.*

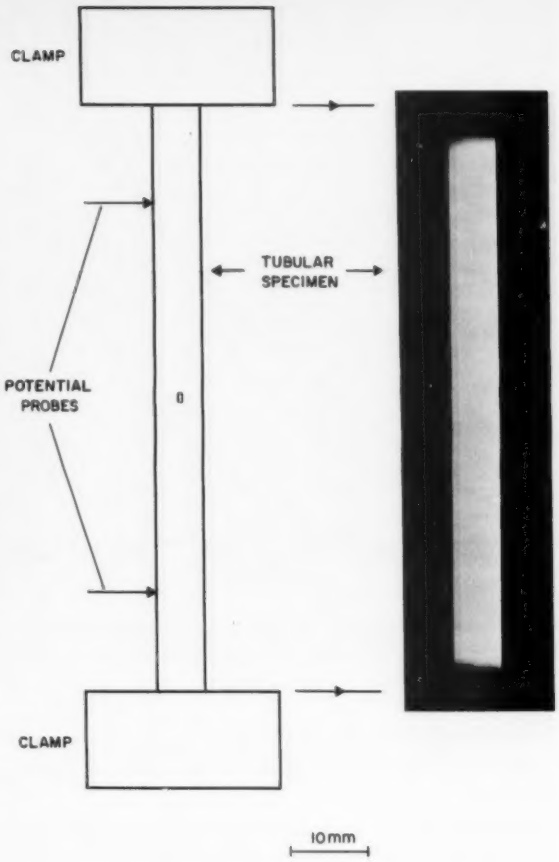

FIGURE 16. *Photograph of a molybdenum specimen during pulse heating to 2500 K.*

In pulse experiments where heat loss from the surface is small compared to power imparted to the specimen, the radial temperature drop (temperature difference between inner and outer surfaces for tubular conductors) may be estimated using the following approximate relation:

$$\Delta T_t = N \, \Delta T_s \tag{13}$$

where

ΔT_t = temperature drop under transient conditions
ΔT_s = temperature drop under steady-state conditions
N = ratio of heat loss from the surface to imparted power under pulse conditions.

The solution of the steady-state radial heat conduction equation, assuming constant properties, for radial temperature drop is:

$$\Delta T_s = \frac{r_o \epsilon \sigma T^4}{2\lambda(r_o^2 - r_i^2)} \left[(R_o^2 - r_i^2) - 2r_i^2 \ln \left(\frac{r_o}{r_i} \right) \right] \tag{14}$$

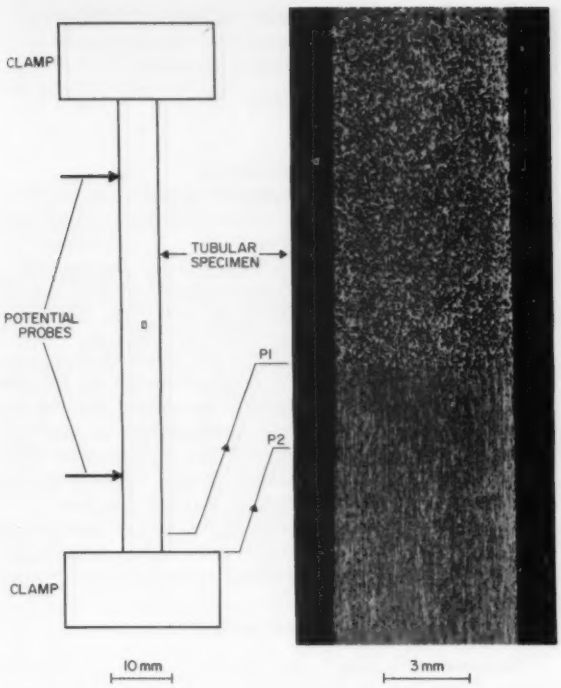

FIGURE 17. *Photomicrograph of a molybdenum specimen after pulse heating to 2800 K for several times.*

where

r_o = outer radius
r_i = inner radius
σ = Stephan-Boltzmann constant
ϵ = hemispherical total emittance
λ = thermal conductivity.

Computations on a molybdenum specimen indicate that radial temperature drop at 2800 K may be approximately 0.3 K for a heating pulse of 0.4 s.

4.3 Evaporation

The rate of evaporation $m(T)$ from metallic surfaces may be expressed by

$$m(T) = A\, e^{-E/T} \tag{15}$$

where, T is temperature in K, A is a constant for a given surface, and E is equal to the energy of evaporation in the units of the Boltzmann constant.

Since in high-speed experiments the heating period is short compared to the cooling period, one may assume that most of the evaporation takes place during cooling of the specimen. Total evaporation during cooling becomes

$$M = \int_{t_1}^{t_2} m(T)\, dt = \int_{t_1}^{t_2} A\, e^{-E/T} dt. \tag{16}$$

After performing a time-to-temperature transformation using eq (9) and integrating eq (16), one obtains

$$M = \frac{A}{BE^3}\left[e^{-\theta_m}\ (2 + 2\theta_m + \theta^2{}_m) - e^{-\theta_f}\ (2 + 2\theta_f + \theta^2{}_f)\right] \tag{17}$$

where

$$\theta_m = \frac{E}{T_m}$$

$$\theta_f = \frac{E}{T_f}$$

B = quantity expressed by eq (8)

and T_m and T_f are initial and final temperatures, respectively.

Computations on a molybdenum specimen indicate that the total weight loss due to evaporation during cooling from 2800 K is approximately 0.003 percent of the specimen weight.

4.4. Inductive Effects

Using equations given in the literature [5], self-inductance of the standard resistance and the specimen were computed to be 0.13 and 0.018 μH, respectively.

The maximum rate of change of the electric current during measurements in a typical high-speed experiment is approximately 3000 A s^{-1}. Then, the possible error (due to self-inductance) in potential measurements across the standard resistance and the specimen is 0.4 mV and 0.054 mV, respectively. Both of these values are smaller than the resolution of the recording system (1 mV).

In order to check the magnitude of mutual-induction between the main circuit and the signal circuits, the following experiment was performed. Potential connections to the standard resistance and the specimen were disconnected and were shorted duplicating, as much as possible, the geometrical configuration that the leads have during an actual high-speed experiment. A heavy pulse current was allowed to flow through the main circuit and the signals were recorded. The output of the recording system did not show any indication of voltage signals (within 1 mV resolution) that could have been generated as the result of mutual inductive coupling between the main circuit and the signal circuits.

4.5. Skin Effect

The skin effect, which is caused by changing currents in a circuit, alters the temperature distribution in the specimen.

For cylindrical conductors the skin effect is a function of the following parameter:

$$x = 2\pi a\sqrt{(2\mu f/10^9\rho)} \tag{18}$$

where

a = radius of the conductor
f = frequency of current
ρ = electrical resistivity of the specimen
μ = permeability of the specimen.

For nonmagnetic materials, $\mu = 1$.

In the case of tubular (thin-wall) specimens, the skin effect is a function of the following parameter:

$$\beta = x\,\tau/a\sqrt{2} \tag{19}$$

where

x = quantity defined by eq (18)
a = outer radius of the specimen
τ = thickness of the specimen.

In general, the contribution of the skin effect in a specimen is expressed in terms of the ratio of its electrical resistance at the frequency in question to that under d-c conditions. Results on the resistance ratio in terms of the parameter x and β are given in tabular form in the literature [5]. Computations indicate that for the specimen geometry and the type of pulses used in the present measurement system, the contribution of the skin effect is less than 0.01 percent.

4.6. Magnetic Forces

Magnetic force (per unit length) on a tubular specimen resulting from current flowing through it is expressed as

$$F = \left(\frac{4i^2}{3b}\right)\left[\frac{1+2m}{(1+m)^2}\right] \tag{20}$$

where i = current, $m = a/b$, b = outside radius, a = inside radius. The corresponding magnetic pressure is given as

$$P_m = \left(\frac{2i^2}{3\pi b^2}\right)\left[\frac{1+2m}{(1+m)^2}\right]. \tag{21}$$

Excessive magnetic forces, which act towards the center of the specimen, tend to collapse it. The collapsing pressure for thin-wall tubes is

$$P_c = \left(\frac{2E}{1-\mu^2}\right)(1-m)^3 \tag{22}$$

where E = modulus of elasticity and μ = Poisson's ratio.

The maximum allowable current is obtained by equating eqs (21) and (22), which yields

$$i = \sqrt{\left(\frac{3\pi b^2 E}{1-\mu^2}\right)\left[\left(\frac{1-m}{1+2m}\right)(1-m^2)^2\right]}. \tag{23}$$

4.7. Thermionic Emission

The contribution of thermionic emission is manifested in the following two forms: (1) energy loss from the specimen as a result of energy carried away by emitted electrons, (2) establishment of undesirable current paths around the specimen.

Dependence of thermionic emission current on temperature is given by

$$I = AT^2 e^{-\frac{e\phi}{kT}} \tag{24}$$

where

A = thermionic emission constant
ϕ = thermionic work function
e = electronic charge
k = the Boltzmann constant.

Considering the values $A = 55 \times 10^4$ A $m^{-2}K^{-2}$ and $\phi = 4.15$ eV [6,7] for molybdenum, thermionic emission current is computed to be approximately 7×10^{-5} A mm^{-2} at 2000 K and 0.15 A mm^{-2} at 2800 K.

It may be noted that computed values are for the case where electrons are continuously removed from the surface, which requires a collector plate at positive potential. In the present system, the chamber wall is electrically neutral and the only electrical potential gradient that exists is that across the specimen, which is less than 10 V. Thus, in the present experiments thermionic emission is most probably space charge limited; its contribution therefore would be much less than above computed values.

4.8. Thermoelectric Effects

Thermoelectric effects play an important role in experiments where temperature gradients exist and where currents flow through interfaces of dissimilar conductors. The Peltier effect between the specimen and clamps and the Thomson effect in the specimen where sharp temperature gradients exist are appreciable. However, they do not affect the measurements in the present experiments since their contribution is negligible in the "effective" specimen. To further reduce the possible contribution of thermoelectric effects, the knife-edges used for potential measurements are made of the same material as that of the specimen. In the high-speed experiments, the record of potential readings at high temperatures after the opening of the main switch shows "zero" for the potential between the probes. This indicates that there are no measurable erroneous signals due to the interaction (in thermoelectric sense) of the probes with the specimen.

4.9. Thermodynamic Equilibrium

Whether a specimen is under thermodynamic equilibrium while measurements are taken during rapid heating and cooling periods may be determined by considering the relaxation times of various rate processes.

Total relaxation time that must be considered for thermodynamic equilibrium calculations may be expressed as

$$\frac{1}{\tau} = \sum_i \frac{1}{\tau_i} \tag{25}$$

where each τ_i represents a different mechanism of relaxation. The various relaxation mechanisms are the results of different scattering processes. The main three relaxation processes are due to electron-phonon, electron-imperfection, and phonon-phonon interactions.

In electrical conductors, electron-phonon interaction is the predominant one in determining the overall relaxation time. For estimative purposes, the relaxation time due to this may be expressed as

$$\tau_{ep} = \frac{\sigma m}{ne^2} \tag{26}$$

where e = electronic charge, m = electronic mass, n = number of electrons per unit volume, and σ = electrical conductivity.

Relaxation time due to electron-phonon interactions for metals at room temperature is of the order of 10^{-12}s. Since relaxation time is directly proportional to electrical conductivity, and since the latter decreases with increasing temperature, it takes a longer time to establish thermal equilibrium at high temperatures. The variation of electrical conductivity in metallic elements between room temperature and their melting points is within a factor of 100; therefore, it can be seen that thermal equilibrium in metals takes place in times of the order of 10^{-10}s.

Information concerning relaxation times for vacancy equilibrium is not readily obtainable; but since the mechanism is related to that of diffusion, the relaxation time is an exponential function of temperature. The magnitude of vacancy relaxation time as observed in quenching experiments at lower temperatures and extrapolated to higher temperatures may be of the order of a millisecond for refractory metals above 2000 K.

5. Experimental Checks

The following sections outline the procedures and the results of selected experiments, which were performed to assess the accuracy of measured quantities under various operational conditions.

5.1. Resistance Comparison

The objective was to determine the value of a test resistance by measuring the current flowing through it and the voltage drop across its terminals under transient conditions and comparing this measurement with its resistance under steady-state conditions as determined by the potentiometric method.

In order to eliminate any doubt of the possibility of the effect of induced voltages on electrical signals, separate experiments were conducted using two geometrically different test resistances. One of the resistances (0.001 Ω) was a flat manganian strip identical to that used for pulse current measurements. The other was an Inconel tube with a nominal resistance of 0.003 Ω. The results on both test resistances do not indicate any dependence attributable to geometry. In these experiments pulse currents in the range 800 to 2100 A were used. The results do not indicate any current dependence. The results on resistance comparison and standard deviation of the measurements are shown in figures 18 and 19, respectively. It may be seen that, in general, resistance measurements by pulse and steady-state techniques are in agreement within 0.03 percent.

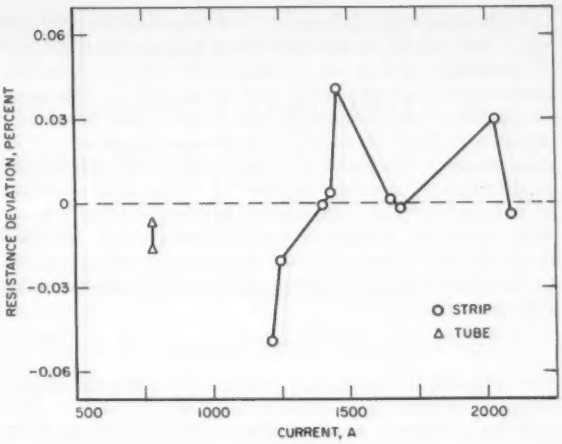

FIGURE 18. *Resistance difference of a test resistor measured under steady-state and pulse conditions.*

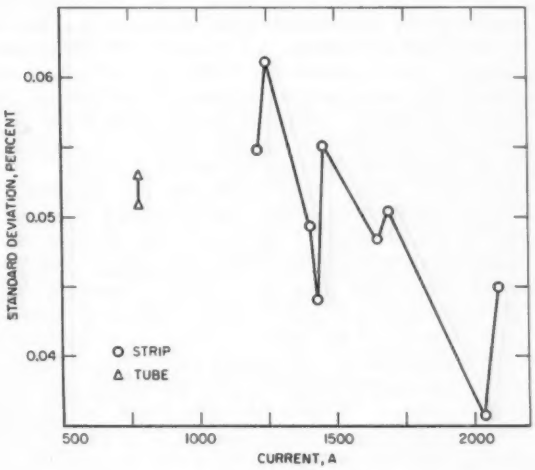

FIGURE 19. *Standard deviation of resistance measurements under pulse conditions.*

5.2. Effect of Different Heating Rates

Several phenomena depend upon the heating rate of the specimen. Heating rate is related, among other factors, to the electric current that flows through the specimen. In high-speed experiments, the rate of change of the current creates a number of problems such as induced voltages in measuring circuits, varying forces in the circuit components, etc. In addition to these extrinsic effects, there is the consideration of the specimen's attaining thermodynamic equilibrium at the time of measurements. To demonstrate partially that the above are negligible, in the present system under present operating conditions, the following experiments were conducted.

A tungsten strip (3.2 mm wide, 0.25 mm thick, 100 mm long) was placed in the high-speed measurement system. Two voltage probes were welded 20 mm apart at the center portion of the strip. Two pulse experiments were conducted in which the strip was heated from room temperature to 2200 K (surface brightness temperature) in approximately 2000 and 250 ms, respectively. During the experiments, quantities required for the determination of voltage, current, and surface brightness temperatures were recorded. Comparison of the resistances obtained from the two (slow and fast) experiments corresponding to the same brightness temperature yields the following average value:

$$R(\text{slow heating}) \,/\, R(\text{fast heating}) = 1.0003.$$

The resultant 0.03 percent deviation is within the uncertainty of resistance measurements. Thus, it may be concluded that approximately eightfold variation in the heating rate does not introduce any significant differences in the measured properties.

5.3. Melting Point of Platinum

As a partial check on the accuracy of temperature measurements, experiments were conducted to obtain the melting point of platinum. A high-purity (99.999 percent) platinum wire (diameter = 0.001 in, 0.025 mm) was wound (half turn) around a thin-wall molybdenum tube (similar to regular specimens) at the plane of the blackbody sighting hole. Two pulleys supported the wire. A 0.5 g weight was attached to each end of the wire to assure good contact between the wire and the tube. The ends of the platinum wire were connected to a special circuit, which indicated the time of the opening of the circuit resulting from the melting of platinum. The break in the circuit took place at a point of contact with the tube as the latter was pulse heated. Duration of an experiment (heating of the specimen from room temperature to its melting point) was approximately 0.8 s. Temperature of the tube corresponding to the time of the break in the platinum wire gave the melting point of platinum.

The results of three experiments gave an average value of 2044.2 K for the melting point of platinum on the 1968 International Practical Temperature Scale [8] with an average deviation from the mean of the three amounting to 1.1 K. This compares favorably with the accepted value of 2045 K [8]. Details regarding the experiments, interpretation of results, and errors are given in another publication [9].

6. Conclusions

Estimates indicate that the imprecision and inaccuracy of measured quantities in high-speed experiments using the present system are: 0.02 and 0.05 percent for voltage, 0.03 and 0.06 percent for current, and 0.5 K and 4 K for temperature at 2000 K.

The high-speed system described in this paper has been used successfully to measure heat capacity, electrical resistivity, hemispherical total and normal spectral emittances of molybdenum [1] and tantalum [11] from 1900 to near their respective melting points. The system was also used to obtain the melting point of molybdenum [12] and the variation of normal spectral emittance of tantalum during melting [13]. The results indicate that at 2000 K accuracy of measured properties by the system described here is about the same as that obtained by conventional methods. At temperatures above 2500 K, it surpasses any other method now known. Estimates of the imprecision and inaccuracy of measured properties are given in the above cited references.

7. References

[1] Cezairliyan, A., Morse, M. S., Berman, H. A., and Beckett, C. W., J. Res. Nat. Bur. Stand. (U.S.), **74A** (Phys. and Chem.), 65 (1970).
[2] Foley, G. M., Rev. Sci. Instr. **41**, 827 (1970).
[3] Morse, M. S., and Cezairliyan, A., in preparation.
[4] Carslaw, H. S., and Jaeger, J. C., Conduction of Heat in Solids (Oxford Univ. Press, Oxford, 1959).
[5] Grover, F. W., Inductance Calculations (Van Nostrand, New York, 1946).
[6] DuBridge, L. A., and Roehr, W. W., Phys. Rev. **42**, 52 (1932).
[7] Stanley, J. K., Electrical and Magnetic Properties of Metals, (Metals Park, Ohio, 1963).
[8] International Practical Temperature Scale of 1968, Metrologia **5**, 35 (1969).
[9] Cezairliyan, A., J. Res. Nat. Bur. Stand. (U.S.), **74C** (Eng. & Instr.), 87 (1970).
[10] De Vos, J. C., Physica **20**, 669 (1954).
[11] Cezairliyan, A., McClure, J. L., and Beckett, C. W., J. Res. Nat. Bur. Stand. (U.S.), **75A** (Phys. and Chem.), 1 (1971).
[12] Cezairliyan, A., Morse, M. S., and Beckett, C. W., Rev. Int. Htes. Tempér., to be published.
[13] Cezairliyan, A., High Temp.–High Pres., to be published.

(Paper 75C1-308)

JOURNAL OF RESEARCH of the National Bureau of Standards — C. Engineering and Instrumentation
Vol. 75C, No. 1, January-March 1971

A New Method of Determining Residual Thiosulfate in Processed Photographic Film

C. I. Pope[1]

Institute for Basic Standards, National Bureau of Standards, Washington, D.C. 20234

(October 7, 1970)

Chromatographic paper, saturated with ammonia, is used to extract the residual thiosulfate from the gelatin layer of processed film. The paper is treated in a silver nitrate solution and fixed in an ammonia-sodium chloride solution. Thiosulfate, if present, forms silver sulfide and the thiosulfate is determined by measuring the transmission density of the paper darkened by silver sulfide. The paper extraction method is simple, rapid, requires only a densitometer as special equipment, and is very sensitive especially when the transmission density is measured for two layers of the paper. No filters are required. The test readily reveals the uneven distribution of residual thiosulfate on the film. By selective removal of thiosulfate from the image silver by ammonia and potassium bromide solutions, it was shown that a small amount of thiosulfate was absorbed on the image silver immediately after processing.

Key words: Archival film; hypo; microfilm; permanent record film.

1. Introduction

Residual thiosulfate is readily determined in processed photographic papers by measuring the transmission density of the silver sulfide formed in situ by the reaction of the silver ion with the residual thiosulfate [1].[2] However, the transmission density of the silver sulfide in the gelatin layer of film is much lower for corresponding thiosulfate concentrations, making it difficult to use the density of the silver sulfide as a measure of residual thiosulfate concentration in film [2, 3].

It has been found that chromatographic paper wetted with an ammonia solution will absorb the residual thiosulfate from the gelatin layer of the film. Such paper was treated in silver nitrate solution forming silver sulfide in situ and the excess silver ion was removed by treating the paper in an ammonia solution. The transmission density of the silver sulfide was large enough to determine thiosulfate concentrations as low as 0.15 $\mu g/cm^2$. The film was not destroyed in the test.

2. Experimental Procedure

Whatman No. 3 MM chromatographic paper[3] was selected for this study. The paper, which was 0.03 cm thick, withstood the treatments in the solutions and drying without distortion. A 2-percent ammonia solution was found to be very efficient in extracting the residual thiosulfate from the gelatin. The ammonia solution should either be used in a hood or covered during the test.

A strip of film 10 to 12 cm long and 1.6 to 2 cm wide was taped, emulsion side up, at the two ends to blotter paper resting on a level glass plate. The chromatographic paper, cut the width of the film sample and of a length to fit between the tape strips at the ends of the film, was soaked 3 min in about 100 ml of a 2-percent ammonia solution. Then the paper was grasped with tweezers at one end, drained briefly, and the other end brought in contact with the film, allowing the paper sample to roll down onto the film to prevent air bells. The paper was rubbed once gently with the back of the tweezers. The blotter paper absorbed any excess ammonia solution at the edges of the film. After 5 min the paper was removed and bathed 4 min in 100 ml of a solution containing 10 g of silver nitrate and 30 ml of glacial acetic acid per liter. A control strip was made by treating a sample of the chromatographic paper in the 2-percent ammonia solution 3 min before the test sample was removed from the film and the two paper samples were processed together. Next, the papers were placed in crystallizing dishes and treated 3 min in each of two solutions containing about 100 ml of 5-percent ammonia solution and 1 g of sodium chloride per liter, to remove the excess silver ion. The solutions were stirred during treatments. Then the papers were removed from the ammonia solution with tweezers and placed on blotting paper but not blotted. The paper was turned over three or four times during a 10-min period and allowed to dry in the room atmosphere. The transmission density was measured for the control and test papers. The effective optical density of the silver sulfide was determined by subtracting the density of the control paper from that of the test paper. The corresponding residual thiosulfate concentration of the film was determined from a calibration curve.

It was found that 3 to 5 percent ammonia solutions containing 1 to 5 g of sodium chloride per liter may be

[1] Retired. Present address: 2911 Dawson Ave., Silver Spring, Md. 20902.
[2] Figures in brackets indicate the literature references at the end of this paper.
[3] Commercial materials and equipment are identified in this paper in order to specify the experimental procedure adequately. Such identification does not imply recommendation nor endorsement by the National Bureau of Standards.

used to fix the paper samples. The sodium chloride stabilized any trace of ammonia-silver complex left in the paper.

The chromatographic paper was sufficiently uniform in density that only an occasional control run would be necessary in routine testing.

A pink dye was absorbed by the paper from some films during the extraction operation. The dye was bleached out by exposing the dried paper sample for 1 h to a 20-W, 20-in daylight fluorescent lamp at a distance of 1 in.

The transmission density measurements reported in this paper were made with an Ansco-Sweet Densitometer, Model 11. In this paper, the concentration of residual thiosulfate is given as micrograms per square centimeter. In most of the literature, the concentration is reported in milligrams or micrograms per square inch. One microgram per square inch is equivalent to 0.155 $\mu g/cm^2$.

Table 1. *Residual thiosulfate found in a second ammonia extraction of processed film.*

	Approximate micrograms of residual thiosulfate per centimeter originally found in the film after processing			
	1.5	3	8	16
	Micrograms of thiosulfate per square centimeter found in the second ammonia extraction			
Six microfilms Two x-ray films One motion picture film One aerial film One print film	0	0	0 to 0.15	0 to 0.7
One motion picture film One professional film	0 to 0.07	0.15	0.7	1.5

3. Evaluation of the Paper Extraction Method

In evaluating the paper extraction method for the determination of residual thiosulfate in processed film, six microfilms, two motion picture films, two x-ray films, one aerial film, one print film, and one professional film were tested. The films were made by five manufacturers. The unexposed film samples were treated 4 min in a solution containing 90 g sodium sulfite, 52 g sodium carbonate monohydrate, and 5 g of potassium bromide per liter. This solution is typical of developers but without a developing agent. The developing agent was eliminated to avoid any reduction of silver in the gelatin layer. Then the film samples were fixed in an acid hardening bath and washed in chlorine-free tap water as described in a previous publication [4]. The excess water was removed from the film samples with wiping tissue. The washing time controlled the residual thiosulfate concentration in the films.

For comparison, the residual thiosulfate concentrations in the processed film samples were determined by the paper extraction method and the modified Crabtree-Ross method [5]. Samples for the two methods were taken adjacent to each other on the film. The thiosulfate concentrations ranged from 0.15 to 16 $\mu g/cm^3$ of sodium thiosulfate. The two methods were in general agreement. However, the paper extraction method revealed the fact that the residual thiosulfate is not always evenly distributed in the gelatin layer, there being higher and lower values for residual thiosulfate concentration than the average value found by liquid extraction using the modified Crabtree-Ross method.

Tests were made to determine if any thiosulfate remained in the gelatin layer of the film after the first extraction. A second extraction was made with the paper extraction method immediately after the first extraction. The effective optical density of the silver sulfide was determined for two layers of the test paper and the residual thiosulfate concentration was read from the calibration curve shown in the next section. The results are tabulated in table 1. For 11 films, no thiosulfate remained where there had been a low original thiosulfate concentration and only a negligible amount remained where it had been high. Two films with a thick layer of gelatin retained about 5 percent in the low thiosulfate concentrations and 10 percent in the high. A third extraction detected no thiosulfate. The presence of thiosulfate in the gelatin layer after the first, second, or third extractions was also determined by processing the film, after extraction, by the procedure used by Crabtree, Eaton, and Muehler [1] for determining the thiosulfate in photographic papers. Using this method, one can detect 0.08 $\mu g/cm^2$ of thiosulfate as silver sulfide by measuring the density of two layers of film with a Kodak 18A filter. No thiosulfate was detected in the film with low original concentrations and the amount found where concentrations had been higher correlated with that found in the second paper extraction.

The effect of a high concentration of silver in the fixing bath on the paper extraction of thiosulfate was investigated. Film was fixed in a fixing bath containing 4 g of silver per liter, the silver being added as silver bromide. The silver thiosulfate complex left in the film did not affect the extraction of the thiosulfate.

Tests were made to determine if any residual developing agents remained in processed film as these would form reduced silver in the test paper in the silver nitrate solution. Unexposed samples of microfilm, motion picture film, and x-ray film were normally processed and washed free of thiosulfate. The samples were treated in a bath containing 10 g sodium sulfite, 5 g boric acid, 10 g potassium aluminum sulfate, 10 ml glacial acetic acid, 0.05 g metol, and 1 g hydroquinone per liter and washed 30 s in running tap water. The above bath contained chemical compounds found in a used fixing bath in addition to thiosulfate. When the paper extraction test was applied, there was no reduction of silver in the paper. The developing agents were rapidly removed from the films and therefore would not interfere with the paper extraction method.

Paper extraction does not remove all of the thiosulfate from areas on the film containing a large amount of image silver. One microfilm was flashed and developed to a density of 4.8 and washed 30 min. The paper extraction method detected no thiosulfate in either the image-free area or the image area, whereas the modified Crabtree-Ross method gave negative results for the clear area but 1.2 $\mu g/cm^2$ of thiosulfate in the image area. A sample of the high-density area was treated 15 min in a

5-percent potassium bromide solution, washed, and bleached with an untreated sample in a dichromate solution. The effective densities of the remaining silver sulfide measured for two layers with a Kodak 94 filter were 0.78 for the untreated sample and 0.72 for the one treated in potassium bromide solution. The silver sulfide density of 0.72 corresponds to the silver sulfide formed in the image during fixation and the difference of 0.06 density corresponds to thiosulfate absorbed on the image silver. These tests, made immediately after the film was washed, showed the absorbed thiosulfate was not removed by ammonia but was by potassium bromide. The amount of thiosulfate absorbed is very small. The above results indicate that the paper extraction method should be applied to an image-free area of the film or one not having more than 0.1 density of silver. The absorbed thiosulfate is unstable and reacts rapidly at high relative humidity with the silver in the image to form silver sulfide.

4. Calibration Curve

A calibration curve was prepared using the Whatman 3 MM chromatographic paper. A sample of the paper, cut 10 by 20 cm, was treated 5 min, with agitation, in two liters of a sodium thiosulfate solution in a photographic tray. Solutions containing 0.050, 0.065, 0.075, 0.10, 0.15, 0.2, 0.3, 0.4, and 0.8 g of $Na_2S_2O_3 \cdot 5H_2O$ per liter were used. The paper sample was removed from the thiosulfate solution and blotted immediately between clean photographic blotters with pressure, blotted a second time between clean blotters, and allowed to dry flat on clean blotters, turning the sample over every 3 or 4 min for the first 30 min to obtain a more even distribution of the sodium thiosulfate in the paper.

The dried paper sample was cut into two parts, 5 by 10 cm, and one part was treated, together with a control sample of the chromatographic paper containing no thiosulfate, 4 min in a 400-ml solution containing 10 g of silver nitrate and 30 ml of glacial acetic acid; fixed 3 min in each of two 400-ml solutions containing 3-percent ammonia and 5 g of sodium chloride per liter; and dried flat on blotter paper. The transmission densities of the paper sample containing silver sulfide and the paper control were measured. The density of the silver sulfide was obtained by subtracting the density of the control from that of the paper sample containing the silver sulfide. A single layer of the chromatographic paper had a density of 1.19 $\pm$ 0.01, two layers had 1.47 $\pm$ 0.01 with an occasional deviation of 0.02. Treatment in the processing solutions did not change the density.

Four 2½-cm squares were cut from the second part of the sample mentioned above, adjacent to the first part and about 5 cm from the ends, and the residual thiosulfate was determined by the modified Crabtree-Ross test method [5]. In this test method 5 ml of a 5-percent solution of mercuric chloride was added, with rapid stirring, to a vial containing 5 ml of a 5-percent solution of potassium bromide and 100 μg of gelatin. The thiosulfate reacted with the mercuric chloride to form a turbidity which was determined with a nephelometer. The thiosulfate concentration was determined from a calibration curve. Four squares were used in the test for sodium thiosulfate concentrations up to 2.5, 2 squares for 5, and 1 square for 10 $\mu g/cm^2$. The 5-percent solutions of potassium bromide and mercuric chloride were added from burets. The samples of paper were treated 5 min in a 50-ml beaker with 5 ml of the potassium bromide solution, while agitating with a thin glass rod, and were transferred to a 10-ml graduate. The samples were treated a second time with 5 ml of the potassium bromide solution to remove any trace of thiosulfate remaining in the paper and the solution transferred to the same graduate. After the paper samples were removed from the beaker the volume of solution in the 10-ml graduate was made up to 10 ml with the 5-percent potassium bromide solution to replace the solution absorbed by the paper and the 10-ml solution was transferred to the beaker in which the extraction was made. Four drops of a 0.1 percent gelatin solution and then 10 ml of the mercuric chloride solution were added to the beaker with rapid stirring. Ten ml of the solution in the beaker were transferred to a vial and allowed to stand 30 min and the turbidity was determined with a Coleman No. 9 nephelometer. The vial was handled gently to avoid stirring up a few fibers of the paper that had settled to the bottom. The concentration of the sodium thiosulfate was determined from a calibrated curve for known concentrations of sodium thiosulfate in the potassium bromide–mercuric chloride solution. This value was

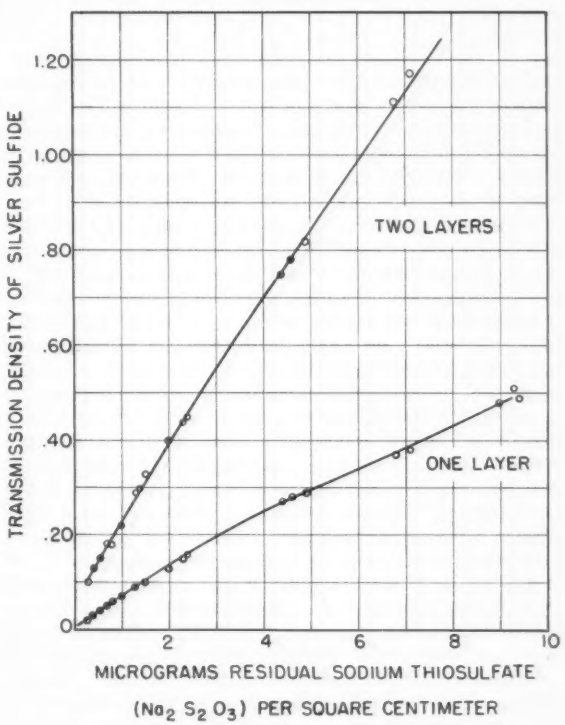

FIGURE 1. *Silver sulfide calibration curve showing the transmission density of silver sulfide formed in the Whatman No. 3 MM chromatographic paper by the reaction of sodium thiosulfate with silver nitrate.*

multiplied by 2 and divided by the area in square centimeters tested to obtain the concentration of the sodium thiosulfate in micrograms per square centimeter in the paper. The transmission densities of the silver sulfide for one layer and two layers of the paper were plotted against the corresponding sodium thiosulfate concentrations to obtain the calibration curves shown in figure 1 for the Whatman No. 3 MM chromatographic paper only. Calibration curves must be prepared for each type of paper used in extracting the thiosulfate from the gelatin layer of film. The calibration procedure is very simple if a nephelometer is available for measuring turbidity.

5. Summary

The new paper extraction method is simple, rapid, and requires no light filters. Only a densitometer is needed as special equipment. The method is nondestructive as tests may be made on roll or sheet film which, after drying, may be returned to storage. The residual thiosulfate may be extracted in the field and the paper may be forwarded for final processing to a laboratory which has a calibration curve for the type of paper used in the extraction. The test should be made in an image-free area of the film or one not having a density greater than 0.1. The test is quite sensitive, especially if the silver sulfide of two layers of the paper is measured. The test demonstrated that the residual thiosulfate is not always evenly distributed in the gelatin layer. Residual sodium thiosulfate as low as 0.15 $\mu g/cm^2$ can be detected if the density of the silver sulfide for two layers of paper is measured. This concentration is visually discernible for one layer viewed with a control. For this reason the paper extraction test is an excellent qualitative test for the detection of residual thiosulfate in processed film. The test method will determine trithionate and tetrathionate as thiosulfate. This is advantageous since these compounds also react with the image silver to form silver sulfide.

6. References

[1] Crabtree, J. I., Eaton, G. T., and Muehler, L. E., A review of hypo testing methods, J. Soc. Motion Picture Engrs. **42,** 34–57 (1944).

[2] Mattey, D. A., and Henn, R. W., Determination of thiosulfate and thionates in film with silver nitrate, Photo. Science and Engr. **10,** No. 4, 202–208 (1966).

[3] Pope, C. I., A simplified method for determining residual thiosulfate in processed microfilm, Photo. Science and Engr. **13,** No. 5, 278–279 (1969).

[4] Pope, C. I., Blemish formation in processed microfilm, J. Res. Nat. Bur. Stand. (U.S.), **72A** (Phys. and Chem.), No. 3, 251–259 (1968).

[5] Pope, C. I., Determination of residual thiosulfate in processed film, J. Res. Nat. Bur. Stand. (U.S.), **67C** (Eng. and Instr.), No. 3, 237–245 (1963).

(Paper 75C1-309)

JOURNAL OF RESEARCH of the National Bureau of Standards — C. Engineering and Instrumentation
Vol. 75C, No. 1, January-March 1971

Scanning Densitometer for Continuous Recording of Spectral Transmission Density at Low Spatial Contrast*

W. L. McLaughlin, M. Rosenstein,[1] E. K. Hussman, and J. J. Lantz, Jr.

Center for Radiation Research, National Bureau of Standards, Washington, D.C. 20234

(October 6, 1970)

A simple photoelectric transmission densitometer can be converted in the laboratory into an instrument for measuring spatial variations in spectral density of small areas of thin, nonturbid films. This is accomplished by adding relatively inexpensive components that are readily available and easily assembled. The basic instrument can be one of a number of commercial densitometers, consisting of stabilized electronics, an adjustable light source, and a photosensitive probe which has a wide range and measures spectral transmission density. For continuous scanning of relatively small sample areas, the followng additions are needed: (1) narrow-bandpass filters; (2) interchangeable field illuminating slits; (3) a short-focal-length illuminating-condenser lens which compromises between a relatively large numerical aperture and a reasonable depth of focus; (4) a motor-driven stage with adjustable speeds; (5) a light diffuser and light guide; and (6) a continuous, relatively fast-response data-recording system (such as a fast-response strip-chart recorder). This instrument has been assembled and tested especially for measuring spatial variations of spectral density produced in irradiated photochromic films; and also for calibrating a train of irradiated film samples, in terms of transmission density at a given wavelength as a function of irradiance, radiation absorbed dose, or photochemical reactivity.

Key words: Densitometer; microdensitometer; radiochromic dye films; spectral transmission density.

1. Introduction

With the increasing use of thin gel, polymer, and photochromic films in chromatography and ionizing radiation applications, such as obtaining beam profiles, registering chemical-reactivity, depth-dose, or penetration distributions, monitoring high-intensity radiation fields, and monitoring beam uniformity in radiation processing of industrial products, there is a need for continuous optical-density scanning at given wavelengths across relatively small areas of these films. A commercial microdensitometer is suitable for very high resolution work, such as determining granularity of images, modulation transfer functions of imaging systems, or acutance of photographic images [1–4],[2] but is expensive and difficult to use for large volumes of routine work. The aim of the present work is to show how a simple, inexpensive photometric apparatus can be assembled and used to measure spectral transmission densities [5] of relatively nonscattering thin-film images with moderate spatial resolution.

Most microdensitometers have two objective lens-slit systems: an illuminating and a scanning system. The illuminating system is situated between the light source and the sample. The scanning objective lens focuses a certain area of the narrow sample image on a reading slit in front of the photocathode. These components are arranged so as to reduce errors due to flare from the sample, diffraction from the apertures caused by partial coherence in the illumination, and film granularity [6, 7]. Great pains have to be taken to improve performance by adjusting the components so as to minimize angular and focal misalinements and non-uniform photocathode sensitivities [8]. The slit images falling on the photosensor are narrow in order to reduce adjacency effects [9].

The instrument described here is not a conventional microdensitometer, in that a scanning lens-aperture system has not been used; rather the slit-image of narrow-band light focused on a small area of the relatively nonscattering photochromic film is transmitted according to the spectral density of that area, and then is diffused and channeled efficiently to the photomultiplier. A schematic chart displaying the main components is shown in figure 1. Relatively turbid samples, such as developed silver halide emulsions, would cause excessive light-scattering in such an arrangement, so that a scanning objective lens would be needed to focus the small portion of sample image through a scanning slit on the photocathode. The instrument diagrammed in figure 1 should be restricted to use with relatively nonturbid, nonreticulated plastic films, photochromic layers, and chromatographic gels. The light passes through a multiple filter system to a slit whose image is reduced and focused on the sample. Essentially all the light transmitted by the sample is first diffused and then collected by the photomultiplier. The photomultiplier current (proportional to spectral density) can be read relative to the lateral film position by an electrometer, an electrometer connected to a strip-chart

* This work was partly supported by the Division of Isotopes Development, U.S. AEC.

[1] Bureau of Radiological Health, Environmental Health Service, Rockville, Md. and Graduate Student, Laboratory for Radiation and Polymer Science, University of Maryland, College Park, Md. Guest worker at the National Bureau of Standards.

[2] Figures in brackets indicate the literature references at the end of this paper.

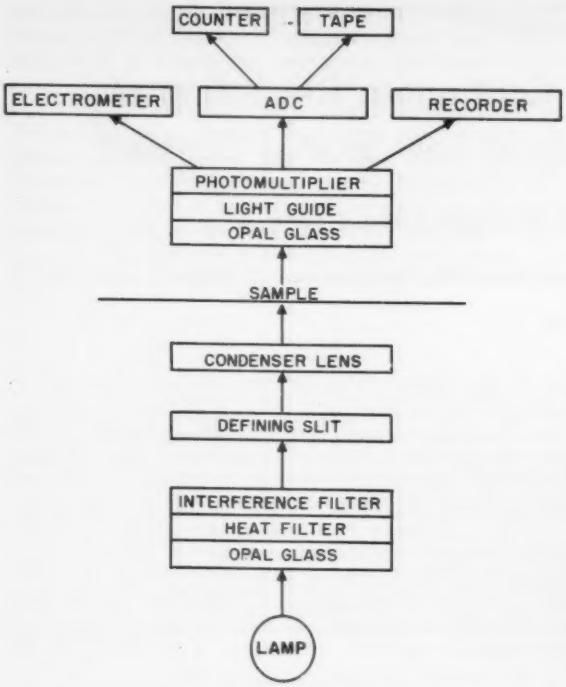

FIGURE 1. *Schematic chart of main components of densitometer scanning slit and light collection system.*

recorder, or, in an expanded system, an analog-to-digital converter may be used and the resulting pulses fed into a tape-recorder readout. The light-collecting system is similar to microscope systems used in recording histophotometers for integral density scanning of small biological specimens or for microscopic spectrophotometry, in that essentially all transmitted light from a small sample area is collected and measured [10–12]. A removable thin focusing screen can be placed into the plane of the sample for sharp focusing of the slit image while viewing with an 8-power lens.

The main limitation of the nonfocusing diffuse-light gathering system is that only moderate spatial resolution is possible, even with relatively nonscattering media. The main advantages are that problems of diffraction, critical slit alinement, focal adjustment, and nonuniformity of photocathode sensitivity are less severe than for a microdensitometer. Even though granularity noise in turbid materials, such as developed silver halide emulsions, would be averaged somewhat by the present system, the scattering of light by the same would result in flare and limited definition of the measured image.

2. Instrumental Details

The basic instrument, adapted for the purposes described here, can be one of a number of photoelectric densitometers with a wide response range, adjustable lamp brightness, and stabilized electronics.[3] The adaptation for continuous recording of spectral densities of small areas can be accomplished at relatively low cost without disturbing the primary function or operation of the original instrument. If necessary, the instrument can easily be returned to its original configuration to measure macroscopic diffuse optical densities of large specimens.

Figures 2 and 3 are photographs of details of the added components. Figure 2 shows the drive, gear, and counter combination which is powered by a variable d-c power supply. Inexpensive permanent-magnet reversible-type motors with integral reduction gearing drive the worm-gear screwjack. Limit switches are mounted to the body of the jack to prevent over-travel. At full voltage, the film

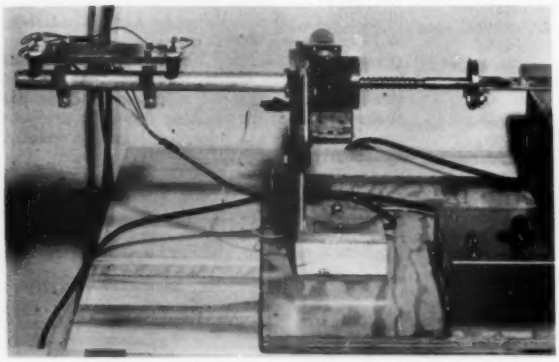

FIGURE 2. *Close-up photograph of drive, gear and counter assembly and d-c power supply.*

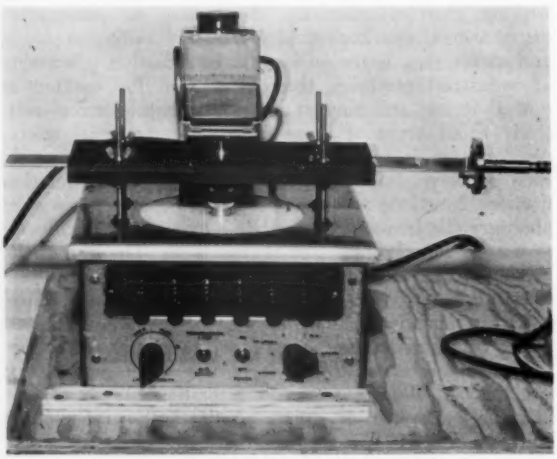

FIGURE 3. *Close-up photograph of scanning densitometer as arranged during operation.*

[3] For example, the apparatus used in this application was a Welsh Densichron Model 400 Photometer and Densichron 3853D Transmission light source. (This equipment is identified here in order to specify the instrumental details adequately. Such identification does not imply recommendation nor endorsement by the National Bureau of Standards.)

holder directly connected to the jack moves laterally in either direction across the photometric aperture at 2 mm/s. Slower speeds variable down to 8 μm/s are possible by lowering the voltage with a rheostat and by using reduction gears. In order to monitor the relative sample position, a calibrated revolution counter is used. These parts provide satisfactory reproducibility and control of the position of samples, without requiring more expensive synchronous motors or stepper motors and gear trains.

Figure 3 shows the scanning densitometer in its operating mode. The sample holder is continuously movable from left to right or vice versa in a horizontal plane across the slit. A vernier scale allows positioning of the sample perpendicular to the scanning direction. The vertical position of this whole assembly is also adjustable for use with different illumination lenses which focus the illumination slit images in a given horizontal plane. The sample holder has a variable opening and can hold films or plates as large as 20 cm long by 3.8 cm wide.

For the purpose of carrying out many simple spatial density gradient readings, an inexpensive drive-strip chart recorder system is satisfactory. If a more sophisticated readout is required, particularly in the case of large-volume data acquisition, an analog-to-digital converter can be used. In the latter case, a ramp voltage can be supplied via a servo loop to drive the motor in stages and thus give a record of optical density as a function of position.

Since one of the main purposes of the instrument is to make spectral-density measurements at optical wavelengths near the absorption maxima of particular photochromic and plastic films, special consideration has been given to providing intense essentially monochromatic light sources corresponding to the wavelengths of the absorption peaks of interest. Interference filters which have been used successfully in spectrophotometry [13] were fitted to the instrument for this purpose. In this case, the optical density measured is standard spectral density [5, 14, 15]. Table 1 lists the filters used, according to wavelength passed, their characteristics in terms of maximum percent transmittance, and spectral bandpass full width at half maximum. Also listed are the plastic or dye films for which the change in absorption characteristics due to irradiation is most pronounced at the indicated wavelength.

TABLE 1. *Interference filter characteristics and corresponding radiochromic film type measured at a particular wavelength*

Transmittance wavelength (nm)	Maximum percent transmittance	Band width at half max. (nm)	Radiochromic film type
401	44.7	10	polyvinylchloride
436	55.5	10	methyl yellow malachite green
559	59.4	10	pararosaniline new fuchsin
601	58.5	10	hexahydroxyethyl violet crystal violet
620	60.0	10	malachite green
640	80.0	10	blue cellophane red Perspex

Several interchangeable slits have been made by an electrical-discharge machining process [16] in aluminum and blackened to reduce reflection from the edges. A list of these slits and their effective image size at the sample plane, when a 4-power, 3.0 numerical aperture condenser lens is used as an illumination condenser system, is given in table 2.

TABLE 2. *Effective image sizes of slits used with scanning densitometer*

Illuminating slit (width × height, mm)	Effective image (width × height, mm)
0.068 × 7.0	0.018 × 1.84
.133 × 1.0	.035 × 0.26
.25 × 2.0	.066 × 0.53
.50 × 3.0	.13 × 0.79
1.0 × 7.5	.26 × 1.97

The lens is an achromatic, spherical-aberration-corrected short focal-length (5.5 mm) lens with an aperture variable from $f/1.8$ to $f/22$. The lens is positioned at a distance from the slit somewhat greater than twice the focal length and the distance between the lens and sample falls between one and two focal lengths. In this geometry, the dimensions of the slit image focused on the sample are between one-third and one-fourth of the slit dimensions. It should be observed from the combination of the smallest effective slit width (18 μm) and the numerical aperture of the lens at full aperture that diffraction at the wavelengths of interest is not a handicap. A slit of this size is still large enough to produce adjacency effects when used for viewing samples with high spatial frequency; however, in most images encountered in the present work, with the exception of edge images, only relatively small variations in optical density occur over a distance the size of the slit width.

3. Instrument Performance

It was noted earlier that the scanning densitometer is not suitable for evaluation of turbid photographic films with high spatial contrast due to excessive light-scattering effects. An example of this limitation is demonstrated in figure 4, where a knife-edge image made on photographic film is shown: (1) as traced by a commercial microdensitometer, and (2) superimposed, as traced by the scanning densitometer. Due to the procedure for calibrating the instrument, data from the scanning densitometer were originally obtained in terms of transmittance. For purposes of comparison with data in figures 4 and 5 from the microdensitometer, these data have been converted to optical density, where

$$\text{Optical Density} = -\log(\text{Transmittance}).$$

Both traces were made with 601 ± 10 nm (full width at half maximum) light provided by an interference filter; the effective slit of the microdensitometer was 16 μm × 800 μm and the effective slit image of the scanning densitometer was 18 μm × 1,840 μm. An objective measure of sharpness for sigmoid-shaped traces is acutance, which is calculated from the relationship [17]:

$$\text{Acutance} = \frac{\sum_{i=1}^{n} (\Delta D/\Delta x)_i^2}{n\,(D_B - D_A)}$$

where,

$(\Delta D/\Delta x)i =$ density change per corresponding trace distance (microns) for each of n equally spaced trace distances between D_A and D_B.

$D_A, D_B =$ optical density at points on knife-edge trace where $\Delta D/\Delta x$ is 0.005 μm^{-1}.

Acutance for the microdensitometric trace of the photographic knife edge, using $n = 10$, was a factor of about 10 higher than for the scanning densitometer. In addition to loss of resolution in the trace of the scanning densitometer, a second degradation of the knife-edge trace is observed due to flare from the illumination of the knife edge. Flare [7, 17] arises from light reflected into the emulsion when a bright region surrounds the image and is within the field of the detector. This is the case when a photographic knife edge is viewed by the scanning densitometer. The result is a reduction in optical density due to collection of extraneous light in the detector. Flare is primarily a function of the material being viewed; it is not a serious problem with the nonturbid films for which the scanning densitometer was designed.

Calculations have been reported of modulation transfer functions (MTF's) for microdensitometer systems from knife-edge traces based on Fourier-transform techniques and convolution methods [17–19]. These computational techniques, with the aid of high-speed computers, can generate separate MTF's for the photographic system and the microdensitometer from knife-edge scans and provide other basic information required for the evaluation of image quality. Such an elaborate analysis was not deemed appropriate for the scanning densitometer because the instrument is not proposed for high-resolution work, but rather as a mechanical apparatus for the purpose of driving a scanning slit across a nonturbid film having relatively low spatial contrast.

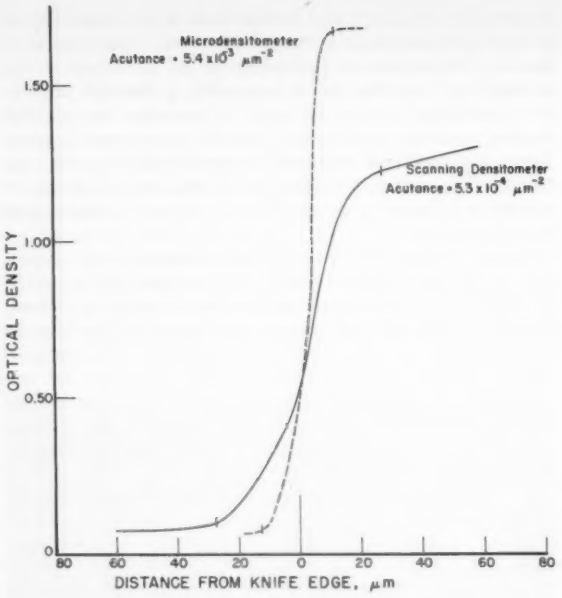

FIGURE 4. *Comparison of photographic knife edge traces for commercial microdensitometer (dotted line) and scanning densitometer (solid line).*

Vertical marks on the traces indicate the points between which acutance was determined ($\Delta D/\Delta x = 0.005\ \mu m^{-1}$).

The most practical measure of the performance of the scanning densitometer is by comparison of optical density traces of nonturbid films with traces produced by a commercial microdensitometer. A typical comparison is shown in figure 5, where traces of an exposed radiochromic dye film, which has recorded the spatial-distribution of dose (proportional to optical density) with depth in a medium, are drawn on the same scale. The important feature of the comparison is the overall agreement in the optical-

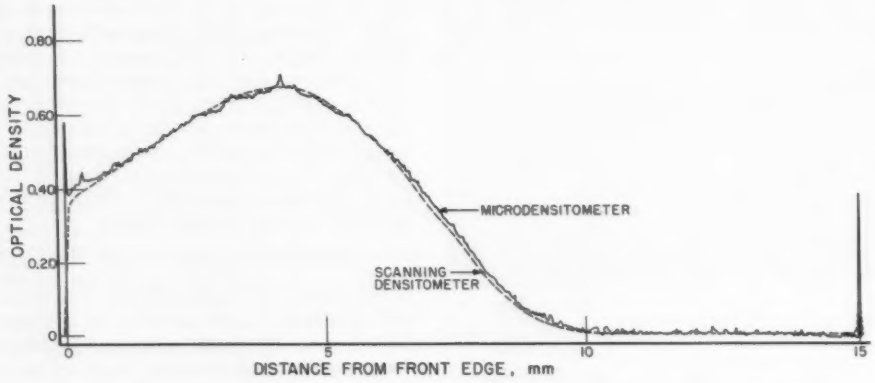

FIGURE 5. *Comparison between spatial optical density tracings of an irradiated radiochromic-dye film for commercial microdensitometer and scanning densitometer.*

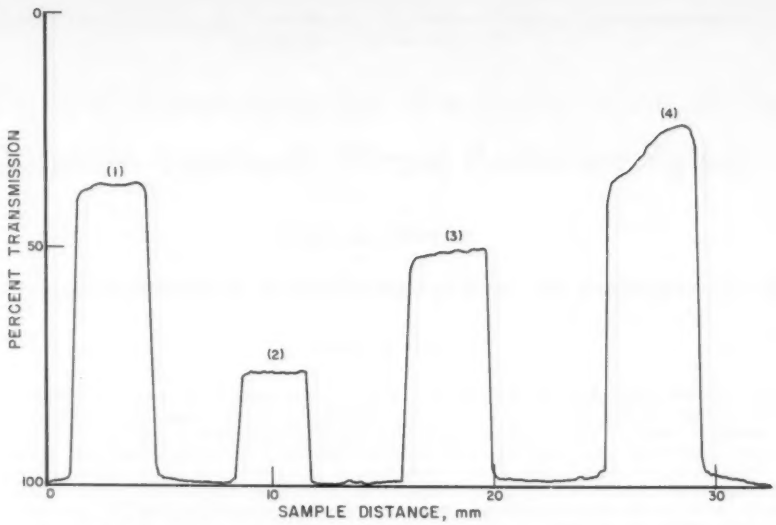

FIGURE 6. *Scanning densitometer trace of a series of irradiated radiochromic dye films.*

(1), (2), and (3) are calibration films exposed to a uniform radiation field, and (4) is the depth-dose response of a film inserted longitudinally in a 4 mm thick phantom. The steep vertical lines represent the edges of the individual films.

density trend between the two traces. As expected, the film edge is more clearly defined in the commercial microdensitometer trace. The sharp spikes evidenced there are responses to small scratches and dust particles which cannot be resolved by the scanning densitometer. It is also observed that the problem of flare noticed with the photographic knife edge is not as pronounced at the edges in the traces of these radiochromic dye films. Except for the improvement in determining the position of the edge of the film, no great advantage would be gained in using the more sophisticated microdensitometer, since the instrument resolution required to register gradual spatial variations in the dye films is available from the scanning densitometer. As an example of a practical application of this instrument, figure 6 shows a trace of a series of irradiated radiochromic-dye films read in tandem on the densitometer.

4. Summary

A simple, inexpensive, scanning densitometer, with effective viewing areas as small as $(0.035 \times 0.26)\,mm^2$ or $(0.018 \times 1.84)\,mm^2$, has been designed and assembled. It is based on existing components, namely a commercial photoelectric densitometer, an illuminating optical-slit system with various wavelengths of monochromatic light, a variable-speed sample driving mechanism and table, and a continuous fast-response readout system. Experiments have shown that images of relatively low spatial contrast on thin nonturbid photochromic films can be scanned competitively with more expensive and complicated microdensitometers. Advantages are that alinement, diffraction, focal adjustment, and photocathode non-uniformity are not severe problems with the instrument described. Disadvantages are that high spatial frequency and sharp knife-edge images on turbid media cannot be handled adequately with this system.

5. References

[1] Altman, J. H., and Stultz, K. F., Rev. Sci. Instr. **27,** 1033 (1956).
[2] Southwold, N. K., and Waters, W. G., J. Photo. Sci. **7,** 174 (1959).
[3] Miller, C. S., Parsons, F. G., and Kofsky, I. L., Nature **203,** 1196 (1964).
[4] Kuttner, P., Appl. Optics **7,** 1029 (1968).
[5] American Standard PH 2.1 (American National Standards Institute, New York, 1952).
[6] Jones, R. A., and Coughlin, J. F., Appl. Opt. **5,** 1411 (1966).
[7] Galburt, D., Jones, R. A., and Bossung, J. W., Photo. Sci. Eng. **13,** 205 (1969).
[8] Charman, W. N., Appl. Optics **4,** 289 (1965).
[9] Linfoot, E. H., Fourier Methods of Optical Image Evaluation, Chapt. III, (Focal Press, London, 1964).
[10] Duecker, H. C., and Lippincott, E. R., Rev. Sci. Instr. **35,** 1108 (1964).
[11] Benedetti, P. A., and Viola-Magni, M. P., J. Sci. Instr. **43,** 141 (1966).
[12] Arndt, U. W., Leigh, J. B., Mallett, J. F. W., and Twinn, K. E., J. Sci. Instr. **2** (Ser. 2), 385 (1969).
[13] Rohner, E., and Strutt, M. J. O., Rev. Sci. Instr. **28,** 1074 (1957).
[14] Simonds, J., The Sensitometry of Color Films and Papers, Chapt. 21 in The Theory of the Photographic Process, eds. C. E. K. Mees and T. H. James (MacMillan Co., New York, 1966).
[15] Powers, S. A., and Miller, D. E., Photo. Sci. Eng. **7,** 59 (1963).
[16] Williams, R. O., Monograph, The Cincinnati Milling Machine Co., from talk at Cincinnati Technical Activities Seminar (1957).
[17] Perrin, F. H., The Structure of the Developed Image, Chapt. 23 in The Theory of the Photographic Process, eds. C. E. K. Mees and T. H. James (MacMillan Co., New York, 1966).
[18] Abbott. F., Opt. Spectra **64** (April 1970).
[19] Jones, R. A., Photo. Sci. Eng. **11,** 102 (1967).

(Paper 75C1–310)

JOURNAL OF RESEARCH of the National Bureau of Standards — C. Engineering and Instrumentation
Vol. 75C, No. 1, January-March 1971

Rotating Optical Attenuator for the Generation of Subsecond Duration Sawtooth Shape Radiance Pulses*

Ared Cezairliyan

Institute for Materials Research, National Bureau of Standards, Washington, D.C. 20234

(August 28, 1970)

A rotating attenuator for the generation of subsecond duration sawtooth shape radiance pulses is described. The attenuator disk is in the form of a cam. The geometry of the opening of a diaphragm used as the aperture stop determines the shape of the radiance pulses. Radiance is determined from the measurements with a high-speed photoelectric pyrometer. Recording of signals is made with a high-speed digital data acquisition system. The combined measuring and recording systems have a full-scale signal resolution of approximately one part in 8000 and a time resolution of 0.4 ms. Two different diaphragms are used in this study yielding radiance pulses (20 to 150 ms long) with linear and quadratic rise. The standard deviation of the experimental points from the pertinent functions describing the radiance variation is less than 0.5 percent.

Key words: High-speed methods; light attenuator; photometry; radiance modulation; radiation.

1. Introduction

A considerable amount of work has been done to develop various techniques to modulate radiance beams in the visible as well as in the ultraviolet and infrared regions. Most of these techniques were confined to generating either repetitive rectangular pulses, or short-duration fast-risetime single pulses. A review of various methods for modulating radiance pulses was given by Jones [1].[1] Optical modulation techniques in the infrared region were discussed by Hudson [2].

Increasing interest in transient techniques for the measurement of properties of matter at high temperatures and related studies has necessitated the development of programmable optical attenuators. Such attenuators are needed to simulate (using steady-state radiance sources) the rapid heating or cooling of the specimen and also to check dynamic characteristics of radiation detectors and of high-speed temperature measurement systems in general.

2. Method and Apparatus

In this study an optical system, including a rotating optical attenuator, is described that is capable of generating repetitive sawtooth shape (either linear or quadratic) radiance pulses, ranging from 20 ms to several seconds in duration. The optical system (fig. 1) consists of a radiance source (tungsten filament lamp), a rotating disk (cam with helical circumference), a special diaphragm, a high-speed pyrometer, and other pertinent optical components. The lenses 01 and 02 shown in figure 1 are 63 mm in diameter with an aperture of $f/2.5$. The circumference of the disk was machined in such a way that its radius r was proportional to the angle from a fixed reference point according to the following relation:

$$r = r_0 - ka \tag{1}$$

where r_0 is the maximum radius, a is the angle, and k is the proportionality constant. The maximum and minimum radii of the disk were 7 in (177.8 mm) and 6 in (152.4 mm), respectively, yielding a maximum difference of 1 in (25.4 mm). The thickness of the disk was 0.12 in (3 mm).

The aperture stop of the optical system was defined by the circumference of the disk and the diaphragm placed in the collimated portion of the beam. As the disk rotated, the effective cross-sectional area of the beam changed, which, in turn, generated sawtooth shape pulses. The shape of the diaphragm opening determined the shape of the radiance pulse. For example, a rectangular opening as seen in figure 2 yields a pulse with linear rise, while a triangular opening gives a pulse with quadratic rise. Rotation of the disk was synchronized with other measuring equipment with a signal obtained from a radiation detector. The radiation detector PM (fig. 1) generated a signal each time a 0.2 mm in diameter hole H (fig. 2) fabricated in the disk was in line with the detector and the light source L (fig. 1). Relative radiance of the source after attenuation was measured with a high-speed photoelectric pyrometer [3]. The electrical signals from the pyrometer were recorded with a high-speed digital data acquisition system [4]. The combined measuring and recording system has a full-scale signal resolution of approximately one part in 8000 and a time resolution of 0.4 ms.

The photomultiplier in the pyrometer was alternately exposed to the radiance from the tungsten filament lamp and to the radiance from a reference lamp. This scheme

* This work was supported in part by the Propulsion Division of the U.S. Air Force Office of Scientific Research under contract ISSA-69-0001.

[1] Figures in brackets indicate the literature references at the end of this paper.

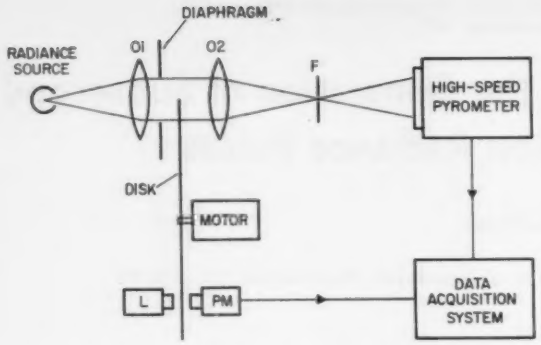

FIGURE 1. *Functional diagram of the optical system for the generation of subsecond duration sawtooth shape radiance pulses.*

eliminated errors that result from photomultiplier fatigue, etc.

Pulse shape as a function of time for various diaphragm geometries is derived in the following paragraphs.

The effective cross-sectional area of the light beam, when the disk circumference is at point x on the diaphragm, may be expressed as

$$A_x = \int_0^x y\,dx \tag{2}$$

where $x = r_0 - r$ and y is the width (height) of the diaphragm at x (fig. 2).

For rectangular geometry, $y =$ constant $= a$, thus

$$A_x = ax. \tag{3}$$

For triangular geometry, $y = bx$, thus

$$A_x = bx^2/2. \tag{4}$$

When the disk rotates at a constant speed, the angle of rotation is proportional to time t, that is

$$a = k't. \tag{5}$$

From eq (1) and the definition of x, it follows that

$$x = r_0 - r = ka. \tag{6}$$

Combination of eqs (5) and (6) yields

$$x = kk't. \tag{7}$$

The radiance L as seen by the pyrometer at a given instant is

$$L = k''A. \tag{8}$$

Combination of eqs (3), (4), (7), and (8) yields the following:

For rectangular geometry

$$L = Kt; \tag{9}$$

For triangular geometry

$$L = K't^2 \tag{10}$$

where K and K' are combination of constants. Equations (9) and (10) represent radiances that are linear and quadratic functions of time, respectively.

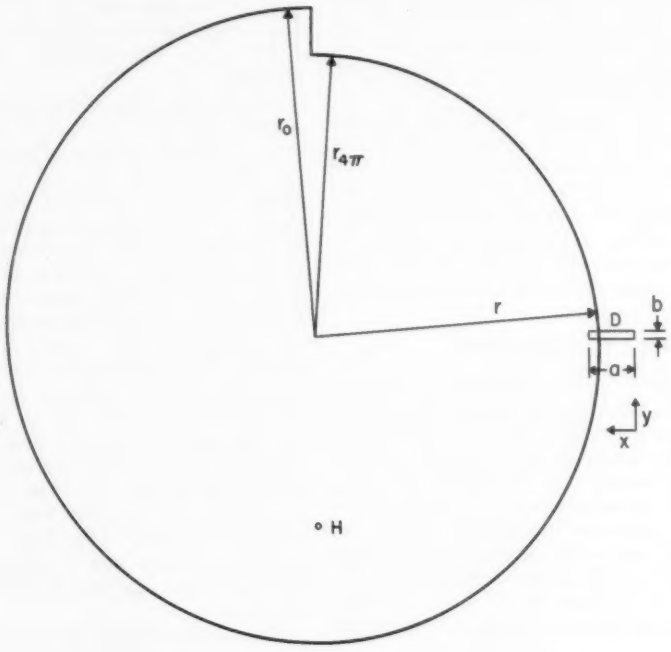

FIGURE 2. *The attenuator disk and the diaphragm opening.*

3. Experimental Results

In order to assess the operational characteristics of the system, experiments were performed using diaphragms of rectangular and triangular openings. These experiments are summarized in the following paragraphs.

Linear radiance pulses: A total of 15 experiments were conducted at five different attenuator speeds yielding radiance pulses (increasing linearly with time) in the range 20 to 150 ms. Additionally, four experiments were performed with the direction of rotation of the attenuator reversed. This scheme generated radiance pulses that decreased linearly with time.

Quadratic radiance pulses: A total of four experiments were conducted at two different attenuator speeds. An additional experiment was performed with the direction of rotation of the attenuator reversed.

Oscilloscope trace photographs of representative radiance pulses are shown in figure 3. The radiances as detected by the high-speed pyrometer and recorded with the digital data acquisition system were fitted to linear and quadratic functions, depending on the pulse shape, using the least squares method. A summary of the experimental parameters and results is given in table 1. It may be seen that average standard deviation (individual point) of the results of both pulse shapes is approximately 0.6 percent corresponding to data covering a radiance ratio of over 10.

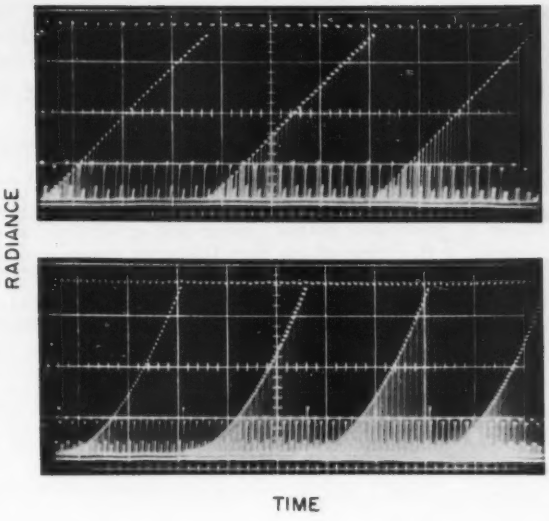

FIGURE 3. *Oscilloscope trace photographs of linear (upper) and quadratic (lower) radiance pulses.*

Horizontal scale: 10 ms (upper), 20 ms (lower) per major division. Vertical scale: arbitrary units. Dots forming the long horizontal lines correspond to radiances from the reference source.

The above value for the standard deviation reflects departure from ideal behavior that may be due to several factors, such as random noise in radiance samples and in the pyrometer operation, nonuniformity in the lenses and in the optical alinement, nonuniformity in the attenuator circumference, variation in the attenuator speed, etc. In order to separate the contribution of the pyrometer and the random noise inherent in radiance measurements from the attenuator and the associated optical system, two separate experiments were conducted under steady-state conditions. In one of the experiments, the attenuator was positioned to provide the maximum opening of the diaphragm as seen by the pyrometer. Then the pyrometer response to the radiance source was recorded. The standard deviation of the results was 0.2 percent. A similar experiment was performed with the attenuator positioned to provide radiance equivalent to that of the lowest level used in the dynamic experiments. The standard deviation of the results of the pyrometer output was 0.8 percent. Assuming an approximately linear variation of randomness between the two extremes, a value of 0.5 percent for the standard deviation contributed by the pyrometer and radiance measurements in general is obtained. Thus, if it is assumed that total standard deviation is the square root of the sum of the squares of individual standard deviations, the standard deviation corresponding to the nonuniformities of the attenuator and the associated optical components becomes approximately 0.3 percent. This value is comparable to the uncertainty with which the pyrometer linearity could be determined in separate experiments.

In order to ascertain the fact that the value obtained for the standard deviation was the result of random deviations in the data, the data on radiance were also fitted

TABLE 1. *Summary of experimental parameters and results*

Item	Radiance variation	Direction of radiance variation	Pulse length *(ms)*	Number of experiments	Number of points per experiment	Average radiance ratio	Average total standard deviation, %
1	Linear	Increasing	23	3	20	10.3	0.6
2	Linear	Increasing	30	3	26	12.1	.7
3	Linear	Increasing	39	3	33	9.0	.6
4	Linear	Increasing	59	3	50	11.8	.5
5	Linear	Increasing	144	3	123	11.3	.6
6	Linear	Decreasing	23	1	20	10.0	.7
7	Linear	Decreasing	30	1	26	9.5	.7
8	Linear	Decreasing	39	1	33	10.4	.6
9	Linear	Decreasing	59	1	50	10.6	.5
10	Quadratic	Increasing	60	3	39	11.0	.6
11	Quadratic	Increasing	40	1	26	10.1	.5
12	Quadratic	Decreasing	60	1	39	11.1	.6

to functions of one and two higher degrees than the pertinent one. No improvement in the standard deviation was observed, indicating that there was no detectable systematic curvature imposed on the proper function.

4. Conclusion

The results of the experiments described above have shown the feasibility of generating subsecond duration pulses of prescribed shapes (linear and quadratic) with a standard deviation of less than 0.5 percent over a radiance ratio of 10. The method allows one to insert appropriate diaphragms in the optical system to obtain radiance pulses of various shapes. For example, in addition to linear and quadratic, it is possible to generate pulses of cubic, exponential, and other shapes.

The scheme of generating radiance pulses allows one to detect the linearity of radiation detectors under dynamic conditions, and also provides the experimenter with means of simulating high-speed heating or cooling experiments.

5. References

[1] Jones, O. C., J. Sci. Instr. **41**, 653 (1964).
[2] Hudson, R. D., Infrared System Engineering (John Wiley & Sons, Inc., New York, 1969), p. 235.
[3] Foley, G. M., Rev. Sci. Instr. **41**, 827 (1970).
[4] Cezairliyan, A., Morse, M. S., Berman, H. A., and Beckett, C. W., J. Res. Nat. Bur. Stand. (U.S.), **74A** (Phys. and Chem.), 65 (1970).

(Paper 75C1–311)

JOURNAL OF RESEARCH of the National Bureau of Standards — C. Engineering and Instrumentation
Vol. 75C, No. 1, January-March 1971

Sound Speed Measurements in solids: Absolute Accuracy of an Improved Transient Pulse Method

Thomas M. Proctor, Jr.

Institute for Basic Standards, National Bureau of Standards, Washington, D.C. 20234

(November 17, 1970)

A modified transient pulse technique for measuring shear and longitudinal sound speeds in solids has been devised. The technique is described and evaluated for both precision and accuracy on a variety of solids. This evaluation has been done by experiments in which the constancy of sound speed with path length is used as the prime test for accuracy. A number of variables such as transducer frequency, transducer size, choice of different coincidence points, etc., have been examined. The transducer bond problem is examined and overcome by the use of a time delay bond. Indicated accuracy of the method is found to be better than one part in 10^4. Advantageous sample geometries for accuracy testing are discussed.

Key words: Acoustical pulse; longitudinal and shear sound waves; solids sound speed accuracy; speed of sound; transient pulse-acoustical.

1. Introduction

For the purpose of this discussion, measurement methods for sound speed can be divided into two groups: (1) equilibrium-monochromatic sinusoidal methods (ES), and (2) nonequilibrium sharp-transient pulse methods (NET). For the ES methods, error evaluation depends upon their described character. The specification of the particular equilibrium condition is important. Many variations of the ES method are discussed in the extensive works of H. J. McSkimin and others [1–5].[1] But in the NET methods the predominant notion is that the first sound arrival proceeds by the shortest path and travels with the sound speed of the infinite medium. The nearer to the first arrival that the measurement is done, the less significant are the various end effects and unwanted boundary reflections.

Because the NET method performs poorly for materials that have frequency dispersion or high losses, its use has been limited in recent years. The monochromatic ES systems are more applicable to these cases. Despite these limitations, various NET methods have been used successfully in this laboratory [6–8]. Recently, the latter has been applied to the measurement of speed of sound in solids with surprisingly good results. Modifications of an older technique have largely overcome the remnant sound energy problem which occurs with continuous pulsing.

The method uses a pair of very short pulses, each approximating a delta function. The pulses are separated by a time interval which is precisely adjusted to correspond to the round-trip time of flight for sound through the sample. The signal pair is followed by a dead time which is sufficiently long enough for the residual sound to have died out. During this dead time, the transducer is used as a receiver in such a manner that the n^{th} return of the second pulse is superimposed on the $(n+1)^{\text{th}}$ return of the first pulse. The earliest recognizable feature of these returning signals is used to make this coincidence. This is related to the most direct path for sound travel. This contrasts sharply with the ES methods. In general, the phase lag of the acoustical signal is measured by comparison to the infinitely long wave train from which the initial pulses are chopped. These ES experiments are essentially monochromatic, as the propagated pulses are made up of many wavelengths in signals of constant amplitude.

The method is discussed with special emphasis on precision and accuracy as determined empirically. The uniformity of the sound speed and the similarity between the two pulses used for coincidence were used as tests for accuracy. The effects of different variables on the sound speed have been examined and are noted. Some guidelines (shape and material) for the choice of a suitable sample for testing the accuracy of the method have been developed.

2. Experimental Features

This transient video pulse technique is used for sound speed measurements in short fat solid samples (3.5 cm long $\times$ 3.8 cm diam) and can be used either single ended or with separate sender and receiver. The single ended way produces the best results and is used for this study. The transit time for a round trip is the principal measurement made.

With continuous pulsing at intervals comparable to the transit time of the sample, remnant sound will build up in small samples of high Q and coincidences for timing the transit time will be impaired. The remnant sound problem is handled by the use of a special sequence of driving pulses. The transducer is driven by two very short

[1] Figures in brackets indicate the literature references at the end of this paper.

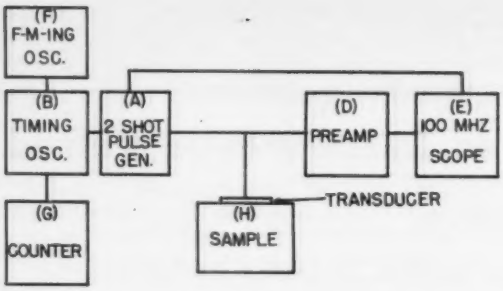

FIGURE 1. *Experimental setup schematic.*

(<30 ns) 50-V pulses, each approximating a delta function, which are separated by a known and adjustable time period, τ. These pulses are followed by a long dead time $(2^n - 1)\tau$ and then the full sequence is repeated. The period τ is determined by the frequency of the control oscillator (B) as measured by the frequency counter (G) (see fig. 1). This drives the two-shot apparatus (A) which produces the pulse sequence.

The dead time generated by the two-shot apparatus can be adjustable to any value $(2^n - 1)\tau$ where n is an integer ranging from 1 to 8. Such adjustments allow for variations in sample losses by permitting the dead time to be adjusted so that, at the beginning of the next sequence, the left-over residual sound is negligible. Most of these measurements were made with $n = 8$ and with a dead time of 255 τ. The two-shot apparatus is a parallel set of 1 MHz binary chains having an adjustable phase difference for pulses traveling down the two chains [9] (see fig. 2). A provision which allows interchanging the firing order of the respective chains is used to cancel slight electronic phase differences between the outputs of the two chains. This function is indicated by the "A before B" switch on figure 2.

The pulses are then amplified and fed to a blocking oscillator which drives the transducer. The transducer, acting as a highly damped resonant sender, sends the sequence of sound pulses into the sample (H), figure 1. In this system a single pulse is reflected back and forth in the sample creating a whole family of successive acoustic reflections: first round trip reflection, second round trip reflection, etc. In this way the two pulses as generated by the apparatus form two overlapping families of acoustical reflections. The superposition of all the acoustical reflections is received by the transducer. The electrical output of the transducer is amplified by a low noise amplifier ((D) of fig. 1) and then the coincidences are displayed on a delayed sweep 100 MHz scope (E).

Coincidences are set between the two overlapped families of reflected pulses. With the control oscillator, the period τ is adjusted until the second reflection generated by the first pulse of the pair coincides with the first reflection generated by the second pulse. Specifically this coincidence is made by aligning the first half cycles of the two reflections. Usually the combination of the two first half cycles is maximized to indicate alinement. This represents a coincidence made at a time between $\frac{1}{3}$ to $\frac{1}{2}$ of the resonant period of the transducer after the receipt of the very first arrival (earlier coincidences can be obtained photographically). The definition of the coincidence setting is improved by a low frequency phase modulation of the control oscillator (fig. 1 [F] modulation oscillator).

Because the two-shot apparatus affords a very low pulse rate, coincidences are especially easy to set even for materials of the highest Q. This condition is due primarily to the absence of driving energy on the transducers at the time of coincidence and to the lack of acoustical reverberation from the previous pulses afforded by the long dead time.

Very thin barium titanate transducers are used for both longitudinal and shear wave generation and reception (see fig. 3). A backing mixture of epoxy resin and tungsten graded powders is attached to the transducers. The high loss characteristics of this mixture helps keep the Q of the transducer system below 10, which is desirable. This reduces long ringing and improves the initial pulse edge.

The transducers are coupled to the sample by an acoustically thick joint. Joints 10 to 25 μm in thickness are constructed of materials having an acoustic impedance much lower than that of either the transducer or sample. This helps isolate the sample from the transducer and the reflections of sound energy in the sample tend to take place at the proper surface. These bonds have the advantage that they are simple and easy to construct. Compressional bonds are usually made with water or

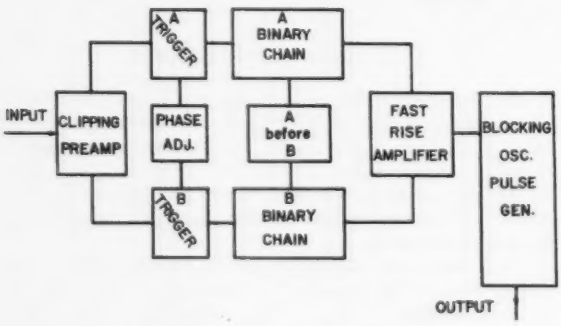

FIGURE 2. *Two-shot pulse generator — a block diagram.*
A before B switch sets the chain firing order, namely A before B or B before A.

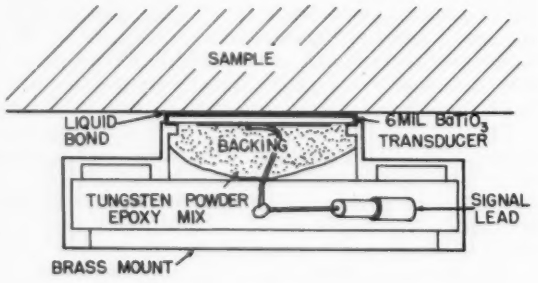

FIGURE 3. *Typical transducer and bond construction.*

alcohol at room temperature and 4-methyl-1-pentene [10] or 2-methyl butane [11] at low temperature (77 to 196 K). A good shear coupling agent at room temperature is Dow Resin 276-V9 [1] (poly-methyl styrene), and at low temperatures is 4-methyl-1-pentene.

3. Technique Evaluation

Errors and accuracy have been evaluated by a number of different experiments for which various accessible variables can be controlled. Two criteria are used for evaluation: sound speed and round-trip transit time. Round-trip transit time is used primarily for studying small time delays associated with bond and end effects. The sound speed is measured whenever the "Crucial Test" is applied.

3.1 The Crucial Test (Sound Speed Uniformity)

The accurate determination of sound speed is hindered greatly by the lack of a uniquely definitive experiment. In general, the toughest convenient test for accuracy that is readily available is to examine the change of sound speed as a function of sample length. In liquids this is relatively simple. The physical limitations of solid samples cause special problems. The following four are examples: (1) The length of a solid sample cannot be changed in a continuous fashion. (2) Material uniformity is always questionable. (3) Spurious reflections occur more readily in the smaller physical sizes commonly used in solid measurements. Finally (4) there are difficulties in bonding the transducer to the sample. The importance of the constancy of sound speed with length cannot be overemphasized. Although it is not a sufficient test, it must necessarily be applied whenever accuracy is of interest.

This test was applied for three different materials. The first sample used was a family of aluminum gage blocks (5 lengths ¾ in thru 4 in long × 2 in diam). The blocks were cut consecutively from a polycrystalline mother bar. Under the best measurement conditions, the longitudinal speed of sound was found constant within $\pm 2 \times 10^{-4}$ parts (18 MHz resonant transducer) and the shear speed within $\pm 1 \times 10^{-3}$ parts (8.5 MHz resonant transducer) for the five lengths. These errors in sound speed for the aluminum sample could easily be explained by the lack of radial stress uniformity in the bar samples and by nonuniform sound scattering caused by the polycrystalline state.

A search for a better material was begun. Commercial grade fused silica was tried and found to be poor for the purpose. Local variations in the internal stress and density as seen in a polarimeter could be roughly correlated with variations in sound speed measured locally. Fused silica of more uniform optical density gave better uniformity in the sound speed. Finally a successful material was found in a borosilicate optical crown glass manufactured by the National Bureau of Standards under the name BSC 517/645. Some physical properties of this glass are given in the Smithsonian Physical Tables [12]. This material was found to have high optical and acoustical uniformity. At room temperature this glass has the bonus property of a near zero velocity temperature coefficient.

A test sample of this material was fabricated so as to have three different path lengths (a parallelepiped of 1 in × 1.5 in × 2.0 in). The question of acoustical uniformity is then isolated to local sound speed uniformity, and this has been determined to be below the threshold of measurement for this method ($< \pm 5 \times 10^{-5}$ parts). Results for compressional waves, using a transducer resonant at 18 MHz on the BSC 517 sample, showed a barely measurable increase in speed for shorter path lengths [V(1 in) >V(2 in) by $\sim 10^{-4}$ parts]. As will be discussed later, adjustments that reduced the bond error made the sound speed on this sample constant to the precision of the method. The same sample was used to test the shear mode (8.5 MHz resonant transducer) and the shear speed was found to be constant to within the precision of $\pm 5 \times 10^{-5}$ parts.

Using different path lengths, another material was measured. With a glass optical absorption cell (nominally 2 in by 3 in) the longitudinal (18 MHz resonant transducer) sound speed of pure water was measured along two path lengths (a third length was obtained from another cell). The transducers were fixed to the outside walls of the container in the same manner as they are for any solid. Thus solid bonding problems are duplicated here although these effects are smaller than normal because of the larger transit times involved. The temperature environment was well isolated and highly controlled. A platinum resistance thermometer was used to measure temperatures to a millidegree. Results on three path lengths (6.3, 8.9, 14.0 cm) indicate that the constancy of sound speed is better than the total precision ($\pm 5 \times 10^{-5}$ parts) and that the measured value agrees extremely well with the recent work of Carnvale et al. [13].

3.2 Effect of Diameter of Transducer

The effects of changing transducer diameter with constant frequency were investigated. Very thin paper masks (25 μm) were used to restrict the radiating area of the transducer. Bonds were made by filling the hole in the mask with the bonding fluid. (It was determined that no sound could be transmitted through the wetted mask area.) Figure 4 shows how the mask hole size is related to the measured transit time through the sample. This experiment was performed on fused silica using three different resonant transducers. In general, the transit time increases (speed decreases) for smaller effective transducer areas. This behavior might be explained by the notions discussed in 4.1. The abrupt change of speed from the unmasked value to the largest masked value is due primarily to the thick bond effect which will be discussed later. When the same experiment was performed using shear waves, very little change in transit time was measured (less than 10^{-4} parts).

3.3 Effect of Resonant Frequency of Transducer

Early experiments on fused silica indicated that the measured sound speed tends to decrease with increasing resonant frequency of the transducer. A similar effect was found with the BSC 517/645 sample. Figure 5 shows the

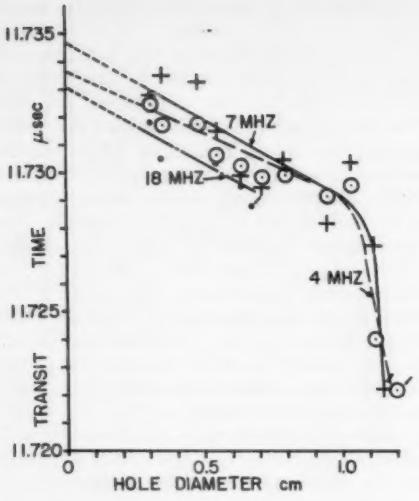

FIGURE 4. *Effect of mask diameter on transit time.*

3.5-cm long fused silica sample with each of three transducers of different frequency. Water forms the bond. Slashes mean "no mask."

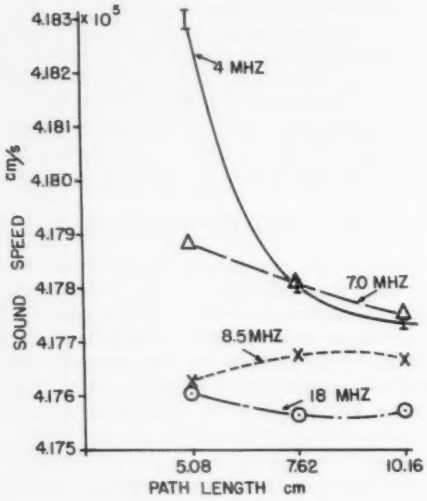

FIGURE 5. *Sound speed (L-waves) in borosilicate crown glass BSC 517/645 for three path lengths and four transducers of different frequency.*

Tight water bond. Flags indicate precision.

constancy test of sound speed as performed with the three lengths of the borosilicate sample using four longitudinal transducers of different resonant frequency. The resonant frequency of each transducer is marked on the appropriate curve. Note that as the resonant frequency increases, the speed decreases and becomes more uniform with path length (maximum spread for all transducer frequencies and sample lengths is 2×10^{-3}). These measurements were made with a tight bond (water bonds of less than 10 μm).

3.4 Earlier Coincidences

As already mentioned in the introduction, it is felt that the closer to the first sound arrival that one sets the timing coincidences the better the resulting accuracy will be. One way to facilitate this is to use transducers of higher resonant frequency as was discussed in section 3.3. Another is to use earlier recognizable features of the transient pulse. Efforts were made to examine the effects on the transit time of the position of the coincidence setting in the received pulse. Transit times for longitudinal sound through a fused silica sample were measured for nine successive half cycles. The coincidences were set by maximizing each half cycle starting with the first and working back to the ninth half cycle in the pulse. These results are shown in figure 6 for two different resonant frequency transducers. The various half cycles at which coincidences were made are appropriately marked and the position of each related to the beginning of the pulse is measured on the abscissa in μs. This test was also performed using shear waves (8.5 MHz resonant transducer) with very similar results.

An arbitrary scheme of obtaining information about coincidences earlier than the first half cycle can be carried out photographically. Photos of the front edge of the first half cycle were obtained from a 100 MHz fast sweep scope. Pictures were taken for both the first and second reflections separately. Amplitude measurements were taken from these as a function of time back to the beginning of the signal from the first half cycle maximum. A

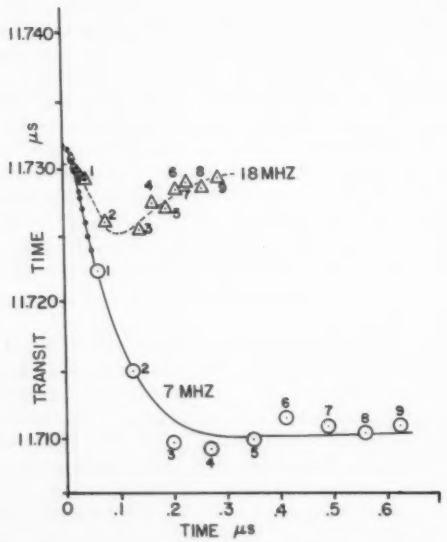

FIGURE 6. *Transit time (L-waves) versus time from the beginning of the signal at which coincidence was made.*

Two transducers (18 and 7 MHz resonance frequency) on 3.5-cm long fused silica sample. Tight water bond.

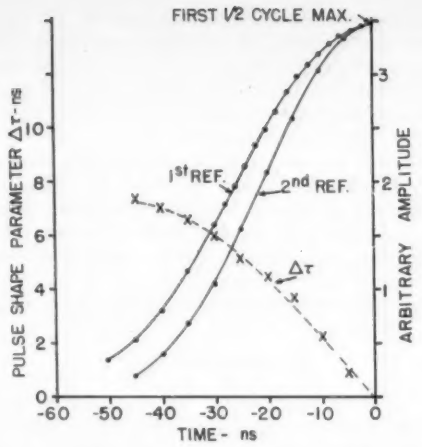

FIGURE 7. *First quarter cycle of first and second reflections normalized at the first ½ cycle maximum.*

Δτ is excess delay for points of equal amplitude (arbitrary time zero at first ½ cycle max.) L-waves in 2.5-cm long borosilicate crown glass. Transducer, 7 MHz. Tight water bond.

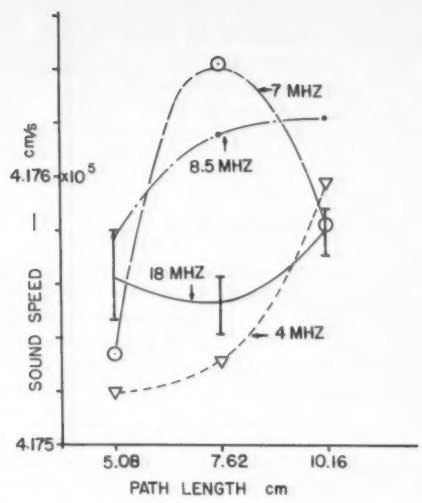

FIGURE 8. *Speed of sound (L-waves) in borosilicate crown glass BSC 517/645 for three path lengths and four transducers of different frequency.*

The data are those of figure 4 corrected according to figure 7. Flags indicate precision.

normalized amplitude graph demonstrates any shape change between the front edges of the first half cycle for the first and second reflections.

Figure 7 is one such normalized comparison. The time reference origin is fixed at the first maximum of each and negative time proceeds forward into the pulse in the normal way. Note that in this case the second reflection rises faster than the first (indicative of some geometric interference effects). The time difference between equal amplitude points of the two pulses is plotted as $\Delta\tau$, the pulse shape parameter. This is associated with pulse shape change and has been used to correct the first half cycle coincidence data to give better values of sound speed. As one goes forward into the pulse the precision of $\Delta\tau$ gets steadily worse making values of $\Delta\tau$ earlier than 30 ns from the first half cycle peak undependable.

Using $\Delta\tau$ to correct the transit times, corrections can be found for the sound speed. These corrected transit times are shown by the small Δ data and the • data for the two different resonant frequency transducers on figure 6. Note that these data tend to converge to the same value at the pulse beginning. Further confirmation for this arbitrary correction is obtained from the favorable results of sound speed uniformity tests shown in figure 8. Figure 8 is figure 4 corrected for the early pulse shape variations using $\Delta\tau$ for the three different path lengths and the four resonant transducers on the BSC 517/645 sample. Note that not only is the sound speed more nearly constant for the three lengths, but the data for the different resonant frequency transducers tends to cluster around the 18MHz transducer value (maximum spread for all lengths and frequencies is 2.5×10^{-4}). In the case of shear waves, the difference in shape of the first two reflections is undetectable and there is no reason for such a correction.

The following general observations can be made about the behavior of $\Delta\tau$, pulse shape, and sound speed.

(1) The higher the resonant frequency of the transducer the smaller the pulse shape factor. In fact for the 18 MHz resonant transducer $\Delta\tau$ is essentially zero.

(2) The smaller $\Delta\tau$ is (or the more nearly alike the first and second reflections are) the more uniform is the sound speed for the three path lengths.

(3) By applying the corrections for the shape factor to the sound speed, the constancy is improved and the values of sound speed, as corrected, bunch closer to the highest frequency value.

3.5 Transducer-Sample Bonds

The effects of a thick bond on the transit time for longitudinal waves were studied by using a variable water bond. Apparatus that allowed continuous fine adjustment of the bond thickness while maintaining parallelism between the transducer and sample was used. Changes in the transit time were measured as a function of bond thickness for a number of different materials, a number of path lengths and different frequency transducers. Figure 9 is typical. It shows the increase in the measured transit time with bond thickness for three transducers of different resonant frequencies. The three path BSC 517 sample was used. Measurements along these three path lengths give essentially the same increase in transit time, indicating that the bond errors are independent of sample length. Furthermore, using transducers of higher resonant frequency reduces the magnitude of the bond error. Similar work using the 8.5 MHz shear resonant transducer with a viscous resin bonding material (Dow 276-V9 Resin) was done. A similar but much smaller increase in transit time was obtained (increase was $\sim 1 \times 10^{-4}$ parts).

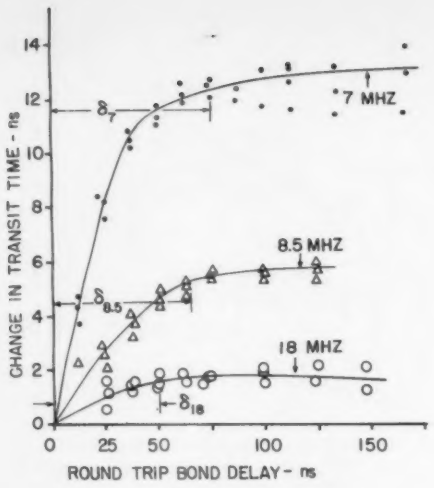

FIGURE 9. *Change in transit time versus water bond thickness.*
L-waves in borosilicate crown glass BSC 517/645. Three transducers of different frequency. Data for three lengths on each curve. δ is the half period of the transducer frequency.

Generally as the thickness is increased to that of the δ bond (thickness corresponding to the time between the first arrival and the first maximum) both the constancy of the sound speed and pulse shape factor are improved. In fact when the sound speed is measured on the three length BSC 517 sample using δ bonds, in a similar manner to figure 4, one finds that all the transducers of different resonant frequencies give more constant values of sound speed and the values obtained cluster much closer to each other than for a thin bond (maximum spread for all frequencies and lengths is 1.5×10^{-4}). At the highest transducer frequency of 18 MHz, measurement of sound speed with a δ bond gives values constant within $\pm 5 \times 10^{-5}$ parts which is lower by 10^{-4} parts than the data of figure 4, taken with thin bond.

3.6 Damping Backing to Transducer

Interference in the leading edge of the received pulses which occurs because of reflections off the back of the transducers was investigated. A number of different backing mixtures were tried in an effort to reduce transducer ringing. It was found that lowering the Q of the transducer by use of a backing with higher damping improved its performance. Both the pulse shape and the constancy of sound speed were improved by a tungsten-epoxy backing which lowered the Q to less than 10. At 18 MHz pulse shapes were made nearly identical by the use of these improved backings.

4. Discussion

4.1 Expected Interference Errors

It is difficult to estimate theoretically the magnitude and the sign of errors in sound speed unless sufficient knowledge about the particular measurement is available. In these experiments, coincidences are made between corresponding points on the front edge of the first and second reflections. Depending on the kind of distortion acquired between these reflections, error of either sign may be expected in the transit time.

Figure 10A represents the condition observed experimentally by this method at the lower frequencies. This shows the leading edges of the first and second reflections as they are related to the first time of arrival. The first reflection rises more slowly to the peak than does the second. The contrary situation has never been observed in all the experiments performed. Let the measured transit time, X, be given by

$$X = \tau + \Delta t_2 - \Delta t_1,$$

where τ is the shortest time of flight, associated with first arrival. Because Δt_2, the time between the first arrival and the first maximum of the second reflection, is smaller than Δt_1, the corresponding time for the first reflection, the measured transit time will be too small when coincidences of the first half cycle are used. Thus, improving the similarity between pulses of the first and second reflections should cause the transit time to increase. This is what is observed experimentally. In fact, it occurs in conjunction with the improvement of sound speed constancy. The following simplification may help to explain the observed differences in the first and second pulse reflections.

Assume that for the leading edge of the signal the sender acts more like a point source than like a plane wave generator. Figure 10B shows the longest and the shortest rays that can connect a point sender and a finite planar receiver for the first two reflections. The difference between the longest received and most direct rays is

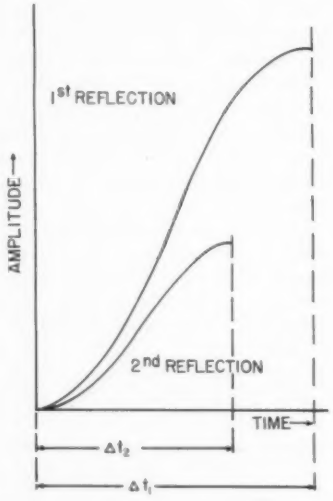

FIGURE 10-A. *Front edge of the first and second reflections.*
Time versus amplitude. First arrival is at the origin.

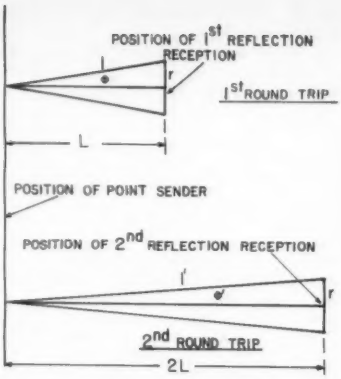

FIGURE 10-B. *Extreme rays connecting a point sender to a finite receiver for two consecutive reflections.*

greater for the first reflection than for the second. Thus one might expect the delay between the first arrival and the initial maximum to be greater for the first reflection than for the second. Although this model fits the qualitative behavior, it oversimplifies a much more complicated geometric interference problem. It is for this and similar reasons that the empirical test has become the guideline for this experiment.

4.2 Bond Errors

In this method one of the biggest sources of error concerns multiple reflections between the two faces of the bond. When sound is sent through a bond of finite thickness some of the energy is transmitted and some internally reflected. In such a manner a whole family of pulses separated by some multiple of twice the transit time of the bond will be transmitted into the sample. The superposition of these reflections changes the shape of the observed pulse. The resultant shape depends on how the intrabond reflections add to the straight-through pulse. The leading edge of the pulse may be sharpened, lengthened, or left essentially unchanged. A similar process will occur at the encounter of the sound with the bond after each round trip.

Not all of the encounters are of the same kind. The most important of these is the one after the sound has completed the first round trip. Part of the sound is transmitted through the bond and the rest is reflected back into the sample. With a thin bond, there are multiple reflections at the faces of the bond which modify both the reflected and transmitted waves. Experiment indicates that the signal received by the transducer after one round trip is lengthened by more than the geometrical effect discussed above. On the other hand, the signal received after two or more round trips is modified less by the bond.

To avoid the influences of these intrabond reflections, a thick bond is used. This "δ bond" delays the unwanted reflections so coincidences formed from the direct pulses will be unhindered by later reflections. Experimentally, when the δ bond is used, one finds that the constancy of sound speed is improved, that the shape differences between first and second reflections become less and that the transit times are longer (measured speeds are lower) than for a thin bond.

5. Summary

The transient pulse technique of sound speed measurement has been shown to be highly accurate when used on nondispersive materials. Accuracies of the order of the precision, which is $\pm 5 \times 10^{-5}$, have been realized. The constancy of sound speed was used as the measure of accuracy. The accuracy of this technique is affected by a number of variables. The observed sound speeds are more nearly constant when using: (a) higher resonant frequency transducers, (b) earlier data in the pulse to set coincidences, (c) thick buffer bonds of δ thickness, which remove interference caused by the intrabond reflections, and (d) transducers of smaller diameter-to-thickness ratio. The obvious has been confirmed in that, as the sound speed constancy is improved, the leading edges of the first two reflections become more identical. Local acoustical uniformity of the test samples is very important and the NBS optical glass BSC 517 fills these requirements quite well. The choice of a multipath sample as opposed to many samples of different length removes much of the question of sample uniformity.

The author is deeply indebted to Martin Greenspan and Frank Breckenridge for discussions about the acoustical aspects, to Carl Tschiegg for help with certain electronic features, and to J. Wilson and C. Smith for typing. This work was supported in part by the U.S. Office of Naval Research.

6. References

[1] McSkimin, H. J., Measurements of elastic constants at low temperatures by means of ultrasonic waves, J. Appl. Phys. **24,** 988–997 (1953).

[2] McSkimin, H. J., Measurement of ultrasonic wave velocities and elastic moduli for small solid specimens at high temperature, J. Acoust. Soc. Am. **31,** 287–295 (1959).

[3] McSkimin, H. J., Empirical study of the effect of diffraction on velocity of propagation of high frequency ultrasonic waves, J. Acoust. Soc. Am. **32,** 1401–1404 (1960).

[4] McSkimin, H. J., Measurement of the 25°C zero-field elastic moduli of quartz by high frequency plane-wave propagation, J. Acoust. Soc. Am. **34,** 1271–1274 (1962).

[5] Papadakis, E. P., Ultrasonic phase velocity by the pulse-echo-overlap method incorporating diffraction phase corrections, J. Acoust. Soc. Am. **42,** 1045–1051 (1967).

[6] Greenspan, M., and Tschiegg, C. E., Sing around ultrasonic velocimeter for liquids, Rev. Sci. Instr. **28,** 897–901 (1957).

[7] Greenspan, M., and Tschiegg, C. E., Speed of sound in water by a direct method, J. Res. Nat. Bur. Stand. (U.S.), **59,** 249–254 (1957).

[8] Proctor, T. M., Low-temperature speed of sound in single-crystal ice, J. Acoust. Soc. Am. **39,** 972–977 (1966).

[9] Tschiegg, C. E., and Greenspan, M., An accurate time modulated pulse circuit, Rev. Sci. Instr. **24,** 183 (1953).

[10] Bateman, T. B., Some materials for ultrasonic transducer bonding at cryogenic temperatures, J. Acoust. Soc. Am. **41**, 1011–1014 (1966).

[11] Stern, R., Natale, G. G., and Rudnick, I., Isopentane bond for low temperature ultrasonics, Rev. Sci. Instr. **35**, 1077–1078 (1964).

[12] Forsythe, W. E., Smithsonian Physical Tables, The Lord Baltimore Press, 1954.

[13] Carnvale, A., Bower, P., Basileo, M., and Sprenke, J., Absolute sound-velocity measurement in distilled water, J. Acoust. Soc. Am. **44**, 1098–1102 (1968).

(Paper 75C1–312)

JOURNAL OF RESEARCH of the National Bureau of Standards — C. Engineering and Instrumentation
Vol. 75C, No. 1 January-March 1971

Seismic Response of Infrasonic Microphones*

Alfred J. Bedard, Jr.**

(November 19, 1970)

Factors affecting the (unwanted) seismic response of infrasonic microphones are indicated. Past measurements of ground motion deduced from the radiated atmospheric sound measured with infrasonic microphones are reviewed, and such measurements are compared with seismometer measurements of ground motion. Seismic motions caused by the Japanese earthquake of May 1968 are used in this example. The seismic response of the infrasonic microphone used for this measurement was experimentally determined and the results are presented. A simple method of compensating for interfering seismic effects on microphones is described.

Key words: Compensation; ground motion; infrasonic microphones; seismic response.

1. Introduction

If seismic motions caused by a distant earthquake are strong enough, an earthquake-associated air-pressure wave may be observed. These air-pressure changes are observed coincident with vertical motions of the earth in the immediate vicinity of the microphone, and are caused by radiation of sound into the atmosphere by the ground motions. Observations on such acoustical radiation have been reported previously [Cook and Young, 1962; Donn and Posmentier, 1965]. The amplitudes of vertical ground motion deduced from the air pressure measurements have been compared with ground motions measured with seismometers operated in the vicinity of the infrasonic microphones [Cook, 1965; Donn and Posmentier, 1965; Golitsyn and Klyatskin, 1967]. In general quite good agreement has been obtained using the two methods.

In addition to the infrasound caused by local ground motions, air pressure waves have been observed originating from both the vicinity of the epicenter of an earthquake [Benioff and Gutenberg, 1939; Mikumo, 1968] and from intermediate regions along the seismic wave propagation path [Benioff et al., 1951; Donn and Posmentier, 1965; Press and Ewing, 1951]. The Alaskan earthquake of 1964 provided examples of both these classes of earthquake-associated atmospheric sound waves [Donn and Posmentier, 1965].

An example of an atmospheric pressure disturbance generated by the local passage of seismic waves from distant seismic activity is the record shown in figure 1. The acoustic data from microphones in the vicinity of Washington, D.C., appear in the upper portion of this figure. The microphone array at a typical station is designed for measuring four principal characteristics of infrasonic waves: (1) the amplitude and waveform of the incident sound pressure, (2) the azimuth of arrival of the wave, (3) the horizontal phase velocity, and (4) the dominant period of the wave. An infrasonic station normally has four or more microphones equipped with noise-reducing devices located at ground level, approximately in the same plane and spaced about 7 to 10 km apart. Figure 2 shows the microphone layout for the Washington, D.C., station.

Each line-microphone produces frequency-modulated voltages proportional to the sound pressure in the atmosphere. The tones are usually transmitted by telephone wires to a recording location. At this central recording location these tones are demodulated, amplified, filtered, and recorded in analog form both as ink-on-translucent-paper traces, and on magnetic tape. The system pass-band is designated N7 and is shown in figure 3.

The disturbance shown in figure 1 is related to an earthquake on May 16, 1968, with the epicenter under the sea floor 100 miles east of Hachinohe, Honshu, Japan (U.S. Coast and Geodetic Survey, Preliminary Determination of Epicenter: $0 = 00^h\ 48^m\ 55.4^s$ UT, 40.84° N, 143.22° E, h = 7 km, $M_s = 7.9$). This disturbance was much smaller at Washington, D.C., than the disturbance following the 1964 Alaskan earthquake. It was thought that the smaller ground motions would make intercomparison with seismic data more feasible. Note that this disturbance was distinguished from local pressure changes caused by turbulent motions of the wind, because of its presence at all of the microphones of a multipartite array.

The analog acoustic record shown in figure 1 is a superposition of the recordings from the various microphone sites. The waveform coherence between the various sites is quite good. Note that the time marks are almost coincident at the chart speed of ¾ in/min, indicating a high horizontal phase velocity. The disturbance was distinguished from acoustic waves propagating in the atmosphere parallel to the earth's surface, by its higher horizontal phase velocity. Rayleigh waves on the earth's surface have a horizontal phase velocity of about 3 km/s, compared with 330 m/s for acoustic waves in the atmosphere.

The disturbance started at 0135 UT and was lost in noise at about 0214 UT. The observed periods ranged from 17 s to 40 s. The maximum amplitude occurred at

* An invited paper.

** Present address: National Oceanic and Atmospheric Administration, Wave Propagation Laboratory, Geoacoustics Group, Rockville, Md. 20852.

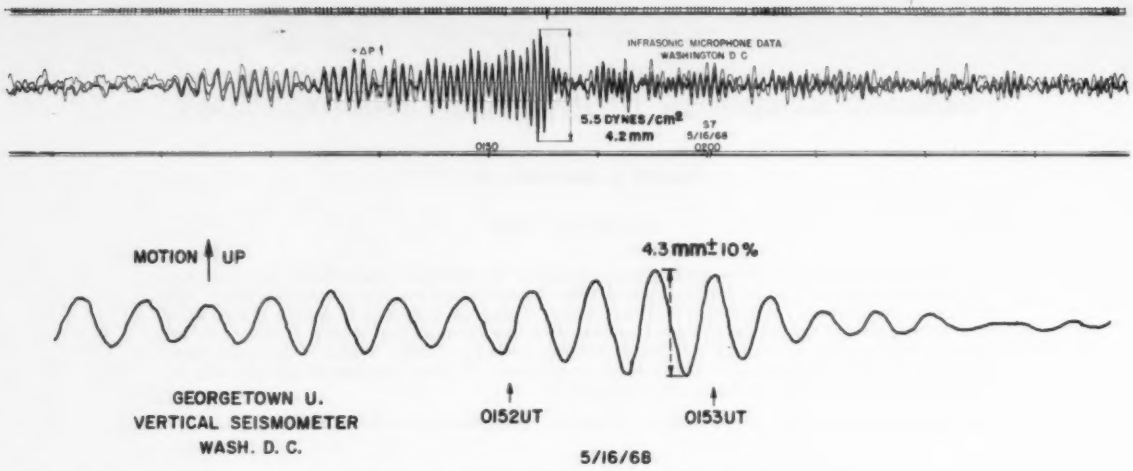

FIGURE 1. *Seismic disturbance of May 16, 1968.*

0153 UT and was 5.5 μbars at a period of 19 s. The ground displacement computed from these pressure data was 4.2 mm. The ground motion determined from seismometers located in Washington, D.C., was 4.3 mm. The Georgetown University Seismometer Laboratory made the recordings of ground motion shown in figure 1 available. The short-period worldwide standard seismograph was used in making the recording. The seismic data were corrected for system amplitude response before being compared with the infrasonic microphone records. Both measurements may be considered accurate to within ± 10 percent.

R. K. Cook [1965] has shown that the air pressures for such a disturbance are due to an integrated effect of the sound radiated by Rayleigh waves over a large area, as opposed to a seismometer which measures motion at a point; hence, it seems reasonable to consider infrasonic microphone data in order to obtain a more representative picture of ground motion over an area of the earth's surface. Infrasonic data will be useful for measurement of very large amplitude ground motions because the sound pressure levels will probably be larger than the pressure variations due to local winds. It is possible that for very large ground motions the dynamic range of sensitive seismometers will be exceeded, and then acoustical measurements can provide the desired measurements of the motions. But the microphones must perforce be

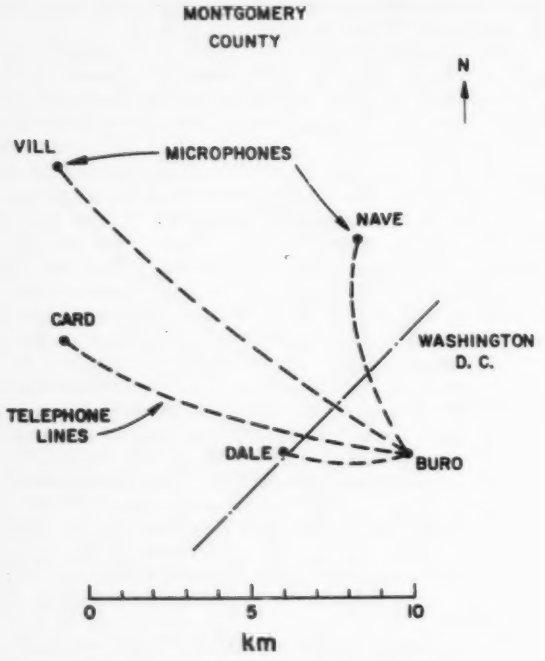

FIGURE 2. *Microphone site layout.*

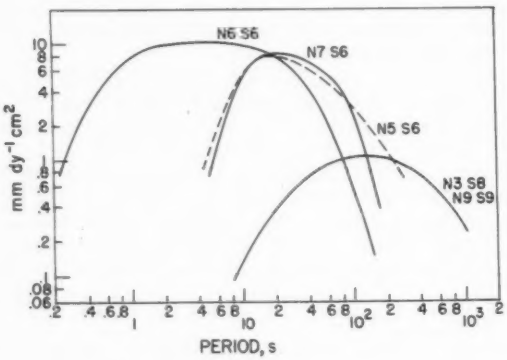

FIGURE 3. *Microphone system response.*

located on the surface of the earth, and they are therefore subjected to the latter's seismic motions. It is therefore necessary to determine the effects of the microphone's seismic motions on its electrical output. The effects might be small or negligible, but they must be known quantitatively.

2. Seismic Response Considerations

In attempting to test and evaluate the seismic response of infrasonic microphones several factors must be considered. Rayleigh waves occurring at the location of the pressure transducer generate peak pressure changes in the atmosphere calculated according to the relation

$$\Delta P = \rho c \omega X$$

where

$\omega = 2\pi f$
f = frequency of the wave
X = double amplitude of ground motion
ΔP = peak-to-peak pressure change in the atmosphere
ρ = density of air
c = velocity of sound in air.

This pressure change would be measured by the microphone together with any other instrumental seismic response effects that might be present. A frequently used form of infrasonic microphone is one that uses the motion of a diaphragm to detect pressure changes. This is the type of detector that will be considered here.

In addition to the pressure $\Delta P = \rho c \omega X$, such a transducer will respond to accelerations independently of any pressure changes occurring in the atmosphere. A transducer such as that shown in figure 4 will show seismic response due to both the diaphragm inertia and the inertia of air columns in the unit. Also, when the transducer is moved vertically through the atmosphere, a pressure change will be introduced whose magnitude will be equal to $\rho g X$. Pressure changes due to air motion past the microphone's openings to the atmosphere could also occur. The various factors contributing in theory to the seismic response are summarized as follows:

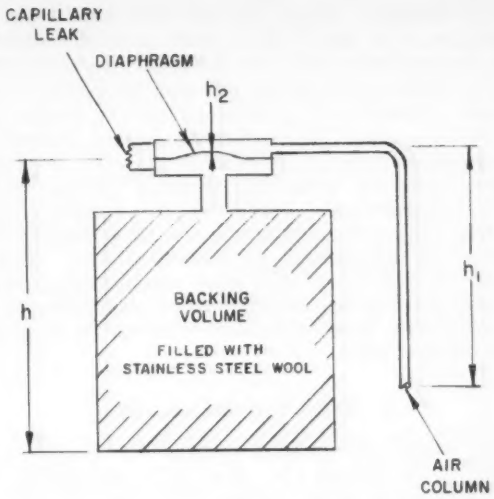

FIGURE 4. *Schematic view of microphone.*

Total Pressure Change		Hydrostatic Equation*		Bernoulli Pressures*
ΔP_{Total}	=	$\rho g X$	+	$1/2\,\rho V^2 + \ldots$

Open Tube Air Column Effects*		Diaphragm Inertia		Local Radiation		Closed Tube Air Column Effects
$\ldots\ \rho\omega^2 h_1 X$	+	$\omega^2 \rho_{\text{brass}} h_2 X$	+	$\rho\omega c X$		$\ldots + 1/2\,\rho\omega^2 h X$

where:

g = local gravitational acceleration
X = displacement double amplitude
h_1 = vertical height of microphone's external air column
h_2 = thickness of diaphragm
h = length of microphone's internal air column
V = maximum velocity of motion
$\omega = 2\pi f$
ρ = density of air
ρ_{brass} = density of the diaphragm
c = velocity of sound in air.

In experimentally testing seismic response on a vibration shaker, the effect of translating the transducer vertically through the atmosphere will have to be taken into account. Effects of local sound radiation by the shaker will be negligible. Note that the relation listed for air column effects is valid for an open-ended tube at low frequencies. The closed tube relation is half of this value. Microphone response to vertical displacements was tested at the National Bureau of Standards at Gaithersburg, Maryland, where Mr. James R. Houghton made available a shaker capable of producing approximately sinusoidal, vertical motions. The tests were performed at an ambient temperature of 22° C, a relative humidity of 20 percent, and an ambient pressure of 757 mm of Hg. The frequency of vertical motion was adjustable over the range 1 Hz to 0.01 Hz. The double amplitude was set to 4 in.

The microbarograph system consisted of a pressure transducer [Cordero et al., 1957] equipped with a 7.5 s high-pass acoustical filter. The system pass-band including Discriminator N4 and Filter Amplifier N10 had 3 dB points at 1 and 20 s. Figure 4 shows a schematic view of the system microphone mechanical configuration. The

* There are no contributions due to the hydrostatic equation or Bernoulli pressures during seismic wave transit. These two effects are important during an experimental evaluation of the microphone with a vibration shaker. The relation shown for open tube air column effects is valid only during vibration shaker type experiments at low frequencies.

microbarographic system was calibrated with a pistonphone, and a portable fixed-frequency pressure calibrator was operated before and after the seismic response tests. The pistonphone was a stainless steel wool-filled 50-gal volume equipped with a brass bellows variable-volume element to produce dynamic pressure changes. Theoretical considerations made it desirable to vary the key parameters while subjecting the infrasonic microphone to vertical displacements on a shaker at a number of frequencies. Since the experiment was performed in the presence of local atmospheric pressure variations, a time of low atmospheric pressure noise was chosen. Further, it was necessary to choose vibration amplitudes large enough for the expected pressure variations to be larger than the local noise level.

3. Experimental Results

The system response on a vibration shaker table was found, within experimental error, to be independent of the orientation of the microphone inlet to the atmosphere. Hence, it is inferred that inlet air blast and Bernoulli effects did not contribute to the electrical output of the microphone.

At longer periods than 5 s per cycle, the observed change in pressure closely approached the value to be expected from the hydrostatic term in the pressure equation. There is no direct frequency dependence involved in this term. Figure 5 shows the pressure measured as a function of frequency.

If the value for ΔP determined from the hydrostatic equation is subtracted from the observed pressure changes and the resulting data plotted as a function of frequency squared, the result is approximately a straight line in agreement with the predicted f^2 dependence. See figure 6 for a log-log plot of ΔP versus frequency squared.

The vertical external tubing length was varied in 5-in increments and the output of the system measured with the frequency of vibration kept constant at 1 Hz. The variation of pressure as a function of length of tubing below this valve is linear and changes as expected

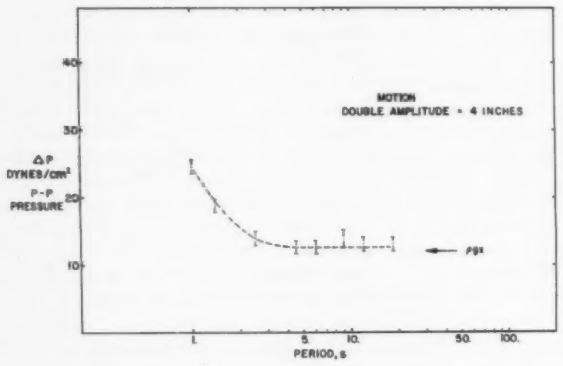

FIGURE 5. *Experimental response of microphone as a function of frequency of vertical motion.*

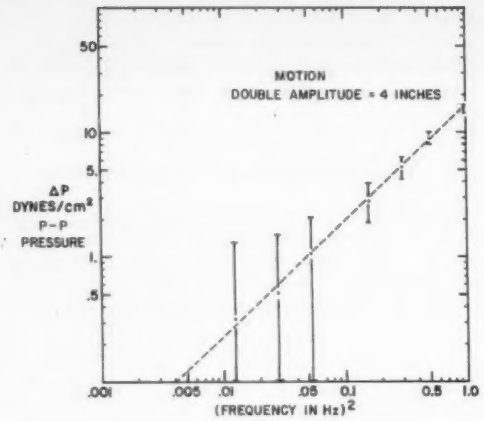

FIGURE 6. *Response of microphone as a function of frequency squared.*

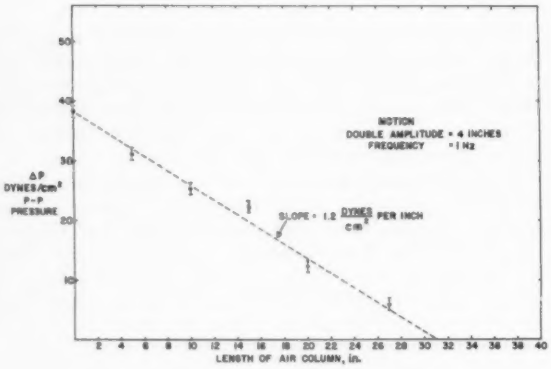

FIGURE 7. *Effect of air column length.*

($\Delta P \approx 1.2\ h_1$ at 1 Hz, where h_1 is in inches; fig. 7). This is approximately the slope of the line in figure 7.

Table 1 presents the contributions of the various seismic response mechanisms to the total pressure change observed. The outputs have been computed at frequencies of 1 Hz and 0.1 Hz and for displacement amplitudes of 0.001 in, 0.01 in, 0.1 in, and 1 in. Typical values are included in this table to show the relative importance of the various effective elements. The hydrostatic relation is also included for comparison purposes, although normally it would not be a factor in determining Rayleigh wave seismic response. The diaphragm compliance and effect of any backing volume sensitivity will reduce the system response, but these effects are not included in this worst-case consideration.

Because local background seismic noise amplitudes can be over 20 μm, the displacement amplitude of 0.001 in is a reasonable reference to use. Table 1 shows that the "loudspeaker action" effect from seismic waves will domi-

TABLE 1. *Seismic response contributions*

Generation mechanism		Displacement X, inches			
		$X = 0.001$	$X = 0.01$	$X = 0.1$	$X = 1$
1 Hz	$\rho g X$	0.003 μbar	0.03 μbar	0.3 μbar	3 μbar
	$\omega c \rho_{air} X$	.638 μbar	6.38 μbar	63.8 μbar	638 μbar
	$\omega^2 \rho_{brass} h_2 X$	.002 μbar	.02 μbar	.2 μbar	2 μbar
	$\omega^2 \rho_{air} h_1 X$	.003 μbar	.03 μbar	.3 μbar	3 μbar
0.1 Hz	$\rho g X$	0.003 μbar	0.03 μbar	0.3 μbar	3 μbar
	$\omega c \rho_{air} X$	.0638 μbar	.638 μbar	6.38 μbar	63.8 μbar
	$\omega^2 \rho_{brass} h_2 X$	$.2 \times 10^{-4}$ μbar	2×10^{-4} μbar	.002 μbar	.02 μbar
	$\omega^2 \rho_{air} h_1 X$	$.3 \times 10^{-4}$ μbar	3×10^{-4} μbar	.003 μbar	.03 μbar

$h_1 = 10$ in
$h_2 = 0.001$ in
$\rho_{brass} = 8.7$ g/cm^3
$g = 980.1$ cm/s^2

nate. The effects due to transducer seismic response are typically less than 1 percent of the "loudspeaker effect" at the pertinent frequencies. Thus, for this infrasonic microphone configuration, it is quite reasonable to deduce ground motions from observed pressure changes without correcting for instrument seismic response. Also, with the proper length of air column termination, one can null out the seismic response of the microphone at infrasonic frequencies. In the NOAA infrasonic microphone, the return hose from the microphone to the noise-reducing array accomplishes this. The open tube relation used here for computing this form of seismic compensation is valid only for shaker-type experiments with negligible local radiation. A seismically compensated microbarograph has been described [Ewing and Press, 1953] for use at periods longer than 20 s. A different method of seismic compensation is used.

Consideration of air column effects would suggest that caution should be exercised, for example, in installing an infrasonic microphone in a deep well and routing a tube to the surface. Since the air column seismic response is directly proportional to the length of the air column, a person might, in fact, be constructing a system sensitive to vibration. For 0.001-in tube displacements at 1 Hz, the seismically induced pressure amplitudes for an air column 10 ft long would be 0.03 μbar. This is over three times the internal noise level of the microphone now used by NOAA. Noise due to local vibrations would be increased.

I am grateful to Mr. Frank Baldwin, who did the art work on the illustrations, and to Rev. McConnell of Georgetown University, who provided the seismic records.

4. References

Benioff, H., Ewing, E. M., and Press, F., (1951), Sound waves in the atmosphere generated by a small earthquake, Proc. Natl. Acad. Sci. **37,** 600–603.

Benioff, H., and Gutenberg, B., (1939), Waves and currents recorded by electromagnetic barographs, Bull. Am. Meteorol. Soc. **20,** 421.

Bolt, B. A., (1964), Seismic air waves from the great 1964 Alaskan earthquake, Nature **202,** 1095–1096.

Cook, R. K., (1965), Radiation of sound by earthquakes, Fifth Congress International D'Acoustique, Liege.

Cook, R. K., and Young, J. M., (1962), Strange sounds in the atmosphere, Sound **1,** No. 3, 25–33.

Cordero, F., Mathesón, H., and Johnson, D. P., (1957), A non linear instrument diaphragm, J. Res. Nat. Bur. Stand. (U.S.), **58,** No. 6, 333–337.

Donn, W. L., and Posmentier, E. S., (1965), Ground-coupled air waves from the great Alaskan earthquake, J. Geophys. Res. **69,** No. 24, 5357–5361.

Ewing, M., and Press, F., (1953), Further study of atmospheric pressure fluctuations recorded on seismographs, Trans. Am. Geophys. Union **34,** No. 1, 95–100.

Golitsyn, G. S., and Klyatskin, V. I., (1967), Atmospheric oscillations caused by movements of the earth's surface, Izv, Atmospheric and Oceanic Physics **3,** No. 10, 1044–1052.

Mikumo, T., (1968), Atmospheric pressure waves and tectonic deformation associated with the Alaskan earthquake of March 28, 1964, J. Geophys. Res. **73,** No. 6, 2009–2025.

Press, F., and Ewing, M., (1951), Ground roll coupling to atmospheric compressional waves, Geophysics **16,** 416–430.

(Paper 75C1–313)

JOURNAL OF RESEARCH of the National Bureau of Standards — C. Engineering and Instrumentation
Vol. 75C, No. 1, January-March 1971

Publications of the National Bureau of Standards*

Selected Abstracts

Achenbach, P. R., Project Director and Coordinator, **Investigation of performance characteristics for sanitary plumbing fixtures,** *Nat. Bur. Stand. (U.S.), Bldg. Sci. Ser. 22, 72 pages (Jan. 1970), 70 cents, SD Catalog No. C13.29/2:22.*

Key words: Abrasion resistance; chemical resistance; cigarette-burn resistance; cleanability and soilability; concentrated static-load capacity; performance characteristics; performance level; santiary plumbing fixtures; scratch resistance; stain resistance; surface-impact resistance; test methods.

This report gives findings and recommendations developed during an investigation of performance characteristics for sanitary plumbing fixtures, conducted at the request of the Building Research Advisory Board of the National Academy of Sciences—National Research Council. The report describes the test methods that are recommended for the evaluation of 16 performance characteristics, and the nature of further work required to complete the development of four or five additional test procedures.
The suitability of various existing test methods for evaluating the functional and performance characteristics of sanitary plumbing fixtures was investigated in the laboratory. In addition, new or modified tests for certain characteristics were developed. The laboratory work was performed only on bathtubs and flat specimens provided by industry through appropriate arrangements with the Building Research Advisory Board. Field inspection trips were made to provide the NBS project staff with up-to-date information on certain manufacturing processes and on installation and use problems. The complexities involved in the selection of valid performance levels are discussed, as well as the elements of judgment involved. A format that might be used in specifying performance is suggested for each test procedure, and the rationale underlying each suggested format is given.

Adams, J. W., Jarvis, S., Jr., **Current distribution in barretters and its application to microwave power measurements,** *IEEE Trans. Micro. Theory Tech.* **MTT-17,** *No. 10, 778–785 (Oct. 1969).*

Key words: Barretter; bolometer; microwave power measurement; substitution error; current distribution in barretter.

This paper describes a mathematical analysis for determining the microwave current distribution in a barretter in a rectangular waveguide. This distribution, when used with another analysis which calculates substitution error for any given current distribution will provide a previously missing step necessary for calibrating microwave and millimeterwave barretters for absolute power measurements.

Alley, C. O., Chang, R. F., Currie, D. G., Poultney, S. K., Bender, P. L., Dicke, R. H., Wilkinson, D. T., Faller, J. E., Kaula, W. M., MacDonald, J. F., Mulholland, J. D., Plotkin, H. H., Carrion, W., Wampler, E. J., **Laser ranging retro-reflector: Continuing measurements and expected results,** *Science* **167,** *No. 3918, 458–460 (Jan. 30, 1970).*

Key words: Geophysics; laser; lunar motion; selenology.

After successful acquisition in August of reflected ruby laser pulses from the Apollo 11 laser ranging retro-reflector (LRRR) with the telescopes at the Lick and McDonald observatories, repeated measurements of the round-trip travel time of light have been made from the McDonald Observatory in September with an equivalent range precision of ±2.5 meters. These acquisition period observations demonstrated the performance of the LRRR through lunar night and during sunlit conditions on the moon. Instrumentation activated at the McDonald Observatory in October has yielded a precision of ±0.3 meter, and improvement to ±0.15 meter is expected shortly. Continued monitoring of the changes in the earth-moon distance as measured by the round-trip time of light from suitably distributed earth stations is expected to contribute to our knowledge of the earth-moon system.

Balcom, M. M., **Influence of red and blue pre-adaptation on hue matching of purple samples,** *J. Opt. Soc. Am.* **60,** *No. 1, 118–121 (Jan. 1970).*

Key words: Adaptation; color; hue; vision.

This experiment was designed to show the effect, if any, of chromatic adaptation on hue matching of purple painted samples of different saturations. Five experienced observers were adapted for one minute to a red field, then asked to find the hue match for each of three test samples from among a set of samples representing the complete hue circuit in 100 steps at middle saturation. The three test samples were of slightly greater saturation and representative of a range of purple samples. The entire procedure was repeated with blue and neutral pre-adapting fields, all under Source C illumination. Results indicated that pre-adaptation did influence the hue-match selections, the average red-blue adaptive shift being about one Munsell hue step. Observers made systematically different hue matches for the same test sample in accordance with their ages. A method for determining graphically the state of adaptation at the time the hue judgments were made showed the chromaticity of the test samples to be at least as influential as either the neutral surround used or the pre-adaptation stimuli.

Beatty, R. W., Editor, **Commission 1 progress in radio measurement methods and standards (Triennial report of progress),** *Radio Sci.* **4,** *No. 7, 579–590 (July 1969).*

Key words: International scientific radio union report; measurement methods; radio measurements; radio standards; URSI XVIth General Assembly.

A review of progress within the USA in Radio Standards and Measurement Methods, covering the period 1966-1968, inclusive, is presented. This review is a part of the Triennial Report of the U. S. National Committee of URSI (International Scientific Radio Union) to the XVIth General Assembly of URSI.
The following topics dealing with the U. S. A. progress in Radio Standards and Measurement Methods are included: 1) Time and Frequency, 2) CW Power, 3) CW Voltage, 4) Noise, 5) Pulsed Voltage and Power, 6) Attenuation, Phase Shift, and Time Delay, 7) Impedance, 8) Antenna Characteristics, 9) Field Strength, 10) RF Properties of Materials, 11) Broadband Measurement Techniques, and 12) Laser Measurements.
The report does not include all the developments which have occurred in the U.S.A. in the period indicated, but rather has attempted to include the most significant developments in each field.

Becker, E. D., Ferretti, J. A., Farrar, T. C., **Driven equilibrium fourier transform spectroscopy. A new method for nuclear magnetic Resonance signal enhancement,** *J. Am. Chem. Soc.* **91,** *7784–7785 (1969).*

Key words: Driven-equilibrium; Fourier-transform; high resolution; nuclear magnetic resonance.

A new method using a high-resolution pulsed NMR spectrometer is described by which the equilibrium magnetization of nuclei with long T_1 may be restored rapidly in order to take full advantage of the Fourier transform technique.

Bender, P. L., Alley, C. O., Currie, D. G., Dicke, R. J., Faller, J. B., **Some implications for physics and geophysics of laser range measurements from earth to a lunar retro-reflector,** *(Proc. Conf. NATO Advanced Study Institute, University of Newcastle, Upon Tyne, England, Mar.-Apr. 1967), Chapter in The Application of Modern Physics to the Earth and Planetary Interiors, S. K. Runcorn, Ed., pp. 523–530 (John Wiley and Sons Inc., London, England, 1969).*

Key words: Astronomy; continental drift; geophysics; gravity; laser; lunar; moon.

The technique of high-accuracy laser range measurements to an optical retro-reflector package on the moon is discussed. The information which can be obtained by this method about the hypotheses of continental drift and ocean floor spreading and about the motion of the pole is described. A method for checking on the constancy of the gravitational constant is also given. The accuracy with which information on all of these questions can be obtained from lunar range measurements is higher than for any other methods which have been suggested.

Berger, M. J., Seltzer, S. M., **Calculation of energy and charge deposition and of the electron flux in a water medium bombarded with 20-MeV electrons,** *(Proc. Conf. High Energy Radiation Therapy Dosimetry under the auspices of the American Association of Physicists in Medicine, New York, N. Y., June 15-17, 1967), Ann. N. Y. Acad. Sci.* **161,** *Art. 1, 8–23 (July 3, 1969).*

Key words: Charge deposition; electrons; energy deposition; flux; Monte Carlo; multiple scattering.

A combination of Monte Carlo and analytical techniques is used to compute the penetration of fast electrons in water, taking into account multiple elastic scattering by atoms, multiple inelastic scattering by atomic electrons, and the production of bremsstrahlung. Secondary electrons are also considered which result from electron-electron collisions, or from the absorption or scattering of bremsstrahlung. The calculation provides information about the spatial distribution of energy deposition, charge deposition and the electron flux (primary and secondary) down to a spectral energy of 400 eV. Representative results are presented, mainly for 20-MeV electrons incident perpendicularly on a semi-infinite water medium.

Birky, M. M., **Simultaneous recording of near-field and far-field patterns of lasers,** *Appl. Opt.* **8,** *No. 11, 2249–2253 (Nov. 1969).*

Key words: Laser; near-field and far-field diffraction; ruby and neodymium.

A technique for simultaneous recording of near-field and far-field diffraction patterns at several exposures for a single laser pulse has been developed. A ruby laser and a neodymium doped glass laser have been investigated. The Nd^{+3} laser shows striking high order cylindrical mode operation as a result of thermal stress. The time resolved output of this laser shows the usual spikes about 500 nenoseconds wide. When the cylindrical mode operation takes place some of the spikes consist of a large number of ultrashort pulses.

Blandford, J. M., **In-plant testing for wash-and-wear apparel performance and labeling,** *Third Annual Tech. Conf. The Apparel Research Foundation, Inc., Washington, D. C., Oct. 14-16, 1969, 12 pages (Oct. 14, 1969).*

Key words: Apparel; care instructions; labeling, apparel; performance, apparel; properties, apparel; testing textiles; wash-and-wear.

A distinction is made between washable garments, in general, and wash-and-wear apparel, in particular, with reference to the properties associated with appearance, performance, and ease of care. The testing equipment, testing procedures, and evaluation materials required by the apparel manufacturer in his assessment of these properties and formulation of ease-of-care instructions for labels and hang tags, are discussed. Tabulations and charts are included.

Brady, E. L., **The National Standard Reference Data System,** *Mater. Res. Std.* **9,** *No. 10, 19–21 (Oct. 1969).*

Key words: Critical evaluation; information centers; information services; NSRDS; physical properties; standard reference data.

The National Standard Reference Data System is a government-wide effort to give to the technical community of the United States optimum access to the quantitative data of physical science, critically evaluated and compiled for convenience. This program was established in 1963 by the President's Office of Science and Technology, acting upon the recommendation of The Federal Council for Science and Technology. The NBS has been assigned responsibility for administering the effort. The general objective of the NSRDS is to coordinate and integrate existing data evaluation and compilation activities into a systematic, comprehensive program, supplementing and expanding technical coverage when necessary, establishing and maintaining standards for the output of the participating groups and providing mechanisms for the dissemination of the output as required. The NSRDS is conducted as a decentralized operation of nation-wide scope with central coordination by NBS. It comprises a complex of data centers and other activities carried on in government agencies, academic institutions and non-governmental laboratories. The independent operational status of existing critical data projects is maintained and encouraged. Data centers that are components of the NSRDS produce compilations of critically evaluated data, critical reviews of the state of quantitative knowledge in specialized areas and computations of useful functions derived from standard reference data.

Branscomb, L. M., **Truth in packaging of scientific information,** *Meas. Data* **3,** *No. 5, 104–105 (Sept.-Oct. 1969).*

Key words: Reviews; science information; scientific literature.

This is an edited version of a talk presented to the Precision Measurements Association meeting in Boulder, Colorado, August 28, 1968.
No new technical information is contained in the manuscript.

Brauer, G. M., Termini, D. J., Burns, C. L., **Characterization of components of dental materials and components of tooth structure by differential thermal analysis,** *J. Dental Res.* **49,** *No. 1, 100–110 (Feb. 1970).*

Key words: Characterization of dental materials; components of tooth structure; dental materials materials; differential thermal analysis (DTA); differential thermal analysis of calcium phosphates.

Differential Thermal analysis (DTA) has been employed to characterize a variety of dental materials, components of tooth structure, as well as certain phosphates related to the mineral components of tooth structure. The technique was applied to the rapid comparison of similar materials, quality control of ingredients and products used in restorative dentistry, determination of melting ranges especially those of dental waxes and gold alloys, and studies of reactions occurring at elevated temperatures. The DTA technique is simple and requires only a few milligram sample. Thus it should prove especially useful for specification testing of melting ranges of dental materials, for establishing proper curing procedures, determining catalyst effectiveness and measuring storage stability in various environments.

Braun, W., Carrington, T., **Line emission sources for concentration measurement and photochemistry,** *J. Quant. Spectr. Radiative Transfer* **9,** *1133–1143 (1969).*

Key words: Absorption; analysis; gas; photochemistry; spectroscopy; vacuum ultraviolet.

When a resonance line is absorbed in its own gas, measurements of this absorption can be used to derive a value of the product, *nf*, of concentration of the absorber and f value of the transition. This line absorption process is also important in the study of fluorescence and photochemistry, where it is possible to produce atoms or molecules in a single quantum state without otherwise

disturbing the system. The interpretation and success of these applications of line absorption depend critically on the shape of the line emitted by the light source. This is strongly influenced by the optical depth in the emitting region, and by the inevitable presence of a reversing layer through which the light must travel on its way out of the lamp. This paper presents a simple model which can be used to estimate the effects of these properties of the light source on the threshold and sensitivity of measurements of *nf*, and on the power which can be delivered to absorbing atoms outside the lamp. Emphasis is on the general principles of lamp design and diagnosis, rather than on accurate description of a particular lamp.

Brenner, F. C., **Research for a uniform quality grading system for tires,** *Rubber Chem. Technol.* **42,** *No. 5, 1446–1449 (Dec. 1969).*

Key words: Bias ply; grading; passenger car; radial; speed capability; tires.

The National Traffic and Motor Vehicle Safety Act of 1966 requires the establishment of a *uniform quality grading system.* This paper discusses the needs for the system and the complexity of the problem. The system proposed here will depend on five properties; tread wear, traction, impact resistance, endurance, and wheel speed capability.

Brenner, F. C., Barton, F. W., **Cuts and cut growth in tires,** *Rubber Chem. Technol.* **42,** *No. 5, 1462–1465 (Dec. 1969).*

Key words: Cut growth; cutting; road test; tires.

Forty tires were subjected to severe road use on a course (approximately 3500 miles) that included Belgian block, over highways at turnpike speeds while overloaded. The course was repeated until the tires were worn smooth. At the end of each course, the number of new cuts and the length of all cuts in grooves was determined. Ten miles of Caliche (sharp stones) road was included between the first and second measuring period.
The tires experienced a total of 169 cuts. Forty seven (47) of these grew, 34 of which grew less than 0.11 inches. No cut grew continuously throughout the test. The cuts grew but not enough to cause tire failure except in one case where the cut exposed the fabric.

Brenner, F. C., Mandel, J., Simson, B. G., **Research for a uniform quality grading system for tires. II. Wheel speed capability test,** *Rubber Chem. Technol.* **42,** *No. 5, 1450–1461 (Dec. 1969).*

Keywords: Bias ply; grading; passenger car; radial; speed capability; tires; winter.

The wheel speed capability of a tire is defined by a test method which determines the speed at which the tire fails on a laboratory test wheel. Data is reported on over 100 different passenger car tires of all grades and types over a range of sizes.
A scaling system is devised for this property. It is found that the system produces consistent results for tires of given manufacturer's nominal grade across the size range tested and for samples produced several months apart.

Cassidy, E. C., Cones, H. N., **Electro-optical observations and measurements of distorted high-intensity electric fields,** *Proc. Conf. Electrical Insulation and Dielectric Phenomena, Buck Hill Falls, Pa., Oct. 20-22, 1969, pp. 77–86 (National Academy of Sciences, Washington, D. C., 1970).*

Key words: Dielectric liquids; electro-optical measurements; electrostatic field measurements; high voltage measurements; kerr cell.

The electric field between electrodes immersed in a dielectric liquid is often distorted by the presence of space change, thus making analytical determination of the field distribution extremely difficult. This work utilizes laser light for Kerr electro-optical analysis of distorted electric fields imposed when high direct voltages are applied to nitrobenzene-filled Kerr cells. Two-dimensional fringe images, similar to those achieved in photoelastic mechanical stress analysis, are observed. Regions of high electrical stress are detected directly from concentrations of a greater number of fringes. Field profiles observed with voltages as high as 90 kV applied to cells with various interelectrode distances are presented. Space-resolved meaurements of relative field strength, actual field strength (in V/cm) and potential are also derived. The measurement techniques employed are believed to be accurate within 1%.

Cassidy, E. C., Cones, H. N., **Use of expanded laser beam to analyze high-intensity electric fields,** *J. Soc. Motion Picture Television Engrs.*

Key words: Electric field measurements; electrooptical measurements; high voltage measurements; Kerr cell; laser applications; pulse measurements and dielectric liquids.

A Kerr electrooptical technique that permits observation and mapping of distorted high-intensity electric fields has been devised at NBS. Analysis of the field profile from two-dimensional fringe images, similar to those observed in photoelastic mechanical stress analysis, permits calibration of the Kerr System for measurement of high-voltage pulses, and determination of relative field strength, actual field strength, and potential.

Catanzaro, E. J., Champion, C. E., Garner, E. L., Marinenko, G., Sappenfield, K. M., Shields, W. R., **Standard reference materials: Boric acid; isotope and assay standard reference materials,** *Nat. Bur. Stand. (U.S.), Spec. Publ. 260-17, 70 pages (Feb. 1970), 65 cents, SD Catalog No. C13.10:260-17.*

Key words: Absolute ratios; assay standards; boron; coulometry; isotopic standards; mass spectrometry.

A precise coulometric titration method has been developed for the assay of boric acid. The method is capable of providing boric acid assays precise to within 0.0025 percent (1 sigma) which is an order of magnitude better than existing techniques. Using this method, a lot of high purity boric acid has been assayed and found to be virtually stoichiometric H_3BO_3. Its acidimetric assay value of 100.00 ± 0.01 percent characterizes this material as a primary chemical standard for boron determinations.
Multiple samples of boric acid were studied and characterized with respect to homogeneity and the effect of relative humidity on stoichiometry. Procedures for precise preparation, aliquoting and storage of boric acid solutions were devised.
A mass spectrometric technique for the precise measurement of boron isotope ratios was developed. Single-filament tantalum-ribbon sources are used, and $^{11}B/^{10}B$ ratios are determined by measuring the relative abundances of $Na_2{}^{11}BO_2{}^+$ and $Na_2{}^{10}BO_2{}^+$ ions, at masses 89 and 88, respectively. The effects of various parameters such as sample mounting procedure, filament material, sample size, total sample composition and sodium concentration were studied and alternative procedures were evaluated.
Absolute values were obtained for the isotopic abundance ratios of two boron isotopic standards, using surface emission mass spectrometry. Samples of known isotopic composition, prepared from nearly pure separated boron isotopes, were used to calibrate the mass spectrometers. The resulting absolute values are: SRM 951, Boric Acid, $^{11}B/^{10}B = 4.04362 \pm 0.00137$; and SRM 952, Boric Acid, $^{11}B/^{10}B = 0.053199 \pm 0.000032$. The indicated uncertainties are overall limits of error based on 95 percent confidence limits for the means and allowances for effects of known sources of possible systematic error.

Cezairliyan, A., **High-speed methods of measuring specific heat of electrical conductors at high temperatures (A review),** *High Temperatures—High Pressures* **1,** *517–529 (1969).*

Key words: High-speed measurements; high temperature; specific heat; thermodynamics; thermophysical properties.

Needs and advantages of high-speed methods (subsecond duration) for the measurement of specific heat of electrical conductors at high temperatures are presented. The high-speed methods are described and classified according to ambient and operational conditions. Measurement and recording of experimental quantities are discussed. A historical development and the major features of

high-speed experiments are summarized. A discussion and conclusions regarding the advantages of various high-speed methods and their application are given.

Chandler, R. F., Christian, R. A., **Crash testing of humans in automobile seats,** *Proc. Society of Automotive Engineers Safety Conf. May 13-15, 1970, Detroit, Mich., and June 8-11, 1970, Brussels, Belgium, Intern. Safety Conf. Compendium No. P-30, 112–132 (Society of Automotive Engineers, Inc., New York, N.Y., June 1970).*

Key words: Automobile; automobile interior; automobile seats; crash testing.

The design of the automobile interior is largely based upon design data gathered under static conditions, where the inertial properties of the human body do not enter into consideration. Anthropometric data based on static measurements are valid for design of clearance and access for normal operation of the vehicle, and have been widely collected and used for these purposes. The requirements of the human operator or passenger during a crash are not as well documented. Clearances, paths of travel, velocities along the path and other dynamic data are of vital interest to the designer. Because of the difficulties in obtaining information about humans under crash conditions, most of the available guidelines are based upon dummy or cadaver tests. Until adequate human data are available, the designer must use the information obtained from human simulators and consider it only an unconfirmed approximation.
To alleviate this shortage of human impact data, the National Bureau of Standards initiated a research program in cooperation with the 6571st Aeromedical Research Laboratory. Tests were conducted on the Daisy Decelerator at Holloman AFB to gather comparative data about human and dummy test subjects under crash conditions using automotive seating and restraint systems. The data presented in this report include 32 human tests of controlled impacts of approximately the same magnitude. Variables are the type of restraint, either lap belt or lap belt plus single diagonal, and subject size. All tests were conducted in the —Gx orientation using a production automobile bucket seat. Data presented include the displacement paths of the subjects during the impact, the maximum velocity along the path, anthropometric data, loads generated in the restraint system, and medical and subjective evaluation of the impacts.

Christ, B. W., **On the mechanism of interstitial-impurity-induced cross-slip in iron deformed near 175°K,** *Acta Met.* **17,** *No. 10, 1317–1321 (Oct. 1969).*

Key words: Cross slip; ductility; interstitial impurity; iron; nitrogen; yield stress.

A mechanism is proposed whereby the elastic dipole distortion of stationary interstitial impurity atoms in lattice solution can promote nucleation and stabilization of double-kink-size dislocation segments on cross-slip planes. Stress relaxation accompanying interstitial-impurity-induced cross-slip can account for the experimental observations that small atom fractions of nitrogen in lattice solution in iron deformed around 175°K decrease yield and flow stresses and increase ductility.

Christ, B. W., Gamble, R. P., Smith, G. V., **On the distinction between alloy softening due to nitrogen and nickel in dilute lattice solution in iron,** *Script. Met.* **3,** *No. 8, 521–530 (Aug. 1969).*

Key words: Alloy softening; elastic; electronic; Fe-N alloys; Fe-Ni alloys; flow stress; lower yield stress; mobile dislocation density; Peierls stress.

Alloy softening (AS) is the decrease in yield and flow stresses of iron and other b.c.c. metals which accompanies increasing quantities of solute in lattice solution, within critical ranges of solute concentration and temperature. This note is a comparison of existing alloy softening data on Fe-N and Fe-Ni. Whereas AS in each alloy system is due to a reduction in the thermal component of stress, the basic cause of the reduction is different in each system. This is inferred from differences in the concentration and temperature dependence of AS for each alloy system. AS in Fe-N is attributed to an increase in mobile dislocation density during yielding and flow, as compared with that of hydrogen-purified iron, arising from the mechanism of interstitial-impurity-induced cross-slip. AS in Fe-Ni is attributed to a systematic reduction in the Peierls stress of iron with increasing Ni. Whereas AS in Fe-N is primarily of elastic origin, AS in Fe-Ni is primarily of electronic origin.

Christensen, R. G., Hoeve, C. A. J., **Comparison between theoretical and experimental values of the volume changes accompanying rubber extension,** *J. Polymer Sci.* **8,** *Part A-1, 1503–1512 (1970).*

Key words: Dilatometer; free energy; intramolecular interactions; intermolecular interactions; rubber elasticity; thermodynamics; volume change.

The molecular theory of rubber elasticity assumes the free energy to consist of two parts: a liquid-like free energy that is governed by intermolecular interactions and is independent of strain at constant volume and an intramolecular interaction free energy equal to the sum of the free energies of the chains making up the network. The volume increases of rubber samples as a function of their length were found to be considerably larger than predicted by the molecular theory. Therefore, contrary to common belief, the values of $(\partial E/\partial L)_{V,T}$ may not be related solely to changes in intramolecular interactions with extension. Also, the usual procedure to obtain values of $(\partial E/\partial L)_{V,T}$ from measurements of $(\partial f/\partial T)_{p,L}$ with the aid of the molecular theory is not strictly correct.

Clark, A. F., Childs, G. E., Wallace, G. H., **Low-temperature electrical resistivity of some engineering alloys,** *(Proc. 1969 Cryogenic Engineering Conf., June 16–18, 1969, Univ. of California, Los Angeles, Calif.), Chapter in Advances in Cryogenic Engineering 15, Paper No. C-5, 85–90 (Plenum Press, Inc., New York, N.Y. 1970).*

Key words: Aluminum alloys; copper alloys; electrical resistivity; iron alloys; nickel alloys; titanium alloys.

The electrical resistivities of several engineering alloys have been measured at 4K, 20K, 76K, 192K, and 273K. Different iron, nickel, copper, titanium and aluminum alloys have been measured, some of them in different heat treated conditions. Most of the alloys have a smooth decrease in resistivity with decreasing temperatures, but some unusual results are reported. Comparisons are made between different alloys and between different heat treatments of the same alloys.

Currie, L. A., **Indirect estimation of component variability in chemical and physical systems,** *Anal. Chem.* **41,** *No. 14, 2051–2054 (Dec. 1969).*

Key words: Chemical microstandards; correlation coefficient; indirect variability estimation; stoichiometry; two-component system.

An indirect method is presented for assessing the variability of a chemical component or a physical property, when that property may not be directly observed. The method is based upon a simple physical model incorporating stoichiometry and the observation of the variability of a second, related property and/or the ratio of the two properties. A principal result of the investigation is an expression giving limits for the relative standard deviation of component-A, ϕ_A: $| \phi^2_{A\,B} - \phi^2_B | \leq \phi^2_A \leq \phi^2_{A\,B} + \phi^2_B$ where $\phi_{A\,B}$ and ϕ_B represent the relative standard deviations of the ratio of components $-A$ and $-B$ and of component-B, respectively. Information is also obtained on bounds for the correlation coefficient.

Deslattes, R. D., **Optical and x-ray interferometry of a silicon lattice spacing,** *Appl. Phys. Letters* **15,** *No. 11, 386–388 (Dec. 1969).*

Key words: Interferometer; lattice parameter; x-ray.

A device permitting simultaneous x-ray and optical interferometry over traverses in excess of 20 μm is reported. Results obtained to

date suggest that such devices will permit measurements of certain crystal lattice parameters with accuracies better than one part per million.

Durst, R. A., **Fluoride microelectrode—fabrication and characteristics,** *Anal. Chem.* **41,** *No. 14, 2089–2090 (Dec. 1969).*

Key words: Fluoride analysis; fluoride microanalysis; fluoride microelectrode; ion-selective microelectrode; microelectrode; potentiometry.

A fluoride ion-selective microelectrode has been constructed with a volume requirement of less than 2 μl. This microelectrode has the advantage of being suitable for *in situ, in vivo,* and continuous analysis of microliter volumes of solution. Details of construction and the response characteristics are given. Nernstian response is observed down to less than $10^{-6}M$ fluoride. Further miniaturization is feasible by extension and refinement of this design.

Ederer, D. L., **Computer analysis of resonance profiles by the method of least squares,** *Appl. Opt.* **8,** *No. 11, 2315–2325 (Nov. 1969).*

Key words: Beutler-Fano resonance profiles; least squares analysis; parameter correlation; random errors; slit function; slit width-resonance ratio; systematic errors.

The method of least squares has been applied to the analysis of resonance profiles described by the Beutler-Fano (BF) absorption cross section. To illustrate the method, parameters were determined for experimental data having BF profiles of (a) the asymmetric, enhanced absorption type, (b) the "window" type, and (c) the Lorentzian absorption type. Systematic and random errors, and correlation among the parameters were studied as a function of the slit width to resonance width ratio by applying the least squares fitting method to data computed by folding the BF transmission profile with a gaussian slit function. High correlation among the parameters and parameter fractional standard deviations of 10% to 20% for data with a standard deviation of 0.01 are an incentive to keep the slit width to resonance width ratio less than two for "window" type resonances. In addition it was found that the parameters describing a resonance could be determined with the greatest precision in a given time when the slit width to resonance width ratio was of order one. It was found that systematic errors greater than about one percent resulted if the number of mesh points used to approximate the convolution integral in the fitting procedure was less than at least two per resonance width. Also, for resonances whose width was equal to the slit width, systematic errors in the parameter values of order ten percent resulted if the width of slit function used in the fitting procedure differed from the "actual" slit function by ten percent.

Eick, J. D., Caul, H. J., Hegdahl, T., Dickson, G., **Chemical composition of dental gold casting alloy and dental wrought gold alloys,** *J. Dental Res.* **48,** *No. 6, 1284–1289 (Nov.-Dec. 1969).*

Key words: Casting gold alloys; chemical composition; dental gold alloys; gold; platinum; wrought gold wire; x-ray emission.

The chemical composition of 136 dental casting gold alloys and 21 dental wrought gold wire alloys was determined by an x-ray emission method. The changes in composition from 1928 and 1932 to the present time are small. There has been a decrease in platinum content in both castings and wires. About 1% nickel is found in the present-day wire which was not present in 1928 and 1932.

Freeman, D. H., Currie, L. A., Kuehner, E. C., Dixon, H. D., Paulson, R. A., **Development and characterization of ion-exchange bead microstandards,** *Anal. Chem.* **42,** *No. 2, 203–209 (Feb. 1970).*

Key words: Ion exchange; microstandards; nanogram.

The encapsulation of Na or Ca by ion exchange beads is investigated in the counterion mass range below one nanogram. Preparative methods are described for obtaining the exchanger in a pure counterion form and for subsequent prevention of ion exchange so that the isolation of a single bead is possible in the absence of significant contamination. Activation Analysis indicated that the network heterogeneity was characterized by a 5% relative standard deviation for Na in measurements extending to 3×10^{-12} grams. A bead diameter measurement is equivalent to a counterion mass determination and this opens the door to the use of the beads as microstandards in the mass region where no other methods are applicable.

Freeman, D. H., Zielinski, W. L., Jr., Editors, **Separation and Purification Section: Summary of activities July 1968 to June 1969,** *Nat. Bur. Stand. (U.S.), Tech. Note 509, 73 pages (Feb. 1970), 70 cents, SD Catalog No. C13.46:509.*

Key words: Gas chromatography; infrared analysis; ion exchange; liquid chromatography; purification; separation; styrene/divinylbenzene; ultra-pure reagents.

This is the annual progress report on the Separation and Purification Section activities. The major task of developing a certified ion exchange microstandard as a Standard Reference Material is presented in terms of the preparative and characterizational work involved. Fundamental studies of ion exchange substrates includes the application of quantitative analytical infrared spectrophotometry to measure crosslinking in the copolymer network, and to determine the degree of sulfonation. Optical microscopy is applied to the study of swelling kinetics for single copolymer particles. Analytical gas chromatography is applied to the isomers of divinylbenzene. The recently acquired quadrupole mass spectrometer is decribed. Liquid chromatography at high pressures and with high resolution has been begun recently. The activities of a project dealing exclusively with ultrapure reagents is described including the problems of contamination free storage.

Gadzuk, J. W., **Resonance tunneling through impurity states in metal-insulator-metal junctions,** *J. Appl. Phys.* **41,** *No. 1, 286–291 (Jan. 1970).*

Key words: Electron tunneling; junctions; impurities; metal-insulator-metal structures.

Motivated by the recent work of Parker and Mead on the effects of impurity trapping states in Schottky barriers, a theory of resonance tunneling through absorbed atoms in field emission is modified to treat resonance tunneling through isolated and uniformly distributed impurities in the insulating layer of a metal-insulator-metal tunnel junction. In analogy with the magnetic impurity tunneling theory of Appelbaum, the effects of resonant tunneling through impurity states opens up new tunneling channels with a concomitant change of slope in the I–V characteristics. These changes should be apparent as definite structure in curves of $d\sigma/dV$ versus voltage although depending upon the impurity concentrations and impurity level positions relative to the Fermi levels of the two metals, the height of the structure reflecting the impurity energy level spectrum may not rise above the noise level. Implications of the theory are discussed and experimental suggestions made.

Green, J. A. S., Mengelberg, H. D., Yolken, H. T., **Oxide growth on copper and alpha-brasses in aqueous ammonia,** *J. Electrochem. Soc.* **117,** *No. 4, 433–437 (Apr. 1970).*

Key words: Alpha-brass; copper; ellipsometry; oxide-growth; season-cracking; stress-corrosion.

An ellipsometric study of the kinetics of oxide growth for pure copper and a series of alpha-brasses immersed in tarnishing ammoniacal environments has established that the growth of the oxide, shown to be cuprous oxide, obeys a linear law in each case, and that the rate of growth increases significantly with (a) increasing zinc content of the solid, (b) increasing temperature and (c) the application of anodic potentials. On the basis of these results it is suggested that the oxide is porous and that oxide growth involves the dissolution of metal ions at the base of the pore (anodic reaction) and their deposition at the oxide surface (cathodic reaction), electrons flowing through the oxide film. The influence of zinc content on the oxide-growth rate is attributed to its effect on the dissolution kinetics. The relevance of these observations to season-cracking is considered.

Haller, W., Blackburn, D. H., Wagstaff, F. E., Charles, R. J., **Metastable immiscibility surface in the system Na_2O–B_2O_3–SiO_2,** *J. Am. Ceram. Soc.* **53,** *No. 1, 34–39 (1970).*

Key words: Glass; immiscibility; melts; microheterogeneities; Na_2O–B_2O_3–SiO_2; B_2O_3–Na_2O–SiO_2, SiO_2–B_2O_3–Na_2O.

Opalescence and clearing techniques have been used to determine the metastable immiscibility surface for sodium borosilicate solutions. These results indicate that a "three-liquid region, which may or may not be metastable to two-liquid regions, underlies the immiscibility surface.

Hamer, W. J., DeWane, H. J., **Electrolytic conductance and the conductances of the halogen acids in water,** *Nat. Stand. Ref. Data Ser., Nat. Bur. Stand. (U.S.), 33, 37 pages (May 1970) 50 cents, SD Catalog No. C13.48:33.*

Key words: Conductances of HF, HCl, HBr, and HI; electrolytic conductance; theories of electrolytic conductance.

Definitions, symbols, general principles, and general laws related to the electrolytic conductance of aqueous solutions are presented. The general laws considered are Coulomb's law for charged bodies, Poisson's equation relating the electrostatic potential to charge distribution, and the Stokes and Oseen laws for the velocity of a sphere in a fluid medium. The relations between electrical resistance, electrical conductance, specific resistance, specific conductance, and equivalent conductance are set forth. Theoretical expressions for the equivalent conductance as derived by Debye, Onsager, and Fuoss are given in general form and in a somewhat more detailed fashion in an appendix. The general methods of treating the equivalent conductances of ionophores and ionogens, especially in regard to the determination of the limiting equivalent conductance, the degree of ionic association, and the degree of ionic dissociation are discussed. Data on the equivalent conductances of the halogen acids, hydrofluoric, hydrochloric, hydrobromic, and hydriodic acids in water are given for a wide range of concentration and temperature.

Heinrich, K. F. J., **Advances in the metallurgical application of electron probe microanalysis,** *Proc. Conf. 5th International Congress on X-ray Optics and Microanalysis, Tubingen, Germany, Sept. 9–14, 1968, G. Mollebstedt and K. H. Gaukler, Eds., pp. 415–423 (Springer-Verlag Publ. Co., Berlin, Germany, Dec. 1969).*

Key words: Applications; electron probe; microanalysis; metallurgy; x-rays; spectrometry.

Electron probe microanalysis is widely used in the investigation of phenomena of general metallurgical interest as well as in the study of specific materials and processes. New devices for x-ray detection, and automatic data collection, increases the usefulness of the microprobe for such applications. Besides the well-known methods for qualitative and quantitative electron probe analysis, the instrument can also be used advantageously for quantitative metallography and related techniques.

Heinrich, K. F. J., Fiori, C., Yakowitz, H., **Image-formation technique for scanning electron microscopy and electron probe microanalysis,** *Science* **167,** *1129–1131 (Feb. 20, 1970).*

Key words: Derivative signal; electron probe; image; scanning electron microscope; secondary electrons; target current.

A technique is described for producing improved topographic images on the scanning electron microscope and the scanning electron probe microanalyzer. In this technique, the brightness of the oscilloscope is modulated by a signal obtained by mixing the signal (from secondary electrons or target current) with its first derivative. This enhances minor topographic features which are poorly reproduced in the conventional technique.

Heinrich, K. F. J., Yakowitz, H., **Propagation of errors in correction models for quantitative electron probe microanalysis,** *Proc. Conf. 5th International Congress on X-ray Optics and Microanalysis, Tubingen, Germany, Sept. 9–14, 1968, G. Mollebstedt and K. H. Gaukler, Eds., pp. 151–159 (Springer-Verlag Publ. Co., Berlin, Germany, Dec. 1969).*

Key words: Absorption of x-rays fluorescence; atomic number effects; error propagation; microprobe analysis; quantitative analysis.

Lack of appropriate standards frequently forces the analysis to use elemental standards. The usefulness of correction models is limited by the accuracy to which the input parameters are known. Uncertainties in presumably known quantities (mass absorption, coefficients, fluorescence yield, mean ionization potentials, etc.) are in many cases the limiting factors. The resulting analytical errors can be minimized by judicious choice of experimental conditons. This paper will give examples involving the corrections for absorption, fluorescence by characteristic lines, and atomic number effects.

Heydemann, P. L., **Ultrasonic measurements at pressures up to 50 kbar,** *Proc. Intern, Collog. Solids at High Pressures, Grenoble, France, Sept. 8, 1969, No. 188, pp. 461–467 (Centre National de la Recherche Scientifique, Paris, France, 1970).*

Key words: Bulk modulus; equation of state; high pressure; phase transitions; potassium chloride; tellurium; ultrasonics.

Ultrasonic measurements as a function of pressure or temperature provide one of the most accurate means to determine the pressure or temperature dependence of the bulk modulus and the density of both liquids and solids. Such measurements are currently carried out with very high accuracy at pressures up to about 4 kbar (1 kbar = 10 Nm^2) in several laboratories.
If the material under investigation undergoes transitions at higher pressures, or if the bulk modulus is noticeably non-linear with pressure, ultrasonic measurements at pressures higher than 4 kbar are needed. This report describes our methods to carry out such measurements at pressures close to 50 kbar, both under hydrostatic and non-hydrostatic conditions.
For most materials the accuracy of the density and bulk modulus data obtained from such measurements is much higher than that obtained from isothermal dilatometric measurements. In the case of tellurium, the accuracies for the bulk modulus at 30 kbar are 1.6 and 23%, respectively.
Another interesting application of ultrasonics at high pressures is the detection of phase transitions and the measurement of the elastic properties as the material undergoes the transition. As an example for measurements through a transition range, our results of ultrasonic and isothermal dilatometric measurements on KCl are presented. We find that the ratio of specific heats also shows a sharp increase in the transition range.

Hust, J. G., **A compilation and historical review of temperature scale differences,** *Cryogenics* **9,** *No. 6, 443–455 (Dec. 1969).*

Key words: Temperature; temperature scales; thermometry.

A brief review is given of temperature, its definition, and measurement. Methods of practical temperature measurement are described. Differences between internationally accepted temperature scales are presented graphically and in tabular form; comparisons are also given for several national temperature scales. Emphasis has been placed on temperatures below 0°C, but some information on temperatures above 0°C has also been included. Suggested methods of conversion between different temperature scales are described.

Ireland, C. T., Ku, H. H. Kullback, S., **Symmetry and marginal homogeneity of an $r \times r$ contingency table,** *J. Am. Statist. Assoc.* **64,** *1323–1341 (Dec. 1969).*

Key words: Contingency table analysis; homogeneity of marginals; minimum discrimination information estimation; test for symmetry.

The principle of minimum discrimination information estimation is employed to obtain RBAN (Regular Best Asymptotically Normal) estimates of the cell frequencies of an $r \times r$ contingency table under hypotheses of symmetry and marginal homogeneity. For the latter

a convergent iterative procedure is given to compute the estimates. The associated minimum discrimination information statistics are distributed asymptotically as χ^2 under the null hypothesis. The procedures differ from those previously presented in the literature and permit of extension to multidimensional contingency tables. An example is given.

Jones, M. C., Giarratano, P. J., Simpson, A. U., **Heat transfer to solid-vapor mixtures of cryogens below their triple points flowing through heated tubes,** *AIChE J.* **15,** *No. 5, 890–897 (Nov. 1969).*

Key words: Boundary layer; cryogenic; heat transfer; hydrogen; low pressure; nitrogen; particle-wall interaction; solid-vapor; tube; two-phase.

Data are presented for wall temperatures and heat transfer coefficients for solid-vapor mixtures of parahydrogen and nitrogen flowing in an electrically heated straight tube of length 40 times its diameter. These are interpreted by the application of flat plate, constant property boundary layer theory to models in which the solid particle geometrical distribution takes on simple limiting forms. The observed enhancement of the heat transfer coefficient over that for gas alone traveling at the same velocity is qualitatively predicted as a function of a dimensionless heat flux, the Sterman parameter $q_w/\rho_v U\lambda$. This parameter is also shown to be an index of particle-wall interaction and is used to correlate observed limiting wall heat fluxes above which free flow may be guaranteed.

Kamper, R. A., **The Josephson effect,** *IEEE Trans. Electron Devices* **ED–16,** *No. 10, 840–844 (Oct. 1969).*

Key words: Electron tunneling; electronics; low temperature; superconducting devices.

This is a review of the Josephson effect in superconductors with emphasis on the electrical properties of Josephson junctions and their application to devices and measurement techniques.

Kilgore, S. B., **Electronic circuit breaker for motor load protection,** *Rev. Sci. Instr.* **41,** *No. 1, 40–41 (Jan. 1970).*

Key words: Electronic circuit breaker; mechanical load protection; surge current; time delay.

An electronic circuit breaker, designed to switch off the power to an electric motor when the mechanical load increases, is described. The circuit operates rapidly and can sense an increase in mechanical load before it reaches destructive proportions. The sensitivity of the electronic circuit makes it necessary to incorporate a time delay that prevents the initial surge current from turning the motor off before it gets started.

Kostkowski, H. J., Erminy, D. C., Hattenburg, A. T., **High-accuracy spectral radiance calibration of tungsten-strip lamps,** *Chapter 4 in Advances in Geophysics 14, 111–127 (Academic Press Inc., New York, N.Y. 1970).*

Key words: Blackbody; high temperature measurement; radiometry; spectral radiance; standards calibration; tungsten strip lamp.

The accuracy of calibrating tungsten strip lamps in terms of absolute spectral radiance has been significantly improved. The standard deviation uncertainty of these calibrations is estimated to vary from 0.3 percent at 850 nm to 1.5 percent at 210 nm. This accuracy has been realized as a result of: (1) The development of a highly stable 3000 °K blackbody and a detailed inevstigation of its quality. (2) Increasing the accuracy with which the blackbody temperature could be determined. (3) Reducing and evaluating errors resulting from scattered light, polarization, and slit-function effects. Highlights of the instrumentation, the temperature measurement and the various error investigations are presented.

Ku, H. H., Varner, R. N., Kullback, S., **Analysis of multi-dimensional contingency tables,** *(Proc. 14th Conf. Design of Experiments in Army Research Development and Testing, Edgewood Arsenal, Md., October 23, 1968), ARO–D Report 69–2, 141–180, (U.S. Army Research Office-Durham, Durham, North Carolina, Sept. 1969).*

Key words: Computer programs; contingency tables; estimation of cell frequencies from marginals; generalized independence; *higher-order interaction;* hypothesis testing; information theory; interaction.

This is an expository paper on the analysis of multi-dimensional contingency tables. The principle of minimum discrimination information estimation is described and used to generate estimates for tests of hypotheses concerning various interactions and effects. All classical hypotheses for contingency tables can be generated by the use of this principle when certain marginals are considered as fixed.
Examples are given and two available computation programs are described in detail.

Kusuda, T., **Algorithms for psychometric calculations (skeleton tables for the thermodynamic properties of moist air),** *Nat. Bur. Stand. (U.S.), Bldg. Sci. Ser. 21, 53 pages (Jan. 1970), 55 cents, SD Catalog No. C13.29/2:21.*

Key words: Computer algorithm; psychrometrics; saturated and unsaturated moist air; thermodynamic properties.

Computer algorithms to obtain thermodynamic properties of saturated and unsaturated moist air are presented in this paper. The sautrated moist air properties are calculated by the methodology developed by J. A. Goff and S. Gratch for their ASHRAE tables (1967 Book of Fundamentals, The American Society of Heating, Refrigerating and Air Conditioning Engineers). Sample calculations were performed using a computer program based upon the algorithms presented herein and the results are attached.

Lang, S. B., Rice, L. H., Shaw, S. A., **Pyroelectric effect in barium titanate ceramic,** *J. Appl. Phys.* **40,** *No. 11, 4335–4340 (Oct. 1969).*

Key words: Barium titanate; ceramics; ferroelectricity; phase transition; pyroelectricity; spontaneous.

The pyroelectric coefficient (at constant stress) of a 95 percent $BaTiO_3$, 5 percent $CaTiO_3$ ceramic composition (Clevite Ceramic B) was measured over the temperature range from 4.9 to 400°K. Extrema in the pyroelectric coefficient were observed at the rhombohedral-orthorhombic transition point (150 to 170°K), the orthorhombic-tetragonal transition point (240 to 260°K), and the tetragonal-cubic transition point (Curie point, at 387°K). The pyroelectric coefficient showed no anomalous behavior below 150°K. A spontaneous polarization curve derived from the pyroelectric results is compared with published single-crystal measurements. A model for ceramic polarization suggests that domain switching at phase transitions is biased by electrical interactions arising from space charges and by mechanical interactions resulting from internal strains.

Latanision, R. M., **On the dislocation distribution near the surface of lightly deformed copper single crystals,** *Scripta Met.* **3,** *No. 7, 465–470 (July 1969).*

Key words: Debris layer; edge dislocation; near surface source; screw dislocation; single crystals; surface source.

Two recent and essentially identical etch-pitting studies on oriented copper single crystals have produced contradictory results. An explanation for the discrepancy is not obvious, but the results of these investigations may be interpreted in terms of either the surface "debris" layer hypothesis or the activation of surface or near-surface dislocation sources. The purpose of this note is to emphasize the ambiguity involved in such studies.

Lawton, R. A., **New standard of electric field strength,** *IEEE Trans. Inst. Meas.* **IM-19,** *No. 1, 45–51 (Feb. 1970).*

Key words: Antenna; electric field strength; measurement; standard field.

A new technique is presented for establishing a standard of field strength using a conducting sphere. An analysis is made to determine the current on the sphere as a function of the electric field strength of an incident plane wave, a method of measuring that current using electronic circuitry and an optical indicator within the sphere is described, and an intercomparison is made with an independent field-strength standard.
This technique is a significant improvement over previous techniques in that it permits the absolute determination of field strength with a maximum uncertainty of 1 percent or less at 30 MHz. This technique is applicable to a broad range of frequencies and field strengths.

McCrackin, F. L., **Analyses and corrections of instrumental errors in ellipsometry,** *J. Opt. Soc. Am.* **60,** *No. 1, 57–63 (Jan. 1970).*

Key words: Birefringence; ellipsometer; thin films.

The errors produced in an ellipsometer due to an imperfect compensator, due to birefringence in windows of a cell containing the sample, and due to tilting of the sample are derived. Methods of analyzing the ellipsometer readings to eliminate these errors are given.

McDonald, D. G., Kose, V. E., Evenson, K. M., Wells, J. S., Cupp, J. D., **Harmonic generation and submillimeter wave mixing with the Josephson effect,** *Appl. Phys. Letters* **15,** *No. 4, 121–122 (Aug. 15, 1969).*

Key words: Infrared; josephson effect; lasers; submillimeter waves; superconductivity.

By observing constant-voltage steps from Josephson junctions at voltages as high as 17 mV we deduce that junctions can generate harmonics up to frequencies as high as 8200 GHz. In consonance with this, submillimeter wave laser detection, harmonic generation and mixing are demonstrated. These results suggest a model for the upper frequency limit of the Josephson effect.

McLaughlin, W. L., Hussmann, E. K., **The measurement of electron and gamma-ray dose distributions in various media** *(Proc. Symp. Utilization of Large Radiation Sources and Accelerators in Industrial Processing, Munich, Germany, Aug. 18–22, 1969), Chapter in Large Radiation Sources for Industrial Processes, IAEA–SM–123/43, pp. 579–590 (International Atomic Energy Agency, Vienna, Austria, 1969).*

Key words: Depth dose; dose distributions; dosimetry; dyes; electron beams; films; gamma rays; microdosimetry; radiographic imaging.

New radiochromic dye films and gels are proposed as simple and relatively accurate devices for imaging and determining the energy deposited locally at different depths and across interfaces of various irradiated media. Depth-dose measurements show remarkable agreement with theoretical computations in various plastics and aluminum, even near the end of the electron range, indicating that the dosimeter response is representative of the energy imparted to the medium over a wide range of electron energies.

Margoshes, M., Rasberry, S. D., **Application of digital computers in spectrochemical analysis—computational methods in photographic microphotometry,** *Spectrochim. Acta* **24B,** *497–513 (1969).*

Key words: Computers; emulsion; microphotometry; photographic emulsion; photographic photometry; photometry; programs; spectrochemical.

A new method is described for calibration of photographic emulsions and conversion of microphotometer readings to relative intensities on a digital computer with special application to spectrochemical analysis. The method for emulsion calibration replaces graphical procedures by a numerical method which is well suited for digital computations. The method of computation and its underlying assumptions are described, and results are given of tests of the procedure. It is recognized that the entire experimental arrangement is being calibrated, not merely the photographic emulsion, and it is shown how malfunctions of the microphotometer which affect the calibration can be recognized from the output of the computer. The program for conversion of microphotometer readings to relative intensities provides for several alternate calculations, including selection of the proper calibration parameters according to the wavelength of the line when these data are supplied for more than one wavelength region, as well as correction for step and background where required. The program is written to provide for automatic selection of the required alternative calculation, based on preliminary analysis of the input data.

Meinke, W. W., **The NBS standard reference materials program: Past, present, and future,** *Mater. Res. Std.* **9,** *No. 10, 15–18 (Oct. 1969).*

Key words: Primary standards; standard reference material; standards.

The past 60 years have been ones of rapid and sweeping technological change in the industrial world. During this time the National Bureau of Standards (NBS), has played a pivotal role in the orderly progress and quality control of the nation's productive process. One of the means by which this progress has been aided is through the production, certification, and issuance of Standard Reference Materials (SRM) from NBS.
The development of our high-technology society is based in large part on the mass production of goods and services. In turn, mass production implies strict quality control of the means of production, an ever-increasing accuracy of measurement, interchangeability of parts, and stringent performance criteria for the wide variety of materials now used. The base of this structure rests firmly on a well-established standards program, national in scope, in which the NBS-SRM program plays a significant role. It is interesting to note that the national standards bodies, the ASTM being among the foremost, have interacted from the earliest days with the NBS-SRM program.

Meyerson, M. R., Friedman, L., Giles, P. M., **Dimensional stability of a 12% nickel maraging steel at ambient temperatures,** *Trans. ASM* **62,** *No. 3, 809–812 (Sept. 1969).*

Key words: Gage blocks; maraging steel; nitriding; precision equipment; surface hardened; temporal dimensional stability; ultrastability.

The maraging steels attain high strength with a relatively simple low temperature heat treatment. The nature of the heat treatment and the low carbon content of the steels indicated low residual stress levels, small lattice distortions, nitridability and other characteristics which are known to promote dimensional stability at high strength levels. A 12% nickel maraging steel was treated to produce a surface hardness of greater than R_c 65 and its dimensional stability at submicroinch levels was observed over a period of about 2½ years. The steel as treated was found to be ultrastable, with an average decrease in length of only 0.05 to 0.10 micrometers per meter per year. Its performance meets or exceeds that of any of the many other materials previously investigated at NBS.

Mosburg, E. R., Jr., **A new probe configuration for plasma diagnostics,** *J. Appl. Phys.* **40,** *No. 13, 5290–5300 (Dec. 1969).*

Key words: Plasma diagnostics; plasma physics; probes.

A new probe geometry using a large array of small, closely spaced electrodes, alternately connected to two different potentials has been developed. The basic characteristics of the current-voltage curve of this probe differ markedly from that of the usual double probe.

Mullen, L. O., **On efficient use of selective vacuum pumping modes,** *J. Environ. Sci.* **12,** *No. 5, 26–30 (Oct. 1969).*

Key words: Cryopumps; getters; ion pumps; pumping efficiency; sublimation pumps; vacuum pumps; vapor pressure.

Most vacuum pumps are selective in the sense that they pump different molecular species at different speeds. Some pumps, such

as sublimation pumps and cryopumps, are extremely selective. Efficient use of selective pumps requires that they be chosen to match the gas load. We present experimental data on some commonly encountered gas loads and discuss the choice of compatible pumps.

Ohashi, M., Paffenbarger, G. C., **Some flow characteristics at 37°C of ternary wax mixtures that may have possible dental uses,** *J. Nihon University School Dentistry* **11,** *No. 3, 109–208 (Sept. 1969).*

Key words: Dental; flow; wax.

One hundred and eighty two ternary diagrams of the flow at 37°C of mixtures of commercial waxes indicate some of these mixtures may have dental use.

Paulsen, P. J., Alvarez, R., Kelleher, D. E., **Determination of trace elements in zinc by isotope dilution spark source mass spectrometry,** *Spectrochim. Acta* **24B,** *535–544 (April 1969).*

Key words: Electrodeposition; isotope dilution; preconcentration; spark source mass spectrometry; trace elements; zinc.

The applicability of the isotope dilution technique in spark source mass spectrometry has been investigated for the determination of Pb, Cu, Cd, Ag, Tl, and Sn in zinc metal. In the procedure developed, a solution of the zinc is spiked with known amounts of stable isotopes of the element to be determined, and the elements are electrodeposited onto gold wires that subsequently serve as electrodes for the mass spectrographic isotopic analysis. Chemical operations, including isothermal distillation of reagents, dissolution of the zinc, and the electrodeposition step are conducted in a closed system to minimize contamination. The results of the analysis of two NBS zinc standard reference materials show determination ranging from 11 ppm (11 ug/g) for Pb to as low as 0.02 ppm (20 ng/g) for Sn. It is concluded that this method is of general utility for simultaneous multi-element trace analysis and is especially applicable in providing much needed standardization in spark source mass spectrometry.

Pizer, R. S., Spinner, S., **An apparatus for determining the actual footprint area of tires,** *Mater. Res. Std.* **10,** *No. 2, 20–23 (Feb. 1970).*

Key words: Contact area; footprint; optical and electrical system; silicon solar cell; tire; tires.

An apparatus is described for measuring the actual contact area of tires regardless of their tread design. The procedure is both rapid and accurate. The method utilizes a bank of lights, an opal glass plate, a simple light focusing system, and a silicon solar cell which linearly transforms the incident light to an electrical current. The reduction in current is the measure of the true contact area of the tire.

Potzick, J., **Low-frequency sine-wave oscillator,** *EEE* **18,** *No. 3, 130 (Mactier Publishing Corp., Mar. 1970).*

Key words: Low frequency oscillator; oscillator.

A simple, inexpensive, low-frequency oscillator which generates a fairly low distortion sine wave at a frequency of about one hertz is described.

Randall, E. B., Jr., Lashof, T. W., **An interlaboratory study of the measurement of the bursting strength of paper,** *Tappi* **53,** *No. 5, 799–809 (May 1970).*

Key words: Bursting strength; evaluation; interlaboratory study; paper; precision; reference materials; standards; test method.

This paper reports on the results of an extensive interlaboratory study, involving more than 175 laboratories in North America and overseas using several different models of bursting strength testers to evaluate 34 papers and 6 foils. Significant differences, both in a statistical and in an economic sense, were found between results obtained on different models and in different laboratories using the same model, confirming previous reports. There were also significant day-to-day variations within a laboratory, and aluminum foil specimens gave results relative to those of paper specimens that depended on the instrument model used. A convenient rule for the number of replications was obtained from the study; namely, make 10 replications unless the range of the first 10 is greater than 20% of their average, then make an additional 10. Two test results, each with 10 or 20 replications as above, are expected to agree with each other within the following values 95% of the time: 5.4% for repeatability within a laboratory, 9.5% for comparability between materials, and 14.3% for reproducibility between laboratories. Between laboratory comparisons may be standardized through the use of a composite reference material of paper, aluminum foils being of only marginal use for this standardization.

Reed, R. P., Durcholz, R. L., **Cryostat and strain measurement for tensile tests to 1.5°K,** *(Proc. 1969 Cryogenic Engineering Conf., June 16–18, 1969, Univ. of California, Los Angeles, Calif.), Chapter in Advances in Cryogenic Engineering* **15,** *Paper No. D–3, 109–116 (Plenum Press, Inc., New York, N.Y. 1970).*

Key words: Capacitance extensometer; cryostat; strain measurement instruments; tensile properties.

A new tensile cryostat has been developed and tested at temperatures between 300 and 1.5K. Better design, insulation, and vacuum-sealed environment reduces the heat leak to about 0.2 watts during continuous pumping above liquid helium. New capacitance strain-sensing equipment has been developed to provide ranges of strain sensitivities between 10^{-6} and 10^{-2} inches per inch. Details are presented of both devices.

Robbins, R. F., **Cryogenic properties of a polyurethane adhesive,** *J. Macro-mol. Sci.* **A3,** *No. 7, 1367–1380 (Nov. 1969).*

Key words: Adhesive; low temperature; mechanical properties; polymer; polyurethane; resilience; thermal properties.

Differential Thermal Analysis (DTA), Rebound Resilience, and Tensile Properties of a polyurethane adhesive were measured at cryogenic temperatures. The experimental methods are described, and test results which aid in evaluating the polyurethane for use at low temperatures are discussed. The DTA thermogram reveals that the glass transition temperature (T_g) is 235°K. The resilience profile indicates a resilience minimum (T_m) at 270°K and a frequency of 3800 Hz, which is consistent with the T_g measured by DTA. The low resilience below T_m, caused by secondary low temperature transitions, shows the high energy absorption capabilities of the polyurethane. Considerable plastic flow at 195°K (40°K below T_g) is evidenced in the results of the tensile tests. The results of the three tests indicate that the polyurethane adhesive will perform well at low temperatures. The test methods should also be useful for evaluating the low temperature performance of new experimental polymers.

Robinson, H. E., Editor, **Durability of insulating glass,** *Proceedings of a seminar held at the National Bureau of Standards, Gaithersburg, Maryland, November 14–15, 1968, Nat. Bur. Stand. (U.S.), Bldg. Sci. Ser. 20, 84 pages (Feb. 1970), 75 cents, SD Catalog No. C13.29/2:20.*

Key words: Accelerated laboratory tests; double-glazed window units; factory-sealed insulating glass units; field performance tests, correlation with laboratory tests; sealant performance; standardized testing; test methods.

A two-day seminar on the Durability of Insulating Glass was attended by some 130 persons on November 14 and 15, 1968. The seminar was held at the Gaithersburg, Maryland, facilities of the National Bureau of Standards and featured fourteen speakers who participated in panel discussions or delivered individual papers. Numerous agencies interested in design, manufacture, specification, purchase, installation or maintenance of windows were represented at the seminar.
Among the topics considered in the panel discussions were: (1) The need for reliability and durability of insulating glass; (2) manufacturers' test methods; (3) proposals for future action. The

Canadian experience with an accelerated test method and acceptance program was presented and discussed, as were the Norwegian accelerated test methods and their correlation with field experience. A review of current practices leading to new test methods and standards was also presented, and a "round robin" program that would compare various test methods now employed in the industry was proposed. Affirmative interest in participating in the proposed round robin was expressed by about a score of manufacturers present at the seminar.

Silverman, S., **The National Measurement System—a concept to assist the private sector,** *Mater. Res. Std.* **9,** *No. 10, 11–14 (Oct. 1969).*

Key words: Measurement; National Bureau of Standards; National Measurement System; national standards; self-calibration; standards, national; systems concept.

The concept of a National Measurement System, involving the entire complex of measurement activities within the United States, is developed. The central element of this Measurement System is the National Bureau of Standards. The role of NBS and of other functional elements of the System, such as private laboratories, is discussed.

Simpson, A. U., Timmerhaus, K. D., Kreith, F., Jones, M. C., **Heat and mass transfer in dispersed, two-phase, single-component flow,** *Intern. J. Heat Mass Transfer* **12,** *No. 9, 1141–1155 (Sept. 1969).*

Key words: Boundary layer; computation; dispersed flow; heat transfer; solid-vapor; two-phase.

The process of heat transfer to a two-phase mixture of well-dispersed subliming particles and vapor, flowing over a heated surface, is analyzed. It is shown by a laminary boundary analysis that, when the surface-area per unit volume of the particle (or solid) phase is large enough, the phase change dominates the heat transfer process and hastens the development of the thermal boundary layer. Under these conditions, the thermal boundary-layer thickness not only becomes uniform a short distance downstream from the starting point, but also is substantially less than it would be were the particle phase absent. For such systems, the equations describing the heat transfer process can be considerably simplified and, if the physical properties of both phases are uniform, a remarkably simple solution results. For systems in which the physical properties are not uniform, a solution involving integration across the boundary layer is developed. The solutions are applicable to developing, as well as fully developed, laminary boundary layers over a flat plate; the solutions also approximate conditions in flow through a tube, provided that the tube radius is large compared to the thermal boundary-layer thickness. The predictions of this theoretical analysis agree satisfactorily with experimental results. With slight modification, the same approach may possibly be applicable for turbulent flow in the boundary layer.

Simpson, J. A., **Electron impact spectroscopy,** *(Proc. 10th Symp. on Electron, Ion & Laser Beam Technology, Gaithersburg, Md., May 21–23, 1969), Chapter in Record of 10th Symposium, Electron, Ion, and Laser Beam Technology, L. Marton, Ed., pp. 345–352 (San Francisco Press, San Francisco, Calif., 1969).*

Key words: Chemical analysis; electron impact spectrometer; uv absorption.

Recent developments in electron spectrometer design have made the application of inelastic electron scattering measurements to gas analysis competitive with other techniques. The energy distribution of electrons of an initially monoenergetic electron beam after an encounter with a gas target, the loss spectrum, contains the optical absorption spectrum of the gas. This absorption data extends from the extreme vacuum ultraviolet into the visible with an energy resolution comparable to a ½ meter optical grating spectrometer. Its response is linear with concentration over a very wide range and contains between 10^3 and 10^4 resolution widths. This spectrum by revealing the valence energy states of the gas is the most intrinsic possible "fingerprint" of the atom or molecule. An instrument has been built to explore the potentialities of this method. The instrument described and its performance as a trace analyzer for air pollution studies discussed.

Smith, R. V., **The influence of surface characteristics on the boiling of cryogenic fluids,** *J. Eng. Ind.* **91,** *No. 4, 1217–1221 (Nov. 1969).*

Key words: Boiling; boiling hysteresis; boiling inception; boiling-site spreading; radiation.

This paper reviews the influence of the characteristics of the solid surface on the boiling of cryogenic fluids. Particular emphasis is placed on papers presented in the cryogenics section of the 1968 Annual ASME meeting.
Hysteresis, boiling-site spreading and the influence of radiation on the surfaces are discussed in detail.

Snelleman, W., Menis, O., Rains, T. C., Yee, K. W., Cook, H. D., **Flame emission spectrometry with repetitive optical scanning in the derivative mode,** *Anal. Chem.* **42,** *No. 3, 394–398 (Mar. 1970).*

Key words: A-c scan; derivative mode; design; detection limits; flame emission spectrometry; interferences; matrix; microsamples.

A flame emission spectrometer using a rapid repetitive scan of a narrow wavelength region has been developed. By this method of wavelength scanning the second derivative of the output intensity is measured. This approach to matrix problems and micro samples greatly enhances the potentialities of flame emission spectrometry, and minimizes the need for a monochromator of high power. A quartz plate, which is vibrating at 145 Hz, is mounted in back of the entrance slit of the monochromator, and a voltage at its frequency of oscillation is used as the reference signal for a lock-in amplifier. When the ac amplifier is tuned to twice the frequency of vibration the second derivative of the intensity is obtained. This permits the measurement of weak line spectra nested in or on a broad band or continuum. It is demonstrated that spectral interference due to CaOH bands and/or a continuum are minimized in the measurement of barium, thus leading to an increase in detection limits of alkali and alkali earth elements in the presence of many matrix ions. An analysis can be performed on 50 μl of sample which makes it applicable to biochemical and air pollution studies.

Strobridge, T. R., **Refrigeration techniques,** *U.S. Bureau Mines Info. Circ. No. 8417, pp. 39–56 (1969).*

Key words: Applications; cryogenic; refrigeration; thermodynamic cycles.

The supply of helium accumulated through the conservation program has allowed technology in many disciplines to freely make use of the unique behavior of helium. Helium is the only fluid that can be conveniently used as a refrigerant below about 14°K and is often used at higher temperatures. The thermodynamic cycles that modern helium refrigerators utilize are reviewed. The Joule-Thomson process is important because it forms the lowest temperature stage of virtually all helium temperature refrigerators. The various processes and cycles for precooling the helium stream prior to the Joule-Thomson process form the essential differences between the closed cycle refrigerators operating today. Typical refrigeration and liquefaction facilities, both large and small, are discussed.

Strohlein, J. N., Bagg, T. C., **A selective roll-to-roll printer for producing duplicate microfilm copies,** *Nat. Bur. Stand. (U.S.), Tech. Note 516, 9 pages (Feb. 1970), 25 cents, SD Catalog No. C13.46:516.*

Key words: Information retrieval device; microcopier; microfilm duplicator; reader-printer; selective copier.

The "Selectaframe" printer, a convenient device for copying onto roll film selected frames from other rolls of film for subsequent automatic enlargement printing is described in detail.

Tighe, N. J., Kreglo, J. R., Jr., **Electron microscopy of periclase brick,** *J. Am. Ceram. Soc.* **49,** *No. 2, 188–192 (Feb. 7, 1970).*

Key words: Ceramics; electron microscopy; MgO; microstructure; sea-water periclase.

Transmission electron microscopy was used to study microtructure of sea-water periclase brick. The material contained 96.7% MgO and had a porosity of 19%. Specimens were cut from the brick and thinned for microscopy by ionic bombardment. MgO was present as single grains (20 to 90 μm) and as a fine precipitate (~100Å) in an amorphous matrix. Dislocations in MgO grains were decorated with impurity precipitates. Second phase material was also present as single grains. Forsterite and monticellite were identified as second phases.

Vidal, C. R., Cooper, Jr., **Heat pipe oven: a new, well-defined metal vapor device for spectroscopic measurements,** *J. Appl. Phys.* **40,** *No. 8, 3370–3374 (July 1969).*

Key words: Absorption spectroscopy; heat pipe; metal vapor device; oven.

A new well defined metal vapor device called the heat pipe oven has been developed on the basis of the heat pipe, a heat conductive element designed by G. Grover and his co-workers in Los Alamos. It generates continuously homogeneous vapors of well defined temperature, pressure and optical path length. The vapor is confined by inert gas boundaries which remove the window problem and allow a direct pressure measurement without relying on vapor pressure curves. Due to the continuous evaporation and condensation the vapor purifies itself during operation.

Viezbicke, P. P., Edward, **NBS Frequency and time broadcast services, Radio stations WWV, WWVH, WWVB, and WWVL,** *Nat. Bur. Stand. (U.S.), Spec. Publ. 236, 16 pages (1970) 25 cents, SD Catalog No. C13.11:236 (Supersedes NBS Special Publication 236, 1969 and previous editions).*

Key words: Broadcast of standard frequencies; high frequency; low frequency; standard frequencies; time signals; very low frequency.

Detailed descriptions are given of the technical services provided by the National Bureau of Standards radio stations WWV, WWVH, WWVB, and WWVL. These services are: 1. Standard radio frequencies; 2. Standard audio frequencies; 3. Standard musical pitch; 4. Standard time intervals; 5. Time signals; 6. UT2 corrections; 7. Radio propagation forecasts; and 8. Geophysical alerts. In order to provide users with the best possible services, occasional changes in broadcasting schedules are required. This publication shows the schedules in effect on February 1, 1970. Annual revisions will be made. Current data relating to standard frequencies and time signals are available monthly in the Time and Frequency Services Bulletin. Advance notices of changes occurring between revisions will be sent to users of NBS broadcast services who request such notice on the basis of need.

Waclawski, B. J., Hughey, L. R., **Adsorption of water vapor on polycrystalline tungsten,** *Surface Sci.* **19,** *464–468 (1970).*

Key words: Adsorption; hydrogen evolution; polycrystalline tungsten; room temperature; ultra-high vacuum; water vapor; work function.

Following an induction period, a spontaneous evolution of hydrogen was observed to occur in the initial stages of adsorption at room temperature when polycrystalline tungsten was exposed to water vapor. Concurrent photoemission measurements indicated that a change in the work function of the sample occurred during the hydrogen evolution. Calculations of the rate of evolution, and the amount of hydrogen evolved are presented.

Wall, L. A., Flynn, J. H., Straus, S., **Rates of molecular vaporization of organic plasticizers,** *Polymer Eng. Sci.* **10,** *No. 1, 19–23 (Jan. 1970).*

Key words: Energy of vaporization; internal energies of vaporization; molecular vaporization; organic plasticizers; plasticizers; solubility parameters.

The kinetics of the molecular vaporization process of 21 plasticizers were investigated in detail. By both isothermal and nonisothermal weight loss methods it was evident that 11 were quite pure single compounds while 10 were clearly mixtures of compounds. For the single component species internal energies, for vaporization and rates of volatilization are obtained from the kinetic data. The internal energies of vaporization are about ½ or less of values one can estimate from solubility parameters estimated by the additive factor method of Small. Thus solubility parameters based on our experimental energies of vaporization are low by about 30%. From this and other work on linear n-alkanes it is concluded that in the molecular vaporization process, the large organic molecules studied evaporate approximately as spheres and hence low values for the energy of vaporization are obtained. Consequently the difference between our experimental energy and that estimated from solubility parameters is the energy for extending the molecule in a vacuum environment.

Walton, W. W., Cadoff, B. C., Editors, **Performance of buildings—concept and measurement,** *Proceeding of the 1st conference in a series of conferences on Man and His Shelter held at the National Bureau of Standards, Gaithersburg, Maryland, September 23–25, 1968, Nat. Bur. Stand. (U.S.), Bldg. Sci. Ser. 1, 132 pages (Jan. 1970), $2.75, SD Catalog No. C13.29/2:1.*

Key words: Building systems; performance of buildings; standards; test methods; urban planning; user needs.

The Conference entitled "Performance of Buildings—Concept and Measurement" was held at the National Bureau of Standards, Gaithersburg, Md. on September 23–25, 1968. This was the first in a planned series of conferences on "Man and His Shelter." The purpose of these conferences is to bring together those people from various disciplines who may contribute to improving the quality of man's shelter. At the present conference, papers were presented by nineteen authors representing government and industry in such diverse disciplines as architecture, engineering, science, urban planning, and standards. These papers emphasize the prime importance of considering user needs in the development of performance criteria, the necessity of test methods to determine whether the desired performance has been achieved, and the development of performance specifications and standards. Application of these ideas to building systems, and to the planning and design of entire communities, is also discussed.

Wampler, R. H., **An evaluation of linear least squares computer programs: A summary report,** *(Proc. 14th Conf. Design of Experiments in Army Research Development and Testing, Edgewood Arsenal, Md., October 23, 1968), ARO–D Report 69–2, 103–126 (U.S. Army Research Office-Durham, Durham, North Carolina, Sept. 1969).*

Key words: Computer programs; curve fitting; Gram-Schmidt orthogonalization; Householder transformations; iterative refinement; least squares; linear equations; orthogonal polynomials; orthogonalization; regression; rounding error; stepwise regression.

Two linear least squares test problems, based on fifth degree polynomials, have been run on more than twenty different computer programs in order to assess their numerical accuracy. Among the programs tested were representatives from various statistical packages as well as some from the SHARE library. Essentially four different algorithms were used in the various programs to obtain the coefficients of the least squares fits. The tests were run on several different computers, in double precision as well as single precision. By comparing the coefficients reported, it was found that those programs using orthogonal Householder transformations or Gram-Schmidt orthonormalization were much more accurate than those using elimination algorithms. Programs using orthogonal polynomials (suitable only for polynomial fits) also proved to be superior to those using elimination algorithms. The most successful programs accumulated inner products in double precision and made use of iterative refinement procedures. In a number of programs, the coefficients reported in one test problem

were sometimes completely erronous, containing not even one correct significant digit.

White, H. J., Jr., **Absorption of cationic surfactants by cellulosic substrates,** *Chapter 9 in Cationic Surfactants* **4,** *311–340 (Marcel Dekker, Inc., New York, N.Y. 1970).*

Key words: Absorption; adsorption; cationic surfactants; cellulosic materials; review.

The physical chemistry of the interaction of cationic surfactants with cellulosic substrates is reviewed.

Wiederhorn, S. M., **Crack propagation in polycrystalline ceramics,** *(Proc. 15th Sagamore Army Materials Research Conf., Sagamore Conference Center, Raquette Lake, New York, Aug. 20–23, 1968), Chapter in Ultrafine-Grain Ceramics* **15,** *317–338 (Syracuse University Press, Syracuse, N.Y., 1970).*

Key words: Ceramics; fracture; fracture surface energy; strength; thermal shock.

In this paper, the strength and shock resistance of ceramic materials will be related to microstructural details and the energy necessary to form fracture surfaces. The influence of grain size, grain orientation, crystal anisotropy and residual stresses on crack propagation will be discussed. It will be argued that the strength of ceramic materials is closely related to the grain boundary or single crystal fracture surface energy while shock resistance is related to the surface energy required to propagate large cracks through polycrystalline materials. The use of fracture surface energies as a research technique and as a design parameter will be discussed.

Wilson, W. K., **Development of specifications for archival record materials,** *Am. Archivist* **33,** *No. 2, 219–223 (April 1970).*

Key words: Acidity; aging; alum sorption; laboratory aging; paper; records; stability; stability of cellulose; stability of paper; thermal analysis.

Work in progress on the development of information on the stability of paper and modified cellulose is described in relation to the objectives of the program. Plans for calendar year 1970 are outlined.

Wilson, W. K., **Reflections on the stability of paper,** *Restaurator* **1,** *No. 2, 79–86 (1969).*

Key words: Degradation; paper; preservation of records; records; stability.

Variables in the composition of paper are discussed in relation to stability, and new approaches to research on preservation of records are described.

Wood, R. E., Hamer, W. J., **Theoretical electromotive forces of metal-halogen cells: Some recalculations based on recent data,** *J. Electrochem. Soc.* **117,** *No. 1, 82–83 (Jan. 1970).*

Key words: Cells; emfs; free energies of formation; fused salts; halides; thermodynamics.

Comparison of the theoretical emfs for cells containing a single solid or molten halide published by Hamer, Malmberg and Rubin in 1956 and 1965 with emfs calculated from tabulations in the JANAF tables published in 1965, 1966, 1967, and 1968 reveals some rather large discrepancies. This note tabulates the 34 cases in which such dicrepancies were found to exceed 100 millivolts, discrepancies equivalent to 2.3 kcal — one thermocalorie (defined) = 4.1840 joules. Equiv^{-1} or more.

Yakowitz, H., **The divergent beam x-ray technique,** *Chapter in Advances in Electronics and Electron Physics, Suppl. 6, Electron Probe Microanalysis, A. J. Toksimis and L. L. Marton, ed., pp. 361–431 (Academic Press Inc., New York, N.Y., 1969).*

Key words: Kossel method; x-ray microdiffraction.

This is a review paper discussing the technique of divergent beam (Kossel) x-ray diffraction. The Kossel method is studied with regard to line intensities, photographic contrast, data reduction, specimen preparation, and contribution to scientific research.

Other NBS Publications

J. Res. Nat. Bur. Stand. (U.S.), 74A (Phys. and Chem.), No. 1 Jan.–Feb. 1970, SD Catalog No. C13.22/sec.A:74/1. $1.75.

Standardization of cesium-137 gamma-ray sources in terms of exposure units (Roentgens). T. P. Loftus.

Calculations of Zn II $3d^9 4,5_s$ and Ag I $4d^9 5,6_s$, and some new levels in these spectra. W. C. Martin and J. Sugar.

New vacuum ultraviolet wavelengths and revised energy levels in the second spectrum of zinc (Zn II). W. C. Martin and V. Kaufman.

CIE 1960 UCS diagram and the Müller theory of color vision. D. B. Judd and G. T. Yonemura.

Blemish formation in processed microfilm. II. C. I. Pope.

Positive and negative ion sublimation from transition metal surfaces: A review of some recent results. M. D. Scheer.

Generation of controlled low pressures of nitrogen by means of dissociation equilibria. R. H. Orcutt.

Temperature coefficient of the bismuth I-II transition pressure. J. C. Houck.

Isothermal diffusion in the dilute range of the system $Ca(OH)_2$-H_3PO_4-H_2O—Theory. E. C. Moreno, P. R. Patel, and W. E. Brown.

High-speed (subsecond) measurement of heat capacity, electrical resistivity, and thermal radiation properties of molybdenum in the range 1900 to 2800 K. A. Cezairliyan, M. S. Morse, H. A. Berman, and C. W. Beckett.

P-V-T, thermodynamic and related properties of oxygen from the triple point to 300 K at pressures to 33 MN/m^2. L. A. Weber.

J. Res. Nat. Bur. Stand. (U.S.), 74A (Phys. and Chem.), No. 2 (March–April 1970), SD Catalog No. C13.22/sec.A:74/2. $2.00.

A theoretical investigation of the configurations $(3d+4s)^4 4p$ in neutral vanadium (V I). C. Roth.

A theorectical investigation of the configurations $(3d+4s)^5 4p$ in neutral chromium (Cr I). C. Roth.

A theoretical investigation of the configurations $(3d+4s)^7 4p$ in neutral iron. C. Roth.

The intensity as a function of temperature of the low-angle x-ray diffraction maxima of the *n*-paraffins: hexatriacontane, tetratetracontane, and tetranonacontane. P. K. Sullivan and J. J. Weeks.

Photoelastic constants of ruby. R. M. Waxler and E. N. Farabaugh.

Estimation of critical constants T_c, ρ_c from the ρ (T) and $T(\rho)$ relations to coexistence. R. D. Goodwin.

Synthesis and growth of fresnoite ($Ba_2TiSi_2O_8$) from a TiO_2 flux and its relation to the system $BaTiO_3$-SiO_2. C. R. Robbins.

Photoionization study of $Fe(CO)_5$ and $Ni(CO)_4$. G. Distefano.

Papers presented at the Conference, Electronic Density of States, National Bureau of Standards, Gaithersburg, Maryland November 3–6, 1969

The band structure problem. J. M. Ziman.

Optical properties and electronic density of states. M. Cardona.

Excitonic effects in x-ray transitions in metals. G. D. Mahan.

Soft x-ray band spectra and their relationship to the density of states. G. A. Rooke.

The electronic structure of disordered alloys. J. L. Beeby.

Summary of the conference on electronic density of states. H. Ehrenreich.

J. Res. Nat. Bur. Stand. (U.S.), 74A (Phys. and Chem.), No. 3 (May–June 1970), SD Catalog No. C13.22/sec.A:74/3. $1.75.

The crystal structure of hydrazinium trinitromethide ($N_2H_5^+$ $[C(NO_2)_3]^-$ at ~—160°C. B. Dickens.

A refinement of the crystal structure of $Na_2CO_3 \cdot H_2O$. B. Dickens, F. A. Mauer, and W. E. Brown.

Anisotropic reaction kinetics of oxygen with pyrolytic graphite. W. S. Horton.

The viscosity and thermal conductivity of dilute gaseous hydrogen from 15 to 5000 K. H. J. M. Hanley, R. D. McCarty, and H. Intemann.

Temperature classification of the spectra of dysprosium (Dy I, Dy II). A. S. King, J. G. Conway, E. F. Worden, and C. E. Moore.

Papers presented at the Conference, Electronic Density of States, National Bureau of Standards, Gaithersburg, Maryland November 3–6, 1969

Optical density of states ultraviolet photoelectric spectroscopy. W. E. Spicer.

Beyond the one-electron approximation: Density of states for interacting electrons. L. Hedin, B. Lundqvist, and S. Lundqvist.

Ion-neutralization spectroscopy. H. D. Hagstrom.

Local theory of disordered systems. W. H. Butler and W. Kohn.

Density of states information from low temperature specific heat measurements. P. A. Beck and H. Claus.

J. Res. Nat. Bur. Stand. (U.S.), 74A (Phys. and Chem.), No. 4 (July–August 1970), SD Catalog No. C13.22/sec.A:74/4. $2.00.

Solubility of $CaHPO_4 \cdot 2H_2O$ in the system $Ca(OH)_2$-H_3PO_4-H_2O at 5, 15, 25, and 37.5°C. T. M. Gregory, E. C. Moreno, and W. E. Brown.

Effect of oxide additions on the polymorphism of tantalum pentoxide II. "Stabilization" of the high temperature structure type. R. S. Roth, J. L. Waring, and W. S. Brower.

Effect of oxide additions on the polymorphism of tantalum pentoxide III. "Stabilization" of the low temperature structure type. R. S. Roth and J. L. Waring.

The dissociation constant of *m*-nitroanilinium ion in water-tetrahydrofuran solvents at 25°C. R. A. Robinson.

Specific heats of fluorine at coexistence. R. D. Goodwin and R. Prydz.

A theoretical investigation of the configurations $(3d+4s)^6$ $4p$ in neutral manganese (Mn I). C. Roth.

A literature survey of the chemistry of flame inhibition. E. C. Creitz.

The NBS Alloy Data Center: Description of Index to the literature. G. C. Carter, D. J. Kahan, L. H. Bennett, J. R. Cuthill, and R. C. Dobbyn.

Papers presented at the Conference, Electronic Density of States, National Bureau of Standards, Gaithersburg, Maryland November 3–6, 1969

What is a quasi-particle? J. R. Schrieffer.

Electronic densities of states from x-ray photoelectron spectroscopy. C. S. Fadley and D. A. Shirley.

Tunneling measurements of superconducting quasi-particle density of states and calculation of phonon spectra. J. M. Rowell.

Pauli paramagnetism in metals with high densities of states. S. Foner.

Relevance of Knight shift measurements to the electronic density of states. L. H. Bennett, R. E. Watson, and G. C. Carter.

J. Res. Nat. Bur. Stand. (U.S.), 74A (Phys. and Chem.), No. 5 (September–October 1970), SD Catalog No. C13.22/sec.A:74/5. $1.75.

Heat capacity and thermodynamic properties of α-beryllium nitride, Be_3N_2, from 20 to 315 K. G. T. Furukawa and M. L. Reilly.

Heat capacity and thermodynamic properties of lithium hexafluoroaluminate, Li_3AlF_6, from 15 to 380 K. G. T. Furukawa, W. G. Saba, and J. C. Ford.

Thermodynamics of hydrochloric acid in 80 weight percent 2-methoxyethanol and 20 weight percent water from 10 to 50°C. H. P. Thun, B. R. Staples, and R. G. Bates.

Vapor pressure and heat of sublimation of platinum. E. R. Plante, A. B. Sessoms, and K. R. Fitch.

Thermophysical properties of methane: Virial coefficients, vapor and melting pressures. R. D. Goodwin.

Specific heats, C_v, of compressed liquid and gaseous fluorine. R. Prydz and R. D. Goodwin.

Acidic dissociation of diprotonated piperazine in methanol-water solvents from 10 to 40°C. M. Paabo and R. G. Bates.

Thermal conductivity standard reference materials from 4 to 300 K. I. Armco iron: Including apparatus description and error analysis. J. G. Hust, R. L. Powell, and D. H. Weitzel.

Mössbauer spectrometer calibration using TiFe. L. J. Swartzendruber and L. H. Bennett.

Energies of $1snl$ $(l \geq 3)$ configurations in He^4 I as calculated from polarization theory. W. C. Martin.

Odd configurations in neutral nickel (Ni I). C. Roth.

A theoretical investigation of the configurations $(3d + 4s)^9$ $4p$ in neutral cobalt (Co I). C. Roth.

Electron-spin resonance study of an alkaline solution of copper (II) oxalate—*meso*-tartrate complex (the Somogyi reagent) and related complexes. A. J. Fatiadi.

J. Res. Nat. Bur. Stand. (U.S.), 74A (Phys. and Chem.), No. 6 (November–December 1970), SD Catalog No. C13.22/sec.A:74/6. $1.75.

PVT measurements, virial coefficients, and Joule-Thomson inversion curve of fluorine. R. Prydz and G. C. Straty.

The activity coefficients of hydrofluoric acid in water from 0 to 35°C. W. J. Hamer and Y.-C. Wu.

Fluoride flame calorimetry III. The heat of formation of chlorine trifluoride at 298.15 K. R. C. King and G. T. Armstrong.

A review of oscillator strengths for lines of Cu I. C. H. Corliss.

Stark effect and hyperfine structure of HCN measured with an electric resonance maser spectrometer. H. E. Radford and C. V. Kurtz.

The second spectrum of nickel (Ni II). A. G. Shenstone.

J. Res. Nat. Bur. Stand. (U.S.), 75A (Phys. and Chem.), No. 1 (Jan.–Feb. 1971), SD Catalog No. C13.22/sec.A:75/1.

High-speed (subsecond) measurement of heat capacity, electrical resistivity, and thermal radiation properties of tantalum in the range 1900 to 3200 K. A. Cezairliyan, J. L. McClure, and C. W. Beckett.

Thermophysical properties of methane: orthobaric densities and some thermal properties. R. D. Goodwin.

The infrared spectrum of matrix isolated BaO_2. S. Abramowitz and N. Acquista.

Refinement of the crystal structure of the aragonite phase of $CaCO_3$. B. Dickens and J. S. Bowen.

Simple shearing flows in polyisobutylene solutions. L. J. Zapas and J. C. Phillips.

Synthesis of fluorodienes. J. E. Fearn.

Quantum corrections to the second virial coefficient for the Lennard-Jones (*m*–6) potential. M. E. Boyd.

J. Res. Nat. Bur. Stand. (U.S.), 74B (Math. and Sci.), No. 2 (April–June 1970), SD Catalog No. C13.22/sec.B:74/2. $1.25.

Acoustic propagation and stability within an inviscid, heat-conducting fluid. J. E. McKinney and H. J. Oser.

On some indefinite integrals of confluent hypergeometric functions. E. W. Ng and M. Geller.

On complementary polar conical sets. C. Witzgall.

On contractive semigroups and uniform asymptotic stability. P. R. Meyers.

Normal subgroups of the modular group. L. Greenberg and M. Newman.

J. Res. Nat. Bur. Stand. (U.S.), 74B (Math. and Sci.), No. 3 (July–September 1970), SD Catalog No. C13.22/sec.B:74/3. $1.25.

Hecke basis theorems for groups of genus O. M. I. Knopp and J. Roderick Smart.

The distribution of eigenvalues of covariance matrices of residuals in analysis of variance. J. Mandel.

Expansions with coefficient algorithms for time domain responses of skin effect lossy coaxial cables. R. D. Holt.

Derivatives of the Grüneisen and Einstein functions. A. Cezairliyan.

Selecting nonlinear transformations for the evaluation of improper integrals. T. A. Atchison.

On the spheroidal functions. D. R. Rhodes.

Automatic computing methods for special functions. I. A. Stegun and R. Zucker.

American National Standard, Radiological safety in the design and operation of particle accelerators, NBS Handb. 107, 22 pages (June 1970), 30 cents, SD Catalog No. C13.11:107.

Anderson, R. L., Guildner, L. A., Edsinger, R. E., Movable and fixed modular vacuum devices with confined fluorocarbon plastic seals, Rev. Sci. Instr. **41,** No. 7, 1076–1082 (July 1970).

Arenhovel, H., Danos, M., Williams, H. T., Baryon resonances in nuclei: magnetic moments of the deuteron, Physics Letters **31B,** No. 3, 109–112 (February 2, 1970).

Armstrong, G. T., Hydrogen fluoride and the thermochemistry of fluorine, Nat. Bur. Stand. (U.S.), Tech. Note 513, 21 pages (Feb. 1970), 30 cents, SD Catalog No. C13.46:513.

Arp, V., Heat transport through helium II, Cryogenics **10,** No. 2, 96–105 (April 1970).

Astin, A. V., Report on the symposium on an International Standard Reference Materials Program, Metrologia **6,** No. 1, 33–34 (Jan. 1970).

Baker, M. A., A Summary of the three year inspection of the 1964 exposure test of porcelain enamels on aluminum, (Chapter in Proceedings of the Porcelain Enamel Institute Technical Forum, Ohio State Univ., Columbus, Ohio, Nov. 4–6, 1969, 31, 106–113 (Porcelain Enamel Institute, Washington, D.C., 1969).

Baker, M. A., Continuity of coating test and suggested applications, Chapter in Proceedings of the Porcelain Enamel Institute Technical Forum, Ohio State Univ., Columbus, Ohio, No. 4–6, 1969, 31, 71–84 (Porcelain Enamel Institute, Washington, D.C. 1969).

Baker, M. A., 1964 exposure test of porcelain enamels on aluminum three year inspection, Nat. Bur. Stand. (U.S.), Bldg. Sci. Ser. 29, 13 pages (Apr. 1970), 25 cents, SD Catalog No. C13.29/2:29.

Ballard, D. B., Yakowitz, H., Investigation of secondary cracks from the failed Point Pleasant, West Virginia Bridge, Proc. Third Annual Scanning Electron Microscope Symp., April 1970, 321–328 (Illinois Institute of Technology, Research Institute, Chicago, Ill. 1970).

Bennett, L. H., Comments on "Fe and Ni hyperfine fields in Ni_3Fe," Phys. Rev. **188,** No. 2, 1048 (Dec. 10, 1969).

Bennett, H. S., F center in ionic crystals. II. Palarizable-ion models, Phys. Rev. **184,** No. 3, 918–935 (Aug. 15, 1969).

Bennett, H. S., Frequency shifts of acoustic phonons in Heisenberg paramagnets. III, Phys. Rev. **185,** No. 2, 801–804 (1970).

Bennett, L. H., Swartzendruber, L. J., On the interpretation of Mössbauer effect spectra as related to the constitution of Cu-Ni-Fe alloys. Acta Met. **18,** No. 5, 485–498 (May 1970).

Bennett, L. H., Swartzendruber, L. J., Watson, R. E., Magnetic clusters associated with isolated Fe atoms in paramagnetic Cu-Ni alloys, Phys. Rev. Letters **23,** No. 20, 1171–1174 (Nov. 17, 1969).

Benson, S. W., O'Neal, H. E., Kinetic data on gas phase unimolecular reactions, NBS NSRDS–21, 645 pages (Feb. 1970) $7.00, SD Catalog No. C13.48:21.

Berger, M. J., Spectrum of energy deposited electrons in spherical regions, Proc. 2nd Symp. Microdosimetry, Stresa, Italy, October 20–24, 1969, Euratom Document No. 4452 d-f-e, 541–559 (1970).

Berger, M. J., Seltzer, S. M., Penetration of electrons and associated bremsstrahlung through aluminum targets, Chapter in Protection Against Space Radiation, NASA SP–169, pp. 285–322, National Aeronautics and Space Administration, Greenbelt, Md. (1968).

Berger, M. J., Seltzer, S. M., Maeda, K., Energy deposition of auroral electrons in the atmosphere, J. Atmospheric Terrest. Phys. **32,** 1015–1045 (1970).

Berry, V. M., Sage, B. H., Phase behavior in binary and multicomponent systems at elevated pressures: *n*-pentane and methane-*n*-pentane, NBS NSRDS–32, 73 pages (June 1970) 70 cents, SD Catalog No. C13.48:32.

Blaine, R. L., Tomes, L. A., Exploratory studies of early strength development in portland cement pastes and mortars, Nat. Bur. Stand. (U.S.), Bldg. Sci. Ser. 28, 14 pages (July 1970) 25 cents, SD Catalog No. C13.29/2:28.

Blake, R. W., Language of performance, an NBS project, Mater. Res. Std. **9,** No. 3, 11–14 (Mar. 1969).

Bjorge, S. E., Urbach, P. F., Earl, P. H., King, D. W., Wiederkehr, R. R. V., An experiment to determine the effectiveness of various announcement media on Clearinghouse For Federal Scientific and Technical Information Sales, Proc. American Society for Information Science Annual Meeting, Columbus, Ohio, Oct. 20–24, 1968, pp. 327–329 (Greenwood Publ. Corp., New York, N.Y., 1969).

Bjorge, S. E., Urbach, P. F., Earl, P. H., King, D. W., Wiederkehr, R. R. V., Experimentation, modeling and analysis to establish a new pricing policy at the Clearinghouse for Federal Scientific and Technical Information, Proc. American Society for Information Science Annual Meeting, Columbus, Ohio, Oct. 20–24, 1968, pp. 311–314 (Greenwood Publ. Corp., New York, N.Y., 1969).

Boesch, L., Napolitano, A., Macedo, P. B., Spectrum of volume relaxation times in B_2O_3, J. Am. Ceram. Soc. **53,** No. 3, 148–153 (1970).

Boswarva, I. M., Semiempirical calculations of ionic polarizabilities and van der Waals potential coefficients for the alkaline-earth chalcogenides, Phys. Rev. B. **1,** No. 4, 1698–1701 (Feb. 15, 1970).

Bowman, R. R., Quantifying hazardous electromagnetic fields: practical considerations, Nat. Bur. Stand. (U.S.), Tech. Note 389, 15 pages (Apr. 1970), 30 cents, SD Catalog No. C13.46:389.

Branscomb, L. M., The photoionization of one- and two-electron atoms, (Proc. Sommerfeld Centennial Memorial Meeting, Munich, Germany, Sept. 10–14, 1968), Chapter in Physics of the One- and Two-Electron Atoms, F. Bopp and H. Kleinpoppen, Eds., pp. 669–699 (North Holland Publ. Co., Amsterdam, The Netherlands, 1969).

Braun, W., Bass, A. M., Pilling, M., Flash photolysis of ketene and diazomethane: the production and reaction kinetics of triplet and singlet methylene, J. Chem. Phys. **52,** No. 10, 5131–5143 (May 15, 1970).

Brenner, A., Sligh, J. L., Electrodeless electrolysis, J. Electrochem. Soc. **117,** No. 5, 602–608 (May 1970).

Bridges, J. M., Wiese, W. L., The Oscillator-strength scale for Fe I, Astrophys. J. **161,** L71–L75 (July 1970).

Broadhurst, M. G., Mopsik, F. I., Bulk modulus and Gruneisen parameters for linear polymers, J. Chem. Phys. **52,** No. 7, 3634–3641 (Apr. 1, 1970).

Brombacher, W. G., Survey of micromanometers, NBS Mono. **114,** 62 pages (June 1970) 60 cents, SD Catalog No. C13.44:114.

Brower, W. S., Jr., Fang, P. H., Dielectric constants of scheelite structure crystals, J. Appl. Phys. **40,** No. 12, 4988–4989 (November 1969).

Brower, W. S., Jr., Fang, P. H., Dielectric constants of zinc tungstate, J. Appl. Phys. **41,** No. 5, 2266 (April 1970).

Brower, W. S., Jr., Farabaugh, E. N., Dislocation etchant for single crystal Y_2O_3, J. Am. Ceram. Soc. **53,** No. 4, 225 (April 1970).

Brown, D. W., Wall, L. A., Glass transition temperatures of several fluorine-containing polymers, J. Polymer Sci.: Part A–2, **7,** 601–608 (1969).

Bryson, J. O., Carpenter, E. F., Flexural behavior of prestressed concrete composite Twee-beams, Nat. Bur. Stand. (U.S.), Bldg. Sci. Ser. 31, 14 pages (July 1970) 25 cents, SD Catalog No. C13.29/2:31.

Catalog of standard reference materials, Nat. Bur. Stand. (U.S.), Spec. Publ. 260–1970 ed., 84 pages (July 1970) 75 cents, SD Catalog No. C13.10:260–1970 ed.

Bullis, W. M., Editor, Methods of measurement for semiconductor materials, process control, and devices. Quarterly report July 1 to September 30, 1969, Nat. Bur. Stand. (U.S.), Tech. Note 520, 69 pages (Mar. 1970), 65 cents, SD Catalog No. C13.46:520.

Bullis, W. M., Editor, Methods of measurement for semiconductor materials, process control, and devices, Quarterly Report Oct. 1 to Dec. 31, 1969, NBS Tech. Note 527, 60 pages (May 1970) 60 cents, SD Catalog No. C13.46:527.

Bullough, R., Simmons, J. A., On the deformation of an imperfect solid, Chapter 5 in Physics of Strength and Plasticity, A. S. Argon, Ed., 47–63 (Massachusetts Institute of Technology Press, Cambridge, Mass., 1969).

Bur, A. J., Extrapolation to single-relaxation-time behavior in solutions of poly(*n*-butylisocyanate), J. Chem. Phys. **52,** No. 7, 3813–3919 (Apr. 1, 1970).

Burgess, A., Hummer, D. G., Tully, J. A., Electron impact excitation of positive ions, Phil. Trans. Roy. Soc. London, Ser. A. **266,** No. 1175, 225–279 (Apr. 23, 1970).

Burke, R. W., Exchange reactions of ternary ion association complexes directly in the organic phase, Talanta **17,** 240–242 (1970).

Burke, R. W., Deardorff, E. R., Simultaneous spectrophotometric determination of cobalt, nickel and copper and 2,3–quinoxaline–Dithiol, Talanta **17,** 255–264 (1970).

Burke, P. G., Gallaher, D. F., Geltman, S., Electron scattering by atomic hydrogen using a pseudo-state expansion. I. Elastic scattering, J. Phys. B. (Proc. Phys. Soc.) **2,** 1142 (1969).

Burns, G. W., Hurst, W. S., An investigation of W–3% Re and W–25% Re thermoelements in vacuum argon and hydrogen, NASA Final Report CR–72639, 1–28 (National Aeronautics and Space Administration, Greenbelt, Md., Mar. 10, 1970).

Caswell, R. S., Danos, M., On the accuracy of the adiabatic separation method, J. Math. Phys. **11,** No. 2, 349–354 (Feb. 1970).

Childs, G. E., Diller, D. E., Refractive index of liquid deuterium, (Proc. 1969 Cryogenic Engineering Conf., June 16–18, 1969, Univ. of California, Los Angeles, Calif.), Chapter in Advances in Cryogenic Engineering 15, Paper No. C–2, 65–69 (Plenum Press, Inc., New York, N.Y., 1970).

Cohen, M. I., Casella, R. C., Blunt, R. F., Forman, R. A., Lattice absorption in strontium titanate, Phys. Rev. **186,** No. 3, 834–838 (Oct. 15, 1969).

Colwell, J. H., Mangum, B. W., Thornton, D. D.; Wright, J. C., Moos, H. W., Low-temperature magnetic properties of $DyPO_4$: An ideal three-dimensional ising antiferromagnet, Phys. Rev. Letters **23,** No. 21, 1245–1247 (Nov. 24, 1969).

Cooper, M. J., Critical indices of the Z–L polymer folding transition, J. Chem. Phys. Letter **52,** No. 1, 473–474 (Jan. 1, 1970).

Coxon, B., Model parameters for the analysis of skew conformations of carbohydrates by p.m.r. spectroscopy, Carbohydrate Res. **13,** 321–330 (1970).

Coxon, B., The synthesis, equilibration, and conformation of diastereoisomeric 1,2–*O*–*isorpopylidene*–3,5–*O*–(*methoxymethylidene*)–6–*O*–*p*–tolysulfonyl–α–D–glucofuranoses. Conformational evidence from a nuclear Overhauser effect, Carbohydrate Res. **12,** 313–334 (May 15, 1970).

Coyle, T. D., Silica, Kirk-Othmer Encyclopedia of Chemical Technology, 2d Edition **18,** 46–61 (1969).

Cuthill, J. R., A soft x-ray spectrometer with improved drive, Rev. Sci. Instr. **41,** No. 3, 422–423 (Mar. 1970).

Daney, D. E., Rapial, A. S., Preparation and characterization of slush hydrogen and nitrogen gels, (Proc. 1969 Cryogenic Engineering Conf., June 16–18, 1969, Univ. of California, Los Angeles, Calif.), Chapter in Advances in Cryogenic Engineering 15, Paper No. L–4, 467–475 (Plenum Press, Inc., New York, N.Y., 1970).

Demtroder, W., McClintock, M., Zare, R. N., Spectroscopy of Na_2 using laser-induced fluorescence, J. Chem. Phys. **51,** No. 12, 5495–5508 (Dec. 1969).

Deslattes, R. D., Relative energy measurements in the K series of argon, Phys. Rev. **186,** No. 1, 1–4 (Oct. 5, 1969).

Diamond, J. J., Editor, Bibliography on the high temperature chemistry and physics of materials. October, November, December 1969, Nat. Bur. Stand. (U.S.), Spec. Publ. 315–4, 85 pages (Jan. 1970), 75 cents, SD Catalog No. C13.10:315–4.

Diamond, J. J., Editor, Bibliography on the high temperature chemistry and physics of materials, Jan., Feb., Mar., 1970, NBS Spec. Publ. 315–5. 82 pages (Apr. 1970) 75 cents, SD Catalog No. C13.10:315.5.

Dickens, B., Brown, W. E., The crystal structure of calcium carbonate hexahydrate at ~−120°, Inorg. Chem. **9,** No. 3, 480–486 (Mar. 1970).

Diller, D. E., Roder, H. M., Thermal conductivity measurements on fluid hydrogen at 17 to 200°K and pressures to 10 MN/m^2, (Proc. 1969 Cryogenic Engineering Conf., June 16–18, 1969, Univ. of California, Los Angeles, Calif.), Chapter in Advances in Cryogenic Engineering 15, Paper No. C–1, 58–64 (Plenum Press, Inc., New York, N.Y., 1970).

DiMarzio, E. A., Guttman, C. M., Separation by flow, Macromolecules **3,** No. 2, 131–146 (Mar.–Apr. 1970).

Duncan, A. G., Hiza, M. J., A multipurpose phase equilibrium apparatus to study mixtures of cryogenic fluids: application to argon-methane, (Proc. 1969 Cryogenic Engineering Conf., June 16–18, 1969 Univ. of California, Los Angeles, Calif.), Chapter in Advances in Cryogenic Engineering 15, Paper No. B–2, 42–45 (Plenum Press, Inc., New York, N.Y., 1970).

Eisele, J. W., Technical Standards Coordinator, Horticultural grade perlite, NBS Voluntary Prod. Stand. 23–70, 9 pages; (May 1970) 10 cents, SD Catalog No. C13.20/2:23–70.

Eisele, J. W., Types and sizes of forms for one-way concrete joist construction, NBS Voluntary Prod. Stand. 16–69, 16 pages (June 1970), 10 cents, SD Catalog No. C13.20/2:16–69.

Eisenhart, C., Anniversaries in 1970 of interest to statisticians, Am. Stat. **24,** No. 1, 25–68 (Feb. 1970).

Engen, G. F., An evaluation of the "back-to-back" method of measuring adapter efficiency, IEEE Trans. Instr. Meas. **IM–19,** No. 1, 18–22 (Feb. 1970).

Ernst, M. H., Dorfman, J. R., Hoegy, W. R., Van Leeuwen, J. M. J., Hard sphere dynamics and binary collision operators, Physica **45,** 127–146 (1969).

Evenson, K. M., Wells, J. S., Matarrese, L. M., Absolute frequency measurements of the CO_2 cw laser at 28 THz (10.6 μm), Appl. Phys. Letters **16,** No. 6, 251–253 (Mar. 15, 1970).

Evenson, K. M., Wells, J. S., Matarrese, L. M., Elwell, L. B., Absolute frequency measurements of the 28– and 78–μm cw water vapor laser lines, Appl. Phys. Letters **16,** No. 4, 159–161 (Feb. 15, 1970).

Faison, T. K., Jr., Davis, J. C., Achenbach, P. R., Performance of louvered devices as air mixers, NBS Bldg. Sci. Ser. 27, 22 pages (Mar. 1970) 30 cents, SD Catalog No. C13.29/2:27.

Farrar, T. C., Tsang, T., Johannesen, R. B., Internal reorientations in K_2ReH_9 via wide-line and pulsed proton resonance studies, J. Chem. Phys. **51,** No. 8, 3595–3596 (Oct. 15, 1969).

Fatiadi, A. J., Conversion of certain cyclic phenylhydrazino derivatives into phenylazo compounds with periodic acid, J. Org. Chem. **35,** No. 3, 831–833 (Mar. 1970).

Fatiadi, A. J., Preparation of inositol hexasulfate, Carbohydrate Res. **12,** 293–296 (1970).

Fatiadi, A. J., Novel aromatization of a trihydroxycyclohexanetrione (triketoinositol) to a dibenzo–*p*–dioxin derivative, Carbohydrate Res. **12,** 130–132 (1970).

Feldman, A., Horowitz, D., Refractive index of cuprous chloride, J. Opt. Soc. Am. **59,** No. 11, 1406–1408 (Nov. 1969).

Fishman, L., Mountain, R. D., Activity coefficients of solutions from the intensity ratio of Rayleigh to Brillouin scattering, J. Phys. Chem. **74,** No. 10, 2178–2182 (May 14, 1970).

The Flammable Fabrics Program, 1968–1969. U.S. Department of Commerce report of activities under the Flammable Fabrics Act, 1968–1969, Nat. Bur. Stand. (U.S.), Tech. Note 525, 84 pages (Apr. 1970), 75 cents, SD Catalog No. C13.46:525.

Fraker, A. C., Ruff, A. W., Jr., Microstructural studies of 7075 Al-relation to the directional sensitivity for stress corrosion cracking, Corrosion Sci. **10,** 191–195 (1970).

Franklin, A. D., Bennett, H. S., Editors, ARPA–NBS program of research on high temperature materials and laser materials. Reporting period January 1 to June 30, 1969, Nat. Bur. Stand. (U.S.), Tech. Note 514, 98 pages (Jan. 1970), $1.00, SD Catalog No. C13.46:514.

Franklin, A. D., Bennett, H. S., Editors, ARPA–NBS program of research on high temperature materials and laser materials. Reporting Period July 1 to December 31, 1969, NBS Tech. Note 531, 75 pages (June 1970) 70 cents, SD Catalog No. C13.46:531.

Frederikse, H. P. R., Superconducting semiconductors, (Proc. Conf. International Advanced Study Institute: Electronic Structures in Solids, Chania, Crete, Greece, June 30–July 14, 1968), Chapter in Electronic Structures in Solids, pp. 270–282 (Plenum Press Inc., New York, N.Y., 1969).

Frederikse, H. P. R., The electronic band structure of strontium titanate: Theory and experiment (Proc. Conf. International Advanced Study Institute: Electronic Structures in Solids, Chania, Crete, Greece, June 30–July 14, 1968), Chapter in Electronic Structures in Solids, 259–269 (Plenum Press, New York, N.Y., 1969).

Freeman, D. H., Goldstein, S., Schmuckler, G., Homogeneous sulfonation of styrene-divinylbenzene copolymers with oleum in organic solvents, Israel J. Chem. **7,** No. 6, 741–749 (1969).

Funkhouser, A. T., Mielenz, K. D., High-speed holographic interferometry, Appl. Opt. **9,** No. 5, 1215 (May 1970).

Furukawa, G. T., Saba, W. G., Sweger, D. M., Plumb, H. H., Normal boiling point and triple point temperatures of neon, Metrologia **6,** No. 1, 35–37 (Jan. 1970).

Gadzuk, J. W., Coupled surface-plasmon modes in metal-thin-film vacuum sandwiches, Phys. Rev. B, **1,** No. 3, 1267–1269 (Feb. 1, 1970).

Gadzuk, J. W., Resonance transmission in electron emmission from surfaces with adsorbed atoms, Surface Sci. **18,** 193–203 (1969).

Gadzuk, J. W., Resonance-tunneling spectroscopy of atoms adsorbed on metal surfaces: theory, Phys. Rev. B. **1,** No. 5, 2110–2129 (March 1, 1970).

Gallagher, A., State-transfer; collisions, (Proc. Sommerfeld Centennial Memorial Meeting, Munich, Germany, Sept. 9–14, 1968), Chapter in Physics of the One- and Two-Electron Atomics, F. Bopp and H. Kleinpoppen, Eds., pp. 788–794 (North Holland Publ. Co., Amsterdam, The Netherland, 1969).

Geil, G. W., Feinberg, I. J., Temperature changes in specimens in microplasticity tests, Met. Trans. **1,** No. 7, 1845–1851 (July 1970).

Giacchetti, A., Stanley, R. W., Zalubas, R., Proposed secondary-standard wavelengths in the spectrum of thorium, J. Opt. Soc. Am. **69,** No. 4, 474–489 (April 1970).

Ginnings, D. C., Editor, Precision measurement and calibration. Selected NBS Papers on heat, NBS Spec. Publ. 300, Vol. 6, 387 pages (February 1970) $5.00, SD Catalog No. C13.10:300/v.6.

Goltz, S. M., Tanner, C. B., Thurtell, G. W., Jones, F. E., Evaporation measurements by an Eddy correlation method, Water Resources Res. **6,** No. 2, 440–446 (Apr. 1970).

Gonano, R., Adams, E. D., In Situ vapor pressure measurement for low temperature thermometry, Rev. Sci. Instr. **41,** No. 5, 716–719 (May 1970).

Graminski, E. L., The stress-strain behavior of accelerated and naturally aged papers, TAPPI **53,** No. 3, 406–410 (Mar. 1970).

Greenfeld, S. H., Warner, E. R., Reinhart, H. W., Bibliographies on fabric flammability. Part 1. Wearing apparel; Part 2. Fabrics used on beds; Part 3. Carpets and rugs, Nat. Bur. Stand. (U.S.), Tech. Note 498, 36 pages (Feb. 1970), 40 cents, SD Catalog No. C13.46:498.

Greenfeld, S. H., Warner, E. R., Reinhart, H. W., Bibliographies on fabric flammability. Part 4. Interior furnishings, NBS Tech. Note 498–1, 24 pages (June 1970) 30 cents, SD Catalog No. C13.46:498–1.

Greenspan, M., Tschiegg, C. E., Cavitation nucleated by $^{10}B(n,\alpha)^{7}Li$, Nucl. Instr. Methods **82,** No. 3, 310–312 (1970).

Gross, D., Natrella, M. G., Interlaboratory comparison of the potential heat test method, Am. Soc. Testing Mater. Spec. Tech. Publ. 464, Fire Test Performance, 127–152 (1970).

Gugeler, A. L., A study of the adherence of porcelain enamel to aluminum, Chapter in Proc. of the Porcelain Enamel Institute Forum, Ohio State Univ., Columbus, Ohio, November 4–6, 1969, 31, 37–45, Porcelain Enamel Institute, Washington, D.C. (1969).

Guildner, L. A., Stimson, H. F., Edsinger, R. E., Anderson, R. L., An accurate mercury manometer for the NBS gas thermometer, Metrologia **6,** No. 1, 1–18 (Jan. 1970).

Haar, L., Sengers, J. M. H. L., The solubility of condensed substances in dense gases, and the effect of PVT properties, J. Chem. Phys. **52,** No. 10, 5069 (May 15, 1970).

Haber, S., Sequences of numbers that are approximately completely equidistributed, J. Assoc. Computing Mach. **17,** No. 2, 269–272 (Apr. 1970).

Haber, S., Stochastic quadrature formulas, Math. Computation 23, No. 108, 751–764 (Oct. 1969).

Haber, S., Osgood, C. F., On the sum $\Sigma<na>^{-1}$ and numerical integration, Pacific J. Math. **31,** No. 2, 383–394 (1969).

Hamilton, W. C., Edmonds, J. W., Tippe, A., Rush, J. J., Methyl group rotation and the low temperature transition in hexamethylbenzene. A neutron diffraction study, Discussions Faraday Soc., No. 48, 192–204 (1969).

Handy, L. B., Brinckman, F. E., Chemistry of the methoxyfluorotungsten (VI) series, Chem. Commun. 214–215 (1970).

Hanson, D. W., Quasi-optical components using total reflection in dielectrics, IEEE Trans. Microwave Theory Tech. **MTT–18,** No. 4, 233–234 (April 1970).

Harvey, J. L., Brenner, F. C., Tire use survey. The physical condition, use, and performance of passenger car tires in the United States of America, NBS Tech. Note 528, 59 pages (May 1970), 60 cents, SD Catalog No. C13.46:528.

Heinrich, K. F. J., Electron and ion microprobe analysis (Proc. 10th Symp. Electron, Ion, and Laser Beam Technology, Gaithersburg, Md., May 21–23, 1969), Chapter in Record of the 10th Symposium on Electron, Ion and Laser Beam Technology, L. Marton, Ed., 353–360 (San Francisco Press, San Francisco, Calif., 1969).

Heinrich, K. F. J., Present state of the classical theory of quantitative electron probe microanalysis, Nat. Bur. Stand. (U.S.), Tech. Note 521, 17 pages (Aug. 1970) 30 cents, SD Catalog No. C13.46:521.

Heinrich, K. F. J., Yakowitz, H., Quantitative electron probe microanalysis: Uncertainty in the atomic number correction, Mikrochim. Acta **7,** No. 1, 123–134 (Jan. 1970).

Hellwig, H., Hydrogen spin exchange frequency shifts, NBS Tech. Note 387, 13 pages (March 1970), 30 cents, SD Catalog No. C13.46:387.

Henderson, B., Stokowski, S. E., Ensign, T. C., Luminescence from F centers in calcium oxide, Phys. Rev. **183,** No. 3, 826–831 (July 15, 1969).

Hendricks, R. C., Simoneau, R. J., Smith, R. V., Survey of heat transfer to near-critical fluids, (Proc. 1969 Cryogenic Engineering Conf., June 16–18, 1969, (Univ. of California, Los Angeles, Calif.), Chapter in Advances in Cryogenic Engineering 15, Paper No. G–1, 197–237 (Plenum Press, Inc., New York, N.Y., 1970).

Hilten, J. S., Accelerometer calibration with the earth's field dynamic calibrator, Nat. Bur. Stand. (U.S.), Tech. Note 517, 30 pages (Mar. 1970), 35 cents, SD Catalog No. C13.46:517.

Hiza, M. J., Solid-vapour equilibria research on systems of interest in cryogenics, Cryogenics **10,** No. 2, 106–115 (April 1970).

Hoegy, W. R., Convergent generalization of the Boltzmann equation for a hard sphere, Phys. Rev. **185,** No. 1, 210–218 (Sept. 5, 1969).

Horn, W. A., Optimal networks joining n points in the plane (Proc. IVth International Symp. The Theory of Traffic Flow, Karlsruhe, Germany, June 18–20, 1968), Chapter in Strassenbau und Strassenverkehrstechnik 86, W. Leutzbach and P. Baron, Eds., 160–166 (Bundesminister fur Verkehr, Germany, 1969).

Hosler, W. R., Frederikse, H. P. R., Magnetoresistive effects in $KTaO_3$, Solid State Commun. **7,** 1443–1449 (1969).

Hougen, J. T., The calculation of rotational energy levels and rotational line intensities in diatomic molecules, Nat. Bur. Stand. (U.S.), Monogr. 115, 52 pages (June 1970) 55 cents, SD Catalog No. C13.44:115.

Hummer, D. G., Observatory Report—Joint Institute for Laboratory Astrophysics of the National Bureau of Standards and the University of Colorado, Bull. Am. Astron. Soc. **2,** No. 1, 59–65 (1970).

Hummer, D. G., Spectral line formation by noncoherent scattering with a dipole phase-function, Astrophysical Letters **5,** 1 (1970).

Jones, M. C., Far infrared absorption in liquefied gases, NBS Tech. Note 390, 39 pages (April 1970), 50 cents, SD Catalog No. C13.46:390.

Jones, M. C., Far infrared absorption in liquid hydrogen, J. Chem. Phys. **51,** No. 9, 3833–3834 (Nov. 1, 1969).

Jones, R. N., Huntley, L. E., A precision, high frequency calibration facility for coaxial capacitance standards, NBS Tech. Note 386, 27 pages (March 1970), 35 cents, SD Catalog No. C13.46:386.

Kasen, M. B., Grain boundary resistivity of aluminum, Phil. Mag. **21,** No. 171, 599–610 (Mar. 1970).

Kaufman, V., Humphreys, C. J., Accurate energy levels and calculater wavelengths of ^{86}Kr I, J. Opt. Soc. Am. **59,** No. 12, 1614–1628 (Dec. 1969).

Kidnay, A. J., Hiza, M. J., Dickson, P. F., Adsorption kinetics in a ternary system containing hydrogen, (Proc. 1969 Cryogenic Engineering, Conf., June 16–18, 1969, Univ. of California, Los Angeles, Calif.), Chapter in Advances in Cryogenic Engineering 15, Paper No. B–3, 46–49 (Plenum Press, Inc., New York, N.Y., 1970).

Kieffer, L. J., Low-energy electron-collision cross-section data. Part I: Ionization, dissociation, vibrational excitation, Atomic Data **1,** 19–89 (1969).

Klein, R., Scheer, M. D., Addition of oxygen atoms to olefins at low temperature. IV. Rearrangements, J. Phys. Chem. **74,** No. 3, 613–616 (Feb. 5, 1970).

Klose, J. Z., Transition probabilities and mean lives of the $3s_2$ laser level in neon I, Phys. Rev. **188,** No. 1, 45–49 (Dec. 5, 1969).

Kokoszka, G. F., Brinckman, F. E., Electron paramagnetic resonance studies of phosphorus-containing reactive intermediates, J. Am. Chem. Soc. **92,** No. 5, 1199–1205 (1970).

Kose, V. E., Sullivan, D. B., Influence of external noise on microwave-induced Josephson steps, J. Appl. Phys. **41,** No. 1, 169–174 (Jan. 1970).

Krauss, M., Mielczarek, S. R., Minima in generalized oscillator strengths: C_2H_4, J. Chem. Phys. **51,** No. 12, 5241–5243 (Dec. 15, 1969).

Kuriyama, M., The dynamical scattering amplitude of an imperfect crystal, Acta Cryst. **A26,** No. 6, 56–59 (Jan. 1970).

Kushner, L. M., Are there standards? (Proc. National Safety Congress Conf., Chicago, Ill., Oct. 28, 1969), National Safety Congress Trans., Civic Leadership 6, 12–16 (1969).

Lafferty, W. J., Maki, A. G., Coyle, T. D., High resolution infrared spectrum and structure of diborane, J. Mol. Spectr. **33,** No. 2, 345–367 (1970).

LaFleur, P. D., Editor, Activation analysis section: Summary of activities July 1968 to June 1969, Nat. Bur. Stand. (U.S.) Tech. Note 508, 147 pages (July 1970) $1.25, SD Catalog No. C13.46:508.

Landgrebe, W. B., Mann, W. B., Schima, F. J., The distribution of 70–kV prasodymium ions in iron foil and a technique for removing thin layers of iron, Intern. J. Appl. Radiation Isotopes **21,** No. 3, 169–171 (Mar. 1970).

Larson, W., Desch, R. F., Gillard, B. F., Further analysis of the off-null versus power ratio method of attenuation measurement, IEEE Trans. Microwave Theory Tech. **MTT–18,** No. 2, 112–113 (Feb. 1970).

Lawton, R. A., Allerd, C. M., Hudson, P. A., A wide-range CW power measurement technique, IEEE Trans. Instr. Meas. **IM–19,** No. 1, 28–34 (Feb. 1970).

Lechner, R. E., Rowe, J. M., Sköld, K., Rush, J. J., Study of molecular reorientation in solid neopentane by quasielastic neutron scattering, J. Chem. Phys. Letters **4,** No. 7, 444–448 (Dec. 15, 1969).

Levin, E. M., X-ray determination of the thermal expansion of silver nitrate, J. Am. Ceram. Soc. **52,** No. 1, 53–54 (January 1969).

Lide, D. R., Jr., Determination of anharmonic potential constants in linear XYZ molecules, J. Mol. Spectr. **33,** No. 3, 448–459 (Mar. 1970).

Locke, J. W., Penn, R., Rick, J., Bunten, E., Hare, G., Compilation and use of criminal court data in relation to Pre-Trial Release of defendants: pilot study, Nat. Bur. Stand. (U.S.), Tech. Note 535, 242 pages (Aug. 1970) $1.75, SD Catalog No. C13.46:535.

Lutz, G. J., Determination of oxygen in sodium by photon activation analysis, Anal. Chem. **42,** No. 4, 531–532 (Apr. 1970).

Lutz, G. J., Editor, Determination of the light elements in metals: A bibliography of activation analysis papers, NBS Tech. Note 524, 66 pages (May 1970), 75 cents, SD Catalog No. C13.46:524.

Lutz, G. J., Editor, Forensic science: A bibliography of activation analysis papers, Nat. Bur. Stand. (U.S.), Tech. Note 519, 47 pages (Mar. 1970), 50 cents, SD Catalog No. C13.46:519.

Lutz, G. J., Editor, Oceanography: a bibliography of selected activation analysis literature, NBS Tech. Note 534, 36 pages (June 1970) 50 cents, SD Catalog No. C13.46:534.

Lutz, G. J., Editor, Pollution analysis: a bibliography of the literature of activation analysis, NBS Tech. Note 532, 32 pages (June 1970) 45 cents, SD Catalog No. C13.46:532.

Lutz, G. J., Editor, 14–MeV neutron generators in activation analysis: a bibliography, NBS Tech. Note 533, 91 pages (June 1970) $1.00, SD Catalog No. C13.46:533.

Lutz, G. J., Boreni, R. J., Maddock, R. S., Meinke, W. W., Editors, Activation Analysis: A bibliography, NBS Tech. Note 467, Part 1, Addendum 1, 176 pages (Dec. 1969) and Part 2, Appendices, Revision 1, NBS Tech. Note 467, 264 pages (Dec. 1969), $8.50 per set of 3 volumes, sold in sets only. Part 1 of September 1968 accompanies these sets, SD Catalog No. C13.46:467.

Lutz, G. J., Masters, L. W., Determination of carbon in high purity metals by photon activation analysis, Anal. Chem. **42,** No. 8, 948–950 (July 1970).

McAlister, A. J., Calculation of the soft x-ray K-emission and absorption spectra of metallic Li, Phys. Rev. **186,** No. 3, 595–599 (Oct. 15, 1969).

McClintock, M., Balling, L. C., Atomic and molecular fluorescence from laser excited diatomic cesium and rubidium, J. Quant. Spectro. Radiative Transfer **9,** 1209–1214 (1969).

McClintock, M., Demtroder, W., Zare, R. N., Level crossing studies of Na_2 using laser-induced fluorescence, J. Chem. Phys. **51,** No. 12, 5509–5521 (Dec. 1969).

McKinney, J. E., Oser, H. J., Stability of acoustic waves within a viscous compressible heat-conduction fluid, J. Acoust. Soc. Am. **47,** No. 3, 781–785 (March 1970).

McLaughlin, W. L., Photographic film dosimeters, Chapter in Manual on Radiation Dosimetry, N. W. Holm and R. J. Berry, Eds., 387–394 (Marcel Dekker, Inc., New York, N.Y., 1970).

McLaughlin, W. L., Radiochromic dye-cyanide dosimeters, Chapter in Manual on Radiation Dosimetry, N. W. Holm and R. J. Berry, Eds., 377–385 (Marcel Dekker, Inc., New York, N.Y., 1970).

McNish, A. G., Progress on the Metric Study Program, Proc. Conf. 18th Annual Meeting of Standards Engineers Society, Washington, D.C., Sept. 17–19, 1969, pp. 53–56 (Standards Engineers Society, Philadelphia, Pa., 1969).

McNish, A. G., The impact of increasing metric usage, Proc. Conf. Industrial Heating Equipment Association, Spring (77th Consecutive) Meeting, Hot Springs, Virginia, May 19–21, 1969,

Exhibit E (Industrial Heating Equipment Assoc., Washington, D.C., 1969).

Machta, L., Hughes, E., Atmospheric oxygen in 1967–1970, Science **168,** No. 3939, 1582–1584 (June 26, 1970).

Mackay, D. R., American Softwood Lumber Standard, NBS Voluntary Prod. Stand. 20–70, 26 pages (Jan. 1970), 35 cents, SD Catalog No. C13.20/2:20–70.

Madey, T. E., Yates, J. T., Jr., Chemisorption on single crystals: H_2 on (100) tungsten, Proc. Colloque Intern. sur la Structure et les Proprietes des Surfaces des Solides, Paris, France, July 7–11, 1969, No. 187, pp. 155–162 (Centre National de la Recherche Scientifique, Paris, France, 1970).

Madey, T. E., Yates, J. T., Jr., King, D. A., Uhlaner, C. J., Isotope effect in electron stimulated desorption: oxygen chemisorbed on tungsten, J. Chem. Phys. **42,** No. 10, 5215–5220 (May 15, 1970).

Mahler, R. J., Nominal $\Delta m = \pm 1$, 2, 3, 4, 5 magnetic nuclear transition probabilities in ruby, Phys. Rev. **188,** No. 2, 584–590 (Dec. 1969).

Mahler, R. J., James, L. W., Acoustic and magnetic effects involving the 19F nuclei in antiferromagnetic KMnF, J. Appl. Phys. **41,** No. 4, 1633–1636 (March 15, 1970).

Manning, J. R., Cross terms in the thermodynamic diffusion equations for multicomponent alloys, Met. Trans. AIME **1,** 499–505 (Feb. 1970).

Margoshes, M., Data acquisition and computation in spectrochemical analysis: a forecast, Spectrochim. Acta **25B,** 113–122 (June 15, 1969).

Margoshes, M., Scribner, B. F., Emission spectrometry, Anal. Chem. **42,** No. 5, 398R–417R (April 1970).

Marsden, C. P., Cowan, R. Y., Tabulation of data on semiconductor amplifiers and oscillators at microwave frequencies, Nat. Bur. Stand. (U.S.), Tech. Note 518, 66 pages (Feb. 1970), 65 cents, SD Catalog No. C13.46:518.

Marton, L., Survey of microanalysis-interpolation and extrapolation, Chapter in Electron Probe Microanalysis, pp. 1–14 (Academic Press Inc., New York, N.Y., 1969).

Marvin, R. S., Rheological Models and measurements, (Proc. 5th. Intern. Congress on Rheology, Kyoto, Japan, Oct. 7–11, 1968), Chapter in Fifth International Congress on Rheology, S. Onogi, Ed., 1, 85–96, (University of Tokyo Press and University Park Press, Tokyo, Japan, 1969).

Mauvais, C. J., Latanision, R. M., Ruff, A. W., Jr., On the anisotropy observed during the passivation of nickel monocrystals, J. Electrochem. Soc. **117,** No. 7, 902–903 (July 1970).

Mazur, J. Higher order Markov chains and statistical thermodynamics of linear polymers, Chapter 6 in Markov Chains and Monte-Carlo calculations in Polymer Science, G. G. Lowry, Ed., 153–185 (Marcel Dekker, Inc., New York, N.Y., 1970).

Melmed, A. J., Carroll, J. J., Ellipsometry, LEED, and FEM study of evaporated epitaxial films of iron on (011) tungsten, Surface Sci., Letters to the Editor **19,** No. 1, 243–248 (January 1970).

Messina, C. G., Hilsenrath, J., Edit-insertion programs for automatic typesetting of computer printout, NBS Tech. Note 500, 50 pages (Apr. 1970), 60 cents, SD Catalog No. C13.46:500.

Michaels, S., Green, M. S., Larsen, S. Y., Equilibrium critical phenomena in fluids and mixtures: a comprehensive bibliography with key-word descriptors, NBS Spec. Publ. 327, 235 pages (June 1970) $4.00 SD Catalog No. C13.10:327.

Mies, F. H., Resonant scattering theory of association reactions and unimolecular decomposition. II. Comparison of the collision theory and the absolute rate theory, J. Chem. Phys. **51,** No. 2, 798–807 (July 1969).

Mighell, A. D., Reimann, C. W., Santoro, A., The crystal structure of the 2:1 dimer $[(\text{pyridine N–oxide})_2CuBr_2]_2$, Chem. Commun. **4,** 204 (1970).

Miles, B. M., Wiese, W. L., Bibliography on atomic transition probabilities, January 1916 through June 1969, Nat. Bur. Stand. (U.S.), Spec. Publ. 320, 111 pages (Feb. 1970), (Supersedes NBS Misc. Publ. 278 and Supplement) $1.25, SD Catalog No. C13.10:320.

Milligan, D. E., Jacox, M. E., Infrared and ultraviolet spectra of the products of the vacuum-ultraviolet photolysis of silane isolated in an argon matrix, J. Chem. Phys. **52,** No. 5, 2594–2608 (Mar. 1, 1970).

Milligan, D. E., Jacox, M. E., Guillory, W. A., Infrared spectrum of NO_2–ion isolated in an argon matrix, J. Chem. Phys. **52,** No. 8, 3864–3868 (April 15, 1970).

Molino, J. A., Noise the growing hazard, Dialog **1,** No. 4, 26–28 (1970).

Mosburg, E. R., Periodic potential probe configuration for plasma diagnostics, J. Appl. Phys. **40,** No. 13, 5290–5300 (Dec. 1969).

Mozer, B., Price, D. L., Keating, D. T., Meister, H., Incoherent neutron scattering from liquid and solid CuNi, Physics Letters **30A,** No. 3, 206–207 (Oct. 6, 1969).

Mountain, R. D., Comments on fluctuation theory calculations of the specific heat near the critical point, J. Chem. Phys. **52,** No. 7, 3852–3853 (April 1, 1970).

Mountain, R. D., Liquids: Dynamics of liquid structure, Critical Reviews in Solid State Sciences **1,** No. 1, 5–46 (Chemical Rubber Co., Cleveland, Ohio, March 1970).

Nargolwalla, S. S., Crambes, M. R., Suddueth, J. E., Photon self-adsorption corrections for the minimization of systematic errors in 14–MeV neutron activation analysis, Anal. Chim. Acta **49,** No. 3, 425–436 (Mar. 1970).

Nargolwalla, S. S., LaFleur, P. D., Characterization of standard reference materials for industry and research by neutron activation analysis, Proc. American Nuclear Society Topical Meeting, San Juan, Puerto Rico, May 4–6, 1969, 183–186 (1969).

Negas, T., Roth, R. S., The system $SrMnO_{3-x}$, J. Solid State Chem. **1,** 409–418 (1970).

Newell, K. G., Jr., Technical Standards Coordinator, Acrylonitrile–butadiene–styrene (ABS) plastic pipe (schedules 40 and 80), NBS Voluntary Prod. Stand. 18–69, 15 pages (June 1970) 15 cents, SD Catalog No. C13.20/2:18–69. Supersedes NBS Commercial Standard CS218–59.

Newell, K. G., Jr., Technical Standards Coordinator, Acrylonitrile–butadiene–styrene (ABS) plastic pipe (standard dimension ratio), NBS Voluntary Prod. Stand. 19–69, 13 pages (June 1970) 15 cents, SD Catalog No. C13.20/2:19–69. Supersedes NBS Commercial Standard CS254–63.

Newell, K. G., Technical Standards Coordinator, Poly(vinyl chloride) (PVC) plastic pipe (schedules 40, 80, and 120), Nat. Bur. Stand. (U.S.), Voluntary Prod. Stand. 21–70, 16 pages (June 1970) 15 cents, SD Catalog No. C13.20/2:21–70.

Newell, K. G., Technical Standards Coordinator, Poly(vinyl chloride) (PVC) plastic pipe (standard dimension ratio), Nat. Bur. Stand. (U.S.), Voluntary Prod. Stand. 22–70, 14 pages (June 1970) 20 cents, SD Catalog No. C13.20/2:22–70.

Newman, M., A table of the first factor for prime cyclotomic fields, Math. Compt. 24, No. 109, 215–219 (Jan. 1970).

Newman, M., Isometric circles of congruence groups, Am. J. Math. **XCI,** No. 3, 648–656 (July 1969).

Olver, F. W. J., Why steepest descents? SIAM Rev., **12,** No. 2, 228–247 (April 19, 1970).

Osgood, C. F., A method in diophantine approximation (III), Acta Arithmetica **XVI,** 5–22 (1969).

Osgood, C. F., A method in diophantine approximation (IV), Acta Arithmetica **XVI,** 23–40 (1969).

Paabo, M., Bates, R. G., Deuterium isotope effects and the dissociation of deuteriophosphoric acid from 5 to 50°, J. Phys. Chem. **74,** No. 4, 706–710 (Feb. 19, 1970).

Paabo, M., Bates, R. G., Dissociation constant of protonated 2,2–bis(hydroxymethyl)–2,2',"–nitrilotriethanol (*bis–tris*) and related thermodynamic functions from 0 to 50°, J. Phys. Chem. **74,** No. 4, 702–705 (Feb. 19, 1970).

Page, C. H., Relations among systems of electromagnetic equations, Am. J. Phys. **38,** No. 4, 421–424 (April 1970).

Page, C. H., The trolley problem, Am. J. Phys. **38,** No. 5, 608–610 (May 1970).

Parke, W. C., Ponzini, R. G., Williams, H. T., Remarks on finite-energy sum rules, Phys. Rev. **1,** No. 1–D, 134–139 (Jan. 1, 1970).

Paule, R. C., Mandel, J., Standard reference materials: Analysis of interlaboratory measurements on the vapor pressure of gold

(certification of standard reference material 745), Nat. Bur. Stand. (U.S.), Spec. Publ. 260–19, 21 pages (Jan. 1970), 30 cents, SD Catalog No. C13.10:260–19.

Paulsen, P. J., Alvarez, R., Mueller, C. W., Spark source mass spectrographic analysis of ingot iron for silver, copper, molybdenum and nickel by isotope dilution and for cobalt by an internal standard technique, Anal. Chem. **42,** 673–675 (May 1970).

Penner, S., Beam handling techniques for electron linear accelerators, NBS Tech. Note 522, 21 pages (Apr. 1970), 30 cents, SD Catalog No. C13.46:522.

Penner, S., Experimental techniques for electron scattering investigations, Nat. Bur. Stand. (U.S.), Tech. Note 523, 46 pages (Apr. 1970), 50 cents, SD Catalog No. C13.46:523.

Pfeiffer, E. R., Schooley, J. F., Effect of stress on the superconducting transition temperature of $SrTiO_3$, J. Low Temp. Phys. **2,** No. ¾, 333–352 (August 7, 1970).

Phillips, S. L., Johnson, C. E., Effect of atmospheric exposure on the contact resistance of selected tin alloys, J. Electrochem. Soc. **117,** No. 6, 827–830 (June 1970).

Philo, H. A., Technical Standards Coordinator, Polyethylene (PE) plastic pipe (SDR), Nat. Bur. Stand. (U.S.), Prod. Stand. 11–69, 14 pages (Mar. 1970), 15 cents, SD Catalog No. C13.20/2:11–69. (Supersedes Commercial Standard CS 255–63.)

Philo, H. A., Technical Standards Coordinator, Polyethylene (PE) plastic pipe (schedule 40—inside diameter dimensions), Nat. Bur. Stand. (U.S.), Prod. Stand. 10–69, 14 pages (Mar. 1970), 15 cents, SD Catalog No. C13.20/2:10–69. (Supersedes Commercial Standard CS 197–60.)

Philo, H. A., Technical Standards Coordinator, Polyethylene (PE) plastic pipe (schedules 40 and 80—outside diameter dimensions), Nat. Bur. Stand. (U.S.), Prod. Stand. 12–69, 14 pages (Mar. 1970), 15 cents, SD Catalog No. C13.20/2:12–69.

Photonuclear data index, Jan. 1965 through Jan. 1970, NBS Spec. Publ. 322, 86 pages (May 1970), 75 cents, SD Catalog No. C13.10:322, (Supersedes Supplement 1 to Misc. Publ. 277).

Phucas, C. B., Technical Standards Coordinator, Salt packages, Nat. Bur. Stand. (U.S.), Prod. Stand. 14–69, 9 pages (May 1970) 10 cents, SD Catalog No. C13.20/2:14–69. (Supersedes Simplified Practice Recommendation 70–54.)

Plummer, E. W., Young, R. D., Field–emission studies of electronic energy levels of adsorbed atoms, Phys. Rev. B, **1,** No. 5, 2088–2109 (March 1, 1970).

Powell, C. J., Analysis of optical- and inelastic-electron-scattering data. II. Application to Al, J. Opt. Soc. Am. **60,** No. 1, 78–93 (Jan. 1970).

Powell, C. J., Analysis of optical- and inelastic-electron-scattering data. III. Reflectance data for beryllium, germanium, antimony, and bismuth, J. Opt. Soc. Am. **60,** No. 2, 214–220 (Feb. 1970).

Powell, F. X., Johnson, D. R., Microwave detection of $H_2{}^{18}O$, Phys. Rev. Letters **24,** No. 12, 637 (Mar. 23, 1979).

Powell, R. L., Cryogenic materials needs, Proc. 5th Annual Natl. Conf. Industrial Research, Sept. 18–19, 1969, Chicago, Ill., Chapter in Applying Emerging Technologies, 102–107 (Industrial Research, Inc., Beverly Shores, Indiana, 1970).

Qureshi, I. H., McClendon, L. T., LaFleur, P. D., Extraction studies of the group IIIB–VIIB elements and the lanthanides utilizing *bis*(2–ethyl–hexyl) orthophosphoric acid, Radiochim. Acta. **12,** No. 2, 107–111 (Aug. 1969).

Rankin, K., Tan, J. L., Component combination and frame-embedding in Chinese character grammars, Nat. Bur. Stand. (U.S.), Tech. Note 492, 36 pages (Feb. 1970), 40 cents, SD Catalog No. C13.46:492.

Raveche, H. J., Mayer, J. E., Theory of diffusion in simple liquid mixtures, J. Chem. Phys. **52,** No. 8, 3990–4004 (April 15, 1970).

Reader, J., Epstein, G. L., Reivsed $4p^6\ {}^2P^\circ_{1\ 2}$, $_{2\ 3\ 2}$ splitting of Y v, J. Opt. Soc. Am. **60,** No. 1, 140 (Jan. 1970).

Ritter, J. J., Coyle, T. D., Halogen exchange reactions of diboron tetrahalides, J. Chem. Soc. Sec. **A,** 1303–1304 (1970).

Robbins, D., Englert, A. J., Editors, Disclosures on: Viscous damped wind vane; nonskid road or runway; regrooved pneumatic tire with removable inserts; device for radially positioning a rotating wheel; method for fabricating precision waveguide sections; distortion-cancelling loudspeaker system; cryogenic fluid density measurement system; and controlled-atmosphere weathering device, NBS Tech. Note 536, 25 pages (June 1970) 35 cents, SD Catalog No. C13.46:536.

Robertson, A. F., Gross, D., Fire load, fire severity, and fire endurance, Am. Soc. Testing Mater. ASTM Spec. Tech. Publ. 464, Fire Performance, pp. 3–29 (January 1970).

Rockett, J. A., Objectives and pitfalls in the simulation of building fires with a computer, Fire Tech. **5,** No. 4, 311–322 (November 1969).

Rogers, E. E., Abramowitz, S., Jacox, M. E., Milligan, D. E. Matrix-isolation studies of the infrared spectra of the free radicals CCl_3 and CBr_3, J. Chem. Phys. **52,** No. 5, 2198–2204 (Mar. 1, 1970).

Romanoff, M., Corrosion evaluation of steel test piles exposed to permafrost soils, Proc. National Association of Corrosion Engineers 24th Conf., Houston, Texas, March 10–14, 1969, 6–13 (National Association of Corrosion Engineers, Houston, Texas, 1970).

Rosenblatt, J. R., Joiner, B. L., Hogben, D., OMNITAB–Rapid statistical manipulation, (Proc. Conf. Small-Area Statistics, American Statistical Association, New York, N.Y., Aug. 21, 1969). Paper in Census Tract Papers Final 1970 Census Plans and Four Programing Systems for Computerized Data Retrieval and Manipulation, Series GE–40, No. 6, pp. 46–59 (Superintendent of Documents, Government Printing Office, Washington, D.C. 20402, 65 cents, 1970).

Roth, R. S., Stephenson, N. C., Chemical and structural investigations in the Ta_2O_5–WO_3 system, (Proc. Institute for Advanced Study on the Chemistry of Extended Defects in Non-Metallic Solids, Scottsdale, Arizona, April 16–26, 1969), Chapter in The Chemistry of Extended Defects in Non-Metallic Solids, L. Erying and M. O'Keeffee, Eds., pp. 167–182 (North-Holland Publ. Co., Amsterdam, The Netherlands, 1970).

Ruegg, F. C., Spijkerman, J. J., DeVoe, J. R., A Mössbauer spectrometer for the structural analysis of materials, (Proc. Symp. Radioisotope Instruments in Industry and Geophysics, Warsaw, Poland, Oct. 18–22, 1965), Chapter in Radioisotope Instruments in Industry and Geophysics **I,** 325–335 (International Atomic Energy Agency, Vienna, Austria, May 1966).

Ryan, J. V., Implementation of the Flammable Fabrics Act, Proc. Conf. Flame Retardant Cotton Batting Workshop, New Orleans, Louisiana, Nov. 15, 1968, ARS 72–72, 1–77 (Oct. 1969).

Santoro, A., Mighell, A. D., Determination of reduced cells, Acta, Cryst. **A26,** No. 6, 124–127 (Jan. 1970).

Schneider, W. E., A one-solar-constant irradiance standard, Appl. Opt. **9,** No. 6, 1410–1418 (June 1970).

Schroeder, L. W., Infrared and raman spectra of $ClHCl^-$ and $BrHBr^-$ ions in $CsCl \cdot k/3H_2OHCl_2$ and $C_nBr \cdot 1/3H_2OHBr_3$, J. Chem. Phys. **52,** No. 4, 1972–1978 (Feb. 1970).

Schwerdtfeger, W. J., Corrosion rates of metals, alloys, and galvanic couples as measured by polarization techniques, Mater. Res. Std. **10,** No. 3, 22–28 (Mar. 1970).

Screw-thread standards for federal services. Part I. Unified UNJ unified miniature screw threads, Nat. Bur. Stand. (U.S.), Handb. 28, 237 pages (Dec. 1969), $2.00, SD Catalog No. C13.11:28. (Superseding H28 (1957) Part I and that applicable to Part I in the 1963 Supplement to H28.)

Searles, S. K., Sieck, L. W., Ausloos, P., Reactions of $C_2H_6{}^+$. Formation of the $(C_2H_6)_2{}^+$ ion, J. Chem. Phys. **53,** No. 2, 849–850 (July 15, 1970).

Sher, A. H., Nomographs for use in the fabrication and testing of Ge(Li) detectors, Nat. Bur. Stand. (U.S.), Tech. Note 537, 18 pages (Aug. 1970) 30 cents, SD Catalog No. C13.46:537.

Sher, A. H., Coleman, J. A., Lithium driftability in detector-grade germanium, IEEE Trans. Nucl. Sci. **NS–17,** No. 3, 125–129 (June 1970).

Sher, A. H., Keery, W. J., Variation in the effective Fano factor in a Ge(Li) detector, IEEE Trans. Nucl. Sci. **NS–17,** No. 1, 39–43 (February 1970).

Shields, W. R., Editor, Analytical Mass Spectrometry Section: Summary of atcivities July 1968 to June 1969, NBS Tech. Note 506, 55 pages (May 1970), 55 cents, SD Catalog No. C13.46:506.

Shipp, W. E., Surface tension of binary mixtures of several organic liquids at 25°C, J. Chem. Eng. Data **15,** No. 2, 308–311 (April 1970).

Sieck, L. W., Searles, S. K., Ausloos, P., High-pressure photionization mass spectrometry. I. Unimolecular and bimolecular reactions of $C_4H_9^+$ from cyclobutane, J. Am. Chem. Soc. **91,** No. 27, 7627–7634 (Dec. 31, 1969).

Simson, B. G., Mandel, J., Brenner, F. C., Research for a uniform quality grading system for tires. III. Breaking energy Rubber Chem. and Tech. **43,** No. 2, 356–369 (March 1970).

Sindt, C. F., Ludtke, P. R., Slush hydrogen flow characteristics and solid fraction upgrading, (Proc. 1969 Cryogenic Engineering Conf., June 16–18, 1969, Univ. of California, Los Angeles, Calif.), Chapter in Advances in Cryogenic Engineering 15, Paper No. I–6, 382–390 (Plenum Press, Inc., New York, N.Y., 1970).

Skolnik, H., Tauber, S. J., Introduction to the symposium on management and operation of information groups and centers, J. Chem. Doc. **9,** No. 4, 195 (Nov. 1969).

Smith, S. J., Survey on electron-atom collision experiments, (Proc. Sommerfeld Centennial Memorial Meeting, Munich, Germany, Sept. 9–14, 1968), Chapter in Physics of the One- and Two-Electron Atoms, F. Bopp and H. Kleinpoppen, Eds., pp. 574–597 (North Holland Publ. Co., Amsterdam, The Netherlands, 1969).

Smith, E. W., Cooper, J., Vidal, C. R., A unified classical path treatment of stark broadening in plasmas, Phys. Rev. **185,** No. 1, 140–151 (Sept. 5, 1969).

Snediker, D. K., The Mössbauer effect of Sn^{119} in palladium-rich palladium-tin solid solutions, (Proc. 2nd Symp. Mössbauer Effect Methodology, New York, N.Y., Jan. 25, 1966). Chapter in Mössbauer Effect Methodology **2,** 161–170 (Jan. 1966).

Snelleman, W., The measurement and calculation of flame temperatures, Chapter 7 in Flame Emission and Atomic Absorption Spectrometry **I,** 213–239 (Marcel Dekker, Inc., New York, N.Y., 1969).

Stevens, M. E., Automatic Indexing: A state-of-the-art report, NBS Mono. 91, 290 pages (Mar. 1970), $2.25, SD Catalog No. C13.44:91. (Reissued with additions and corrections Feb. 1970).

Stevens, M. E., Research and development in the computer and information sciences. 1. Information acquisition, sensing, and input: A selective literature review, Nat. Bur. Stand. (U.S.), Monogr. 113 Vol. 1, 170 pages (Mar. 1970), $1.50, SD Catalog No. C13.44:113/Vol. 1.

Stevens, M. E., Research and development in the computer and information sciences. 2. Processing, storage, and output requirements in information processing systems: A selective literature review, NBS Mono. 113 Vol. 2, 125 pages (May 1970), $1.25, SD Catalog No. C13.44:113/Vol. 2.

Stevens, M. E., Research and development in the computer and information sciences. 3. Overall system design considerations a selective literature review, Nat. Bur. Stand. (U.S.), Monogr. 113, Vol. 3, 147 pages (June 1970) $1.25, SD Catalog No. C13.44:113, Vol. 3.

Stevenson, D. R., Technical Standards Coordinator, Custom contact-molded reinforced-polyester chemical-resistant process equipment, NBS Prod. Stand. 15–69, 28 pages (June 1970) 20 cents, SD Catalog No. C13.20/2:15–69.

Stevenson, D. R., Technical Standards Coordinator, Heavy-duty alpha-cellulose-filled melamine tableware, Nat. Bur. Stand. (U.S.), Voluntary Prod. Stand. 25–70, 8 pages (Aug. 1970) 10 cents, SD Catalog No. C13.20/2:25–70. Supersedes Commercial Standard CS 173–50.

Stevenson, D. R., Technical Standards Coordinator, Melamine dinnerware (alpha-cellulose-filled) for household use, Nat. Bur. Stand. (U.S.), Voluntary Prod. Stand. 24–70, 9 pages (Aug. 1970) 10 cents, SD Catalog No. C13.20/2:24–70. Supersedes Commercial Standard CS 210–57.

Stevenson, D. R., Technical Standards Coordinator, Polyethylene sheeting (construction, industrial, and agricultural applications), Nat. Bur. Stand. (U.S.), Prod. Stand. 17–69, 20 pages (June 1970) 15 cents, SD Catalog No. C13.20/2:17–69 (Supersedes Commercial Standard CS 238–61).

Steward, W. G., Smith, R. V., Brennan, J. A., Cooldown transients in cryogenic transfer lines, (Proc. 1969 Cryogenic Engineering Conf., June 16–18, 1969, Univ. of California, Los Angeles, Calif.), Chapter in Advances in Cryogenic Engineering 15, Paper No. I–2, 354–363 (Plenum Press, Inc., New York, N.Y., 1970).

Stief, L. J., Payne, W. A., DeCarlo, V. J., Gorden, R., Jr., Ausloos, P., Comment on "Xenon sensitized photolysis of carbon dioxide," J. Chem. Phys. **53,** No. 1, 475–476 (July 1, 1970).

Straty, G. C., Prydz, R., Melting curve and triple-point properties of fluorine, Physics Letters **31A,** No. 6, 301–302 (March 23, 1970).

Sugar, J., Spectrum of doubly ionized thulium (Tm III), J. Opt. Soc. Am. **69,** No. 4, 454–466 (April 1970).

Swartz, J. C., Swartzendruber, L. J., Bennett, L. H., Watson, R. E., Nuclear magnetic resonance of ^{57}Fe in the paramagnetic alloys $TiFe_{1-x}Co_x$, Phys. Rev. **1,** No. 1, 146–152 (Jan. 1, 1970).

Swiggard, E. M., Clabaugh, W. S., Preparation of barium titanate semiconductors containing controlled amounts of neodymium, Am. Ceram. Soc. Bull. **45,** No. 9, 777–781 (Sept. 1966).

Thurber, W. R., Determination of oxygen concentration in silicon and germanium by infrared absorption, Nat. Bur. Stand. (U.S.), Tech. Note 529, 21 pages (May 1970) 30 cents, SD Catalog No. C13.46:529.

Tighe, N. J., Hockey, B. J., Ion thinning of electron microscope specimens, (Proc. 10th Symp. Electron, Ion and Laser Beam Tech., May 21–23, 1969, National Bureau of Standards, Gaithersburg, Md.), Record of 10th Symposium on Electron, Ion, and Laser Beam Technology, L. Marton, Ed., pp. 375–380 (San Francisco Press Inc., San Francisco, Calif., 1970).

Torrance, K. E., Orloff, L., Rockett, J. A., Experiments on natural convection in enclosures with localized heating from below, J. Fluid Mech. **36,** Part I, 21–31 (1969).

Torrance, K. E., Orloff, L., Rockett, J. A., Numerical study of natural convection in an enclosure with localized heating from below—creeping flow to the onset of laminar instability, J. Fluid Mech. **36,** Part I, 33–54 (June 1969).

Utech, H. P., Growing crystals in space, Proc. Conf. Manufacturing Technology Unique to Zero Gravity Environment, George C. Marshall Space Flight Center, Nov. 1, 1968, Huntsville, Alabama, pp. 197–214 (National Aeronautics and Space Administration, Greenbelt, Md., 1969).

Vicentini-Missoni, M., Joseph, R. I., Green, M. S., Sengers, J. M. H. L., Scaled equation of state and critical exponents in magnets and fluids, Phys. Rev. B, **1,** No. 5, 2312–2331 (March 1, 1970).

Vidal, C. R., Cooper, J., Smith, E. W., Hydrogen stark broadening calculations with the unified classical path theory, Nat. Bur. Stand. (U.S.), Monogr. 116, 143 pages (May 1970) $1.50, SD Catalog No. C13.44:116.

Venable, W. H., Jr., Effects upon radiant intensity measurements due to scattering by optical elements, Appl. Opt. **9,** No. 3, 609–615 (Mar. 1970).

Verdier, P. H., Relaxation behavior of the freely jointed chain, J. Chem. Phys. **52,** No. 11, 5512–5517 (June 1, 1970).

Wacker, P. F., Quantifying hazardous microwave fields: Analysis, Nat. Bur. Stand. (U.S.), Tech. Note 391, 19 pages (Apr. 1970), 30 cents, SD Catalog No. C13.46:391.

Weber, L. A., Saturation densities of oxygen in the critical region, Physics Letters **30A,** No. 7, 390–391 (Dec. 1, 1969).

Weber, L. A., The P–V–T surface of oxygen in the critical region; densities of saturated liquid and vapor, (Proc. 1969 Cryogenic Engineering Conf., June 16–18, 1969, Univ. of California, Los Angeles, Calif.), Chapter in Advances in Cryogenic Engineering 15, Paper No. B–4, 50–57 (Plenum Press, Inc., New York, N.Y., 1970).

Wegstein, J. H., Automated fingerprint identification, Nat. Bur. Stand. (U.S.), Tech. Note 538, 33 pages (Aug. 1970) 40 cents, SD Catalog No. C13.46:538.

Weisman, H. M., In the beginning was the word—information needs and uses in science and technology, Paper E 4–2 in Proceedings of the Seventeenth International Technical Communications Conference, Minneapolis, Minn., June 3–6, 1970, B. F.

Hylen and R. R. McDaniel, Ed., pp. 1–5 (Society of Technical Writers and Publishers Inc., 1010 Vermont Ave., N.W., Washington, D.C. 20005, 1970).

Weiss, A. W., Superposition of configurations and atomic oscillator strengths—boron isoelectronic sequence, Phys. Rev. **188,** No. 1, 119–130 (Dec. 5, 1969).

Weiss, A. W., Krauss, M., Bound-state calculation of scattering resonance energies, J. Chem. Phys. **52,** No. 9, 4363–4368 (May 1, 1970).

Wells, J. S., Evenson, K. M., A new LEPR spectrometer, Rev. Sci. Instr. **41,** No. 2, 226–227 (Feb. 1970).

West, E. D., Jennings, D. A., Power measurement of large laser beams with a small dual-cone calorimeter, Rev. Sci. Instr. **41,** No. 1, 142 (Jan. 1970).

White, H. J., Jr., Counties and county equivalents of the states of the United States, Nat. Bur. Stand. (U.S.), Fed. Info. Process. Stand. Publ. (FIPS Pub.) 6–1, 34 pages (1970) 45 cents, SD Catalog No. C13.52:6–1. Supersedes FIPS PUB 6, Nov. 1, 1968.

White, H. J., Jr., States and outlying areas of the United States, Nat. Bur. Stand. (U.S.), Fed. Info. Process. Stand. Publ. (FIPS Pub) 5–1, 4 pages, (1970) 20 cents, SD Catalog No. C13.52:5–1. Supersedes FIPS PUB 5, Nov. 1, 1968.

Wiederhorn, S. M., Moses, R. L., Bean, B. L., Plastic deformation and the fracture surface energy of sodium chloride, J. Am. Ceram. Soc. **53,** No. 1, 18–23 (Jan. 21, 1970).

Wilson, W. K., Discussion of paper "New Approaches to Preservation," by Richard D. Smith, Library Quart. **40,** No. 1, 171–175 (Jan. 1970).

Wilson, W. K., Record papers and their preservation, Chemistry **43,** No. 3, 8–12 (Mar. 1970).

Wims, A. M., Sengers, J. V. McIntyre, D., Shereshefsky, J., Interfacial tension of 3–methylpentane–nitroethane near the critical point, J. Chem. Phys. **52,** No. 6, 3042–3049 (Mar. 15, 1970).

Winogradoff, N. N., Neill, A. H., Petrescu-Prahova, J. B., Band tailing and the spontaneous spectra of compensated epitaxial GaAs laser junctions, IEEE J. Quantum Electron. Q.E. **6,** No. 6, 305–310 (June 1970).

Winogradoff, N. N., Neill, A. H., Jr., Temperature dependence of the power output of the spontaneous emission from GaAs laser diodes, Intern. J. Electron. **28,** No. 5, 401–406 (1970).

Wolfe, W. C., Performance tests for floor coverings, Mater. Res. Stand. **10,** No. 7, 15–18 (July 1970).

Wood, L. A., Creep of "pure-gum" vulcanisates of natural rubber, (Proc. Intern. Natural Rubber Conf., Kuala Lumpur, Malaya, Sept. 1968), J. Rubber Inst. Malaya 22, No. 3, 309–316 (1969).

Wood, L. A., Shouse, P. J., Passaglia, E., How just appreciable fading of AATCC L–4 wool standard is related to exposure time, Textile Chem. Colorist 2, No. 11, 182–190 (June 3, 1970).

Yakowitz, H., Comments on "application of color photography to electron microbeam probe samples," Rev. Sci. Instr. 41, No. 4, 601 (April 1970).

Young, K. F., Frederikse, H. P. R., Temperature and pressure dependence of dielectric constant of cadmium fluoride, J. Appl. Phys. 40, No. 8, 3115–3118 (July 1969).

Zielinzki, W. L., Freeman, D. H., Martire, D. E., Chow, L. C., Gas chromatography and thermodynamics of divinylbenzene separations on 4,4′–dihexoxyazoxybenzene liquid crystal, Anal. Chem. 42, No. 2, 176–180 (Feb. 1970).

** Publications for which a price is indicated are available by purchase from the Superintendent of Documents, U.S. Government Printing Office, Washington, D.C. 20402 (foreign postage, one-fourth additional). The NBS non-periodical series are also available from the National Technical Information Service, Springfield, Va. 22151. Reprints from outside journals and the NBS Journal of Research may often be obtained directly from the authors.*

☆U.S GOVERNMENT PRINTING OFFICE: 1971 O—413–272

UNITED STATES
GOVERNMENT PRINTING OFFICE
PUBLIC DOCUMENTS DEPARTMENT
WASHINGTON, D.C. 20402

OFFICIAL BUSINESS
PENALTY FOR PRIVATE USE, $300

POSTAGE AND FEES PAID
U.S. GOVERNMENT PRINTING OFFICE

JOURNAL OF RESEARCH of the National Bureau of Standards — Vol. 75C, No. 1 — January-March 1971
C. Engineering and Instrumentation

Contents

	Page
Rotary-vane attenuator with an optical readout. W. E. Little, W. Larson, and B. J. Kinder.	1
Design and operational characteristics of a high-speed (millisecond) system for measurement of properties at high temperature. Ared Cezairliyan.	7
New method of determining residual thiosulfate in processed photographic film. C. I. Pope.	19
Scanning densitometer for continuous recording of spectral transmission density at low spatial contrast. W. L. McLauglin, M. Rosenstein, E. Husmann, and J. J. Lantz, Jr.	23
Rotating optical attenuator for the generation of subsecond duration sawtooth shape radiance pulses. Ared Cezairliyan.	29
Sound speed measurements in solids; absolute accuracy of an improved transient pulse method. Thomas M. Proctor, Jr.	33
Seismic response of infransonic microphones. Alfred J. Bedard, Jr.	41
Publications of the National Bureau of Standards.	47

For sale by the Superintendent of Documents, U.S. Government Printing Office, Washington, D.C. 20402. (Order by SD Catalog No. C 13.22/sec. C: 75 (1). Price $1.25 (single copy). Subscription price: $5.00 a year; $1.25 additional for foreign mailing.

UNITED STATES GOVERNMENT PRINTING OFFICE, WASHINGTON : 1971